# Activity and Mechanism Studies on Novel Antibacterial Molecules Targeting Menaquinone Biosynthesis and Fatty Acid Biosynthesis in Drug Resistant *S. aureus*

A Dissertation Presented

by

**Yang Lu**

to

The Graduate School

in Partial Fulfillment of the

Requirements

for the Degree of

**Doctor of Philosophy**

in

**Chemistry**

Stony Brook University

**August 2014**

**Stony Brook University**

The Graduate School

**Yang Lu**

We, the dissertation committee for the above candidate for the

Doctor of Philosophy degree, hereby recommend

acceptance of this dissertation.

**Peter J. Tonge– Dissertation Advisor**
**Professor of Chemistry**

**Dale G. Drueckhammer - Chairperson of Defense**
**Professor of Chemistry**

**Erwin London – Committee Member of Defense**
**Professor of Chemistry**

**Stephen G. Walker – External Committee Member of Defense**
**Associate Professor in Department of Oral Biology and Pathology**

This dissertation is accepted by the Graduate School

Charles Taber
Dean of the Graduate School

Abstract of the Dissertation

**Activity and Mechanism Studies on Novel Antibacterial Molecules Targeting Menaquinone Biosynthesis and Fatty Acid Biosynthesis in Drug Resistant *S. aureus***

by

**Yang Lu**

**Doctor of Philosophy**

in

**Chemistry**

Stony Brook University

**2014**

Drug resistance in bacteria has become a global threat to public health care. The emergence of methicillin resistant *Staphylococcus aureus* (MRSA) exemplifies the eroding clinical efficacy of first-line antibiotics and emphasizes the need for new antibacterial drugs with novel mechanisms of action. The bacterial menaquinone (MK) biosynthesis pathway and fatty acid biosynthesis pathway (FAS-II) represent potential yet relatively underexploited targets for antibiotic development. My research is mainly focused on: 1) activity evaluation and mechanistic exploration of novel inhibitors targeting 1,4-dihydroxynaphthoyl-CoA synthase (MenB) from MRSA; 2) identification of a menaquinone salvage pathway in a defect *S. aureus* strain; 3) evaluation of a series of enoyl-ACP reductase (FabI) inhibitors against MRSA in animal infection models, investigating the impact of residence time ($t_R$) on *in vivo* antibacterial efficacy.

We first demonstrated that a series of 4-oxo-4-phenylbut-2-enoate compounds were active against MRSA with promising minimum inhibitory concentrations (MIC). Subsequently, we elucidated the mode of action of these compounds. The results support our 'prodrug' hypothesis by showing that the butenoyl methyl esters penetrated into bacterial cells where they were hydrolyzed and converted into corresponding CoA adducts. We then confirmed by quantitating menaquinone levels in bacteria before and after drug treatment that the 4-oxo-4-phenylbut-2-enoates acted through a specific effect on menaquinone biosynthesis. Additionally, we evaluated the *in vivo* efficacy of the most potent compound in a mouse model of MRSA, and demonstrated its potential as a new anti-MRSA candidate.

Small colony variants (SCVs) in *S. aureus* have recently attracted great interest. The aberrant bacteria have been identified to be auxotrophic to exogenous supplements such as menadioine (MD). Here, we discovered that a menaquinone-defect *S. aureus* strain (*menD*$^-$) was viable in rich growth media but not in minimal media. We subsequently identified that a series of quinone-based molecules, in addition to menadione, were able to restore the growth of the *menD*$^-$ strain. By showing the recovery of menaquinone biosynthesis in complemented bacteria, we demonstrated that the quinones were converted into a complete set of menaquinone species in *S. aureus*. We further identified that this conversion was catalyzed by 1,4-dihydroxy-2-naphtoate octaprenyl transferase (MenA).

Our lab has developed a library of diphenyl ether-based compounds targeting FabI as novel antibacterial candidates. The kinetics of drug-target interaction, which is described by the parameter of $t_R$, has been extensively studied. In my research, a series of FabI inhibitors that have distinctive $t_R$ values were selected, and their antibacterial activity was

evaluated in a mouse model of MRSA. The *in vivo* efficacy of the tested molecules were demonstrated to correlate more directly with $t_R$ rather than minimum inhibitory concentration (MIC) or the equilibrium dissociation constant ($K_i$). This observation supports the concept that the kinetics of drug-target interaction is more important than thermodynamic parameters when predicting drug efficacy in an open system.

Imaging techniques, such as positron emission tomography (PET), have been important medical probes that provide a non-invasive approach to perform examination in a living animal or human. Here, we labeled two FabI inhibitors with $^{11}C$ radionuclide and investigated their biological properties, such as *in vitro* cell uptake and *in vivo* drug distribution, using PET. In addition, an initial assay of imaging infections in living animals with FabI inhibitor-based radiotracers was performed. The results provide us important information to modify our PET imaging studies, which will ultimately facilitate infection diagnosis.

## Table of Contents

Abstract of the Dissertation ..... iii

Table of Contents ..... vi

List of Figures .....x

List of Tables .....xv

List of Abbreviations ..... xvii

Acknowledgments ..... xxii

Chapter I: Menaquinone and Fatty Acid Biosynthesis Pathways as Novel Antibacterial Targets .....1

*The history of antibiotics* .....1

*The emergence of antibiotic resistance in microorganisms and the need for new chemotherapeutics* .....3

*Menaquinone biosynthesis pathway as a potential antibacterial target* .....5

*Fatty acid biosynthesis pathway as a potential antibacterial target* .....11

*Research project overview* .....17

Chapter II: *In vitro* Activity, Cellular Mechanism, and *in vivo* Efficacy of 4-Oxo-4-Phenylbut-2-Enoate Compounds against *Staphylococcus. aureus* .....31

Background .....31

*Staphylococcus aureus and MRSA*.....31

*Previous work: discovery of a series of 4-oxo-4-phenylbut-2-enate compounds as MenB inhibitors* .....33

*Project overview* .....37

Results and Discussion .....39

*In vitro activity of the 4-oxo-4-phenylbut-2-enoate compounds against S. aureus and MRSA* .....39

*Antibacterial spectrum of M-8* .....42

*Mode of action of M-8: hydrolysis and CoA addition in S. aureus cells* .....44

*Cellular inhibitory mechanism of the 4-oxo-4-phenylbut-2-enoates: the effect on menaquinone biosynthesis in S. aureus* .....47
*In vivo antibacterial activity of M-8 in a mouse model of MRSA* .....54
Summary .....59
Experimental Procedures .....60
*Compound synthesis* .....60
*Determination of MIC values* .....60
*Hydrolysis and CoA addition of the butenoyl methyl esters in S. aureus cells* .....61
*MK extraction from S. aureus cells* .....62
*MK identification and quantification using MS/MS* .....63
*In vivo activity of M-8 in mouse models with MRSA* .....66

Chapter III. Demonstration of Cellular MK Conversion from Various Quinone-Based Molecules in *S. aureus*, and Identification of MenA as a Candidate Catalyzing the Reaction .....76
Introduction .....76
*Small colony variants in S. aureus* .....76
*S. aureus SCVs and menaquinone biosynthesis* .....77
*Project overview* .....80
Results and Discussion .....81
*Viability of the menD$^-$ S. aureus* .....81
*Growth recovery of the menD$^-$ strain in CDM by supplementing with various quinone-based molecules* .....84
*Recovery of MK biosynthesis in the menD$^-$ S. aureus* .....87
*Identification of a candidate enzyme catalyzing MK conversion in S. aureus* .....93
Summary .....100
Experimental Procedures .....102
*Materials and bacterial strains* .....102
*Cell growth recovering experiments* .....102

*MK extraction from rescued menD- bacteria and MK identification using MS/MS* .....103

*Synthesis of deuterium label quinone molecules and identification of D-MKs in complemented cells* .....104

*Antibacterial activity of CSU-20* .....105

*Cloning, overexpression and separation of saMenA* .....106

*In vitro MenA reaction* .....107

Chapter IV: *In vivo* Antibacterial Activity of Enoyl-ACP Reductase (FabI) Inhibitors and the Impact of Drug-Target Kinetics on Therapeutic Efficacy .....115

Introduction .....115

Results and Discussion .....117

*MIC of FabI inhibitors against MRSA* .....117

*In vivo activity of FabI inhibitors against MRSA infections* .....118

*Correlation between in vivo anti-MRSA activities and residence time* .....121

*Pharmacokinetic measurements on FabI inhibitors* .....125

*Determination of in vivo PAE* .....126

*In vivo efficacy and target specificity of a 4-pyridone-based FabI inhibitor, PT-166* .....128

*Antibacterial activity of thiolactomycin (TLM) derivatives against MRSA* .....132

Summary .....138

Experimental Procedures .....139

*Determination of MIC values* .....139

*Identification of in vivo efficacy, in vivo PAE and PK profile* .....139

*Selection for S. aureus RN4220 resistance to PT166* .....140

Chapter V: Biological Evaluation of Enoyl-ACP Reductase Inhibitors using Positron Emission Tomography (PET) .....147

Introduction .....147

Results and Discussion .....151

*In vitro uptake of radiolabeled compounds by S. aureus* .....151

*Biodistribution of radiolabeled [11C]-PT-119 in mice* .....154
*Distribution of [18F]-FDG, [11C]-PT-70 and [11C]-PT-119 in a mouse model of MRSA* .....155
*In vivo imaging of [18F]-FDG, [11C]-PT-70 and [11C]-PT-119 in mouse models* .....158
Summary .....162
Experimental Procedures .....163
*Chemistry* .....163
*In vitro assay for the uptake of radiolabeled compounds by bacteria* .....163
*In vivo radioactive studies* .....163

Bibliography .....170
Chapter I .....170
Chapter II .....177
Chapter III .....182
Chapter IV .....185
Chapter V .....188

## List of Figures

Figure 1.1: Timeline of antibiotic discovery .....3

Figure 1.2: The structure of phylloquinone, menaquinone and ubiquinone .....5

Figure 1.3: The function of menaquinone (MK) in the bacterial electron transport chain.....6

Figure 1.4: The bacterial menaquinone biosynthesis pathway .....7

Figure 1.5: The alternative menaquinone biosynthetic pathway in *S. coelicolor A3(2)*.....8

Figure 1.6: Representative inhibitors targeting the bacterial menaquinone biosynthesis pathway .....10

Figure 1.7: Fatty acid biosynthesis pathway in *E. coli* .....12

Figure 1.8: Activation of INH by KatG to form INH-$NAD^+$ adduct .....13

Figure 1.9: Structure of the INH-$NAD^+$ adduct binding to InhA (PDB: 2PR2) .....13

Figure 1.10: Structures of triclosan and a representative diphenyl ether-based FabI inhibitor previously synthesized by our group .....17

Figure 2.1: Evolution of drug resistance in *S. aureus* .....32

Figure 2.2: The MenB reaction in menaquinone biosynthesis pathway .....34

Figure 2.3: Representative structures of screened MenB inhibitors .....34

Figure 2.4: The hypothetic mechanism of retro-Michael addition and CoA addition .....37

Figure 2.5: The proposed mode of action of 4-oxo-4-phenylbut-2-enoates .....44

Figure 2.6: The structure of M-8 and its analogue M-8-$H_2$ .....45

Figure 2.7: The MALDI-TOF spectra acquired from (a) treated bacteria, (b) untreated bacteria, and (c) CoA adduct standard .....47

Figure 2.8: Mass spectra from (a) the primary ionization and (b) the secondary ionization of MK-4 .....50

Figure 2.9: MK calibration curve generated with MK-4 standard .....51

Figure 2.10: Distribution of MK species in *WT S. aureus* .....52

Figure 2.11: MK-8 concentration in drug treated *S. aureus*, in comparison to that in wild type bacteria .....53

Figure 2.12: Inhibition of all MK species in drug treated bacteria .....54

Figure 2.13: MK-8 concentration in drug treated MRSA cells, in comparison to that in wild type MRSA .....54

Figure 2.14: Decrease of MK-8 concentration in MSSA cells in response to escalating doses of M-8 treatment .....55

Figure 2.15: Investigation of the lethal dose of *S. aureus* BAA 1762 in Swiss Webster mice .....56

Figure 2.16: Survival of infected mice after received treatments of vehicle, oxacillin, M-8 and vancomycin .....57

Figure 2.17: Bacterial growth in thigh muscle in neutropenic mice and immune competent mice .....58

Figure 2.18: Thigh muscle bacterial load in infected mice treated with vehicle, oxacillin, M-8, and vancomycin .....59

Figure 2.19: Synthesis of 2-CoA-4-(4-chloro)-phenyl-4-oxo-butanoic acid.....61

Figure 2.20: MRM signals of MK species from cell extract ..... 65-66

Figure 3.1: Sheep blood-agar plates that show the normal and the small colony variant phenotype of *S. aureus*.....78

Figure 3.2: Bacterial electron transport chain .....79

Figure 3.3: The bacterial menaquinone biosynthesis pathway .....80

Figure 3.4: Growth of WT and *menD- S. aureus* in (a) Tryptic Soy broth (TSB) and (b) Mueller Hinton II broth (MH-II) .....83

Figure 3.5: Viability of the *menD- S. aureus* (a) in chemically defined media (CDM), and (b) on minimal agar plates .....84

Figure 3.6: GC-MS spectra of menadione (MD) .....85

Figure 3.7: Structure of quinone-based supplements .....86

Figure 3.8: Recovery of growth of the *menD*- strain in chemically defined media (CDM) by supplementing with different quinone-based molecules.....87

Figure 3.9: Recovery of menaquinone (MK) biosynthesis in the complemented *menD- S. aureus* .....89

Figure 3.10: Recovery of bacterial growth and cellular MK biosynthesis in *menD- S. aureus* supplemented with MK-7 .....91

Figure 3.11: Synthetic route of MD-$d_3$ and diMe-$d_3$ .....92

Figure 3.12: MK-n-$d_3$ in the *menD- S. aureus* complemented with MD-d3 and diMe-d3 .....92

Figure 3.13: Proposed mechanism of MD-MK conversion via DHNA .....93

Figure 3.14: Hypothetic mechanism of MK conversion via menadione .....94

Figure 3.15: The conversion of different Vitamin K into MK-4 catalyzed by UBIAD1 .....95

Figure 3.16: Identification of *sa*MenA in lipid fraction .....98

Figure 3.17: *In vitro* MenA reaction of DHNA and GGPPi .....100

Figure 3.18: *In vitro* MenA reaction of GGPPi and MD or PQ.....100

Figure 3.19: Mechanism of the radical reaction used for MD-$d_3$ and diMe-$d_3$ synthesis .....105

Figure 3.20: Cloning of *samenA* into plasmid pET15b .....107

Figure 4.1: Correlation between residence times of a series of FabI inhibitors and their *in vivo* efficacy against tularemia in mice .....117

Figure 4.2: Survival of systemically infected mice treated with FabI inhibitors .....120

Figure 4.3: Thigh muscle bacterial load in mice treated with FabI inhibitors.....121

Figure 4.4: Reduction of bacterial burden in thigh infection model .....122

Figure 4.5: Correlation between *in vivo* activities of FabI inhibitors against systemic (left) and thigh (right) infection and their corresponding MIC values .....123

Figure 4.6: Correlation between *in vivo* activities of FabI inhibitors against systemic (left) and thigh (right) infection and their corresponding $K_i$ values .....124

Figure 4.7: Correlation between *in vivo* activities of FabI inhibitors against systemic (left) and thigh (right) infection and their corresponding $t_R$ values .....125

Figure 4.8: Representative drug concentration-time curve in PT52 treated mice .....127

Figure 4.9: Bacterial burdens at the early phase of thigh infection in mice treated with vehicle, PT-04, PT-52, and PT-119 .....129

Figure 4.10: Reduction of thigh bacterial burden in PT-166 treated mice .....131

Figure 4.11: Survival of systemically infected mice treated with TLM derivatives .....138

Figure 4.12: Average survival times of the infected mice treated with escalating doses of TLM-6 .....138

Figure 5.1: Mechanism of positron emission .....149

Figure 5.2: *In vitro* uptake of [$^{18}$F]-FDG (left) and [$^{11}$C]-PT-119 (right) by *S. aureus* cells .....152

Figure 5.3: *In vitro* uptake of [$^{18}$F]-FDG (left) and [$^{11}$C]-PT-119 (right) by *S. aureus* cells at different temperatures .....153

Figure 5.4: *In vitro* uptake of [$^{18}$F]-FDG (left) and [$^{11}$C]-PT-119 (right) by *S. aureus* cells pretreated with 'cold' glucose or PT-119 .....154

Figure 5.5: Distribution of [$^{11}$C]-PT-119 in peripheral organs / tissues in mice .....155

Figure 5.6: Radioactivity counts in different organs in healthy (control), low-dose infected and high-dose infected mice .....156

Figure 5.7: Ratio of radioactivity accumulated in the infected thighs (L) over that in the uninfected thighs (R).....157

Figure 5.8: Biodistribution of [$^{11}$C]-PT-119 in systemic infection model of MRSA .....158

Figure 5.9: Accumulation of [$^{11}$C]-PT-70 (top) and [$^{11}$C]-PT-119 (bottom) in thigh infection model of MRSA.....158

Figure 5.10: PET images acquired from healthy mice that were administered [$^{18}$F]-FDG, [$^{11}$C]-PT-70, or [$^{11}$C]-PT-119.....160

Figure 5.11: Dynamics of the *in vivo* distribution of [$^{11}$C]-PT-119.....160

Figure 5.12: Images acquired from (a) healthy, (b) systemic infection, and (c) thigh infection mice after administration of [$^{11}$C]-PT-119 .....161

## List of Tables

Table 1.1: Examples of menaquinone biosynthesis inhibitors.....10

Table 1.2: Examples of synthetic FabI inhibitors .....14

Table 1.3: Examples of natural product-based FabI inhibitors.....15

Table 2.1: *In vitro* activity of 1548L21 analogues.....36

Table 2.2: MenB inhibition by the 2-CoA-4-oxo-4-phenylbutanoic acids.....37

Table 2.3: Antibacterial activity of the butenoyl methyl esters .....40

Table 2.4: Antibacterial activity of the butenoic acids .....41

Table 2.5: Comparative antibacterial efficacy of M-8 and several first-line antibiotics against MSSA and MRSA .....42

Table 2.6: MIC values of M-8 against various bacterial species.....43

Table 2.7: Viability of MenB inhibitor-treated *S. aureus* with or without DNHA supplementation .....48

Table 2.8: Primary and secondary ionization of MK components .....50

Table 3.1: Antibacterial activity of CSU-20 and several MenB inhibitors with or without quinone supplementations.....96

Table 3.2: Primary and secondary ionization of MK-n-$d_3$.....106

Table 4.1: MIC values of diphenyl ether FabI inhibitors against MRSA (BAA1762)..... .....118

Table 4.2: Survival rate and average survival time of infected animals treated with different drugs.....120

Table 4.3: *In vitro* and *in vivo* data of studied FabI inhibitors.....122

Table 4.4: Core PK parameters of studied FabI inhibitors .....127

Table 4.5: *In vitro* activity of reprehensive pyridone-based FabI inhibitors against *S. aureus* .....130

Table 4.6: Core PK parameters of PT-166 and PT-04 .....132

Table 4.7: Point mutations observed in PT166 resistant *S. aureus* strains .....133

Table 4.8: *In vitro* antibacterial activity of TLM derivatives against MSSA and MRSA ..... ..... 135-137

Table 5.1: Commonly used positron-emitting isotopes .....149

## List of Abbreviations

| | |
|---|---|
| 2,3-diMe-NQ | 2,3-dimethyl-1,4-naphthoquinone |
| ACP | Acyl carrier protein |
| ADP | Adenosine diphosphate |
| APCI | Atmospheric pressure chemical ionization |
| ATP | Adenosine triphosphate |
| AUC | Area under the curve |
| *B. mallei* | *Burkholderia mallei* |
| *B. subtilis* | *Bacillus subtilis* |
| BNL | Brookhaven National Laboratory |
| CDC | Centers of Disease Control and Prevention |
| CDM | Chemically defined media |
| CFU | Colony forming unit |
| *c*logP | Calculated logarithm of the partition coefficient between *n*-octanol and water |
| $C_{max}$ | Peak plasma concentration |
| CNS | Central nervous system |
| CoA | Coenzyme A |
| CPA | Cyclophosphamide |
| CT | Computerized tomography |
| Da | Dalton |
| DHB | 2,5-dihydroxybenzoic acid |
| DHNA | 1,4-dihydroxy-2-naphthoic acid |
| DMMK | Demethylmenaquinone |
| DMSO | Dimethyl sulfoxide |

| | |
|---|---|
| *E. coli* | *Escherichia coli* |
| *E. faecium* | *Enterococcus faecium* |
| *E. faecalis* | *Enterococcus faecalis* |
| FabI | Enoyl-ACP reductase |
| FAS-I | Type I fatty acid biosynthesis |
| FAS-2 | Type II fatty acid biosynthesis |
| FDA | Food and Drug Administration |
| [$^{18}$F]-FDG | 2-deoxy-2-($^{18}$F)fluoro-D-glucose |
| GC-MS | Gas chromatography-mass spectrometry |
| GGPPi | Geranylgeranyl pyrophosphate |
| HIV | Human immunodeficiency virus |
| HPLC | High-performance liquid chromatography |
| HTS | High throughput screening |
| $IC_{50}$ | Half maximal inhibitory concentration |
| IM | Intramuscular injection |
| INH | Isoniazid |
| InhA | Enoyl-ACP reductase from *M. tuberculosis* |
| IP | Intraperitoneal injection |
| IPTG | Isopropyl β-D-1-thiogalactopyranoside |
| IV | Intravenous injection |
| *K. pneumoniae* | *Klebsiella pneumoniae* |
| KatG | *Mycobacterial* catalase-peroxidase |
| $K_i$ | Dissociation constant of inhibitors |
| $k_{off}$ | Dissociation rate constant |
| LB | Luria Broth |

| | |
|---|---|
| *M. smegmatis* | *Mycobacterium smegmatis* |
| *M. tuberculosis* | *Mycobacterium tuberculosis* |
| MALDI | Matrix-assisted laser desorption/ionization |
| MD | Menadione |
| MenA | 1,4-dihydroxy-2-naphthoate-octaprenyltransferase |
| MenB | 1,4-dihydroxy-2-naphthoyl-CoA synthase |
| MenD | 2-succinyl-5-enolpyruvyl-6-hydroxy-3-cyclohexadiene-1-carboxylate synthase |
| MenE | OSB-CoA synthase |
| MenG | (SAM)-dependent methyl transferase |
| MH-II | Mueller Hinton II broth |
| MIC | Minimum inhibitory concentration |
| MK | Menaquinone |
| MRI | Magnetic resonance imaging |
| MRSA | Methicillin resistant *S. aureus* |
| MS | Mass spectrometry |
| MS/MS | Tandem mass spectrometry |
| MSSA | Methicillin susceptible *S. aureus* |
| $NAD^+$ | Nicotinamide adenine dinucleotide (oxidized) |
| NADH | Nicotinamide adenine dinucleotide (reduced) |
| NQ | 1,4-naphthoquinone |
| $OD_{600}$ | Optical density at 600 nm |
| OSB | *O*-succinylbenzoic acid |
| *P. aeruginosa* | *Pseudomonas aeruginosa* |
| *P. mirabilis* | *Proteous mirabilis* |
| PAE | Post-antibiotic effect |

| | |
|---|---|
| PCR | Polymerase chain reaction |
| PEG | Polyethylene glycol |
| PET | Positron emission tomography |
| PK | Pharmacokinetics |
| PQ | Phylloquinone |
| PRSA | Penicillin resistant *S. aureus* |
| *S. aureus* | *Staphylococcus aureus* |
| *sa*FabI | Enoyl-ACP reductase from *S. aureus* |
| SAM | *S*-adenosylmethionine |
| *sa*MenA | 1,4-dihydroxy-2-naphthoate-octaprenyltransferase from *S. aureus* |
| *sa*MenB | 1,4-dihydroxy-2-naphthoyl-CoA synthase from *S. aureus* |
| *sa*MenD | 2-succinyl-5-enolpyruvyl-6-hydroxy-3-cyclohexadiene-1-carboxylate synthase from *S. aureus* |
| SAR | Structure-activity relationship |
| SC | Subcutaneous injection |
| SCVs | Small colony variants |
| SD | Standard deviation |
| SDS-PAGE | Sodium dodecyl sulfate-polyacrylamide gel electrophoresis |
| SEM | Standard error of the mean |
| SI | Selective index |
| SSI | Surgery site infection |
| $t_{1/2}$ | Half-life |
| TB | Tuberculosis |
| TLM | Thiolactomycin |
| TOF | Time-of-flight |
| $t_R$ | Residence time |

| | |
|---|---|
| TSB | Tryptic soy broth |
| UBIAD1 | UbiA prenyltransferase containing domain 1 |
| UBQ | Ubiquinone |
| VISA | Vancomycin intermediate *S. aureus* |
| VRSA | Vancomycin resistant *S. aureus* |
| WHO | World Health Organization |
| WT | Wild type |

**Acknowledgment**

It is a great opportunity to express my sincere respect to those who have contributed to this dissertation. Without you, this dissertation would not have been possible. Moreover, you made my graduate experience one of the brightest sparks in my life.

I would like to give the deepest thanks to my advisor Prof. Peter J. Tonge, who has provided support and advice on my research, and more importantly encouraged me to think and work creatively. More than showing interest and appreciation on my experiments, Prof. Tonge always lead me to pursue the story behind a simple sign, which truly represents the essence of science. His enthusiasm, preciseness, diligence, and immense knowledge posted a great example for me in my future career and my life.

I would like to thank Prof. Dale Drueckhammer for serving as the chairperson of my dissertation committee. I learned so much in Dr. Drueckhammer's classes and from his suggestions on my experiments. It has been a privilege having Prof. Erwin London as the third member of my committee. His patience and knowledge benefitted my Ph.D. career a lot. It is also an honor to invite Prof. Stephen Walker as the external member of my committee. In addition to his comments on my research and thesis, Prof. Walker's optimistic spirit always inspired me to conquer many difficulties.

I must pass my thanks to Dr. Thomas Zimmerman (DLAR), Dr. Robert Rieger (Proteomics Center), Dr. Bela Ruzsicska (ICB&DD), and Dr. David Alexoff (BNL) for teaching me the amazing expertise that lead my research going forward. I would also like to thank my lab mates for all the stimulating discussion and kind help. The experience of being a member of Tonge group will be my precious memory forever.

Nothing can describe my gratefulness to my incredible parents for their continuous support and encouragement. I am very proud of being their son, and words are never enough to express my love to them. Finally yet importantly, I owe a great many thanks to my special one Li Tan whose love put me through the ebbs and flows of my life.

# Chapter I: Menaquinone and Fatty Acid Biosynthesis Pathways as Novel Antibacterial Targets

*The History of antibiotics*

Infectious diseases are caused by pathogenic microorganisms and can be spread, directly or indirectly, from one person to another. Since the permanent settlement of hominid civilizations beginning some 10,000 years ago, infectious diseases have played an important role in human history. The first recorded emergence of infectious disease dates back to the biblical times and it has since been a huge threat for human beings (1, 2). The establishment of large cities and the accumulation of regional populations heightened the devastating consequences of infection outbreaks (3, 4). A dramatic example is the Black Death of the late 14$^{th}$ century, in which the infection caused by *Yersinia pestis* swept across Europe and eliminated at least one quarter of the total European population in one decade (5). Meanwhile, tuberculosis (TB) is estimated to have claimed approximately one billion lives by the end of the 19$^{th}$ century (6, 7), and still ranks as the second leading cause of death worldwide by a single infectious agent, just behind human immunodeficiency virus (HIV) (8). In history, unsanitary living conditions, poor nutrition and the lack of effective treatment have been the major causes for routine outbreaks and the high mortality of infectious diseases (9).

The use of "drugs" to combat human infections dates back to more than 2,000 years ago in ancient Greece, Egypt and China, but was primarily based on medicinal folklore such as mixtures of specific plants and molds (10). Treatments for infectious diseases were not rationalized until Louis Pasteur revealed the relationship between microorganisms and

infections, and announced "if we could intervene in the antagonism observed between some bacteria, it would offer perhaps the greatest hopes for therapeutics" (11). The term 'antibiosis', meaning "against life", was first introduced by a French bacteriologist Jean Paul Vuillemin and was subsequently verified by Louis Pasteur and Robert Koch in 1877 as they observed that the growth of a microorganism, *Bacillus anthracis*, could be inhibited by another airborne bacillus bacterium (12). The first chemical approach in the intervention of bacterial growth was conducted by a German scientist Paul Ehrlich who screened hundreds of dyes and discovered the first ever antibacterial chemical Salvarsan, an anti-syphilis drug that is now called Arsphenamine (13).

The most significant hallmark in the history of antibiotics was the discovery of penicillin by Sir Alexander Fleming in 1928 (14, 15). This achievement has been widely appreciated as one of the most important scientific events in the 20$^{th}$ century. Purification of penicillin was accomplished in 1942; however, the use of this antibiotic was limited to the allied military. Mass production of penicillin became available in 1945 after Dorothy Crowfoot Hodgkin determined its chemical structure. The clinical use of penicillin was a great success as the mortality of bacterial infections dropped by an estimated 85% from 1920 to 1950 (16). Moreover, the success of penicillin ushered "the golden era of antibiotic discovery" from the 1940s to the 1960s (**Figure 1.1**), during which most of the antibiotic classes we use today were identified (17). Although it is impossible to estimate how many lives have been saved, the discovery of antibiotics has drastically affected the world.

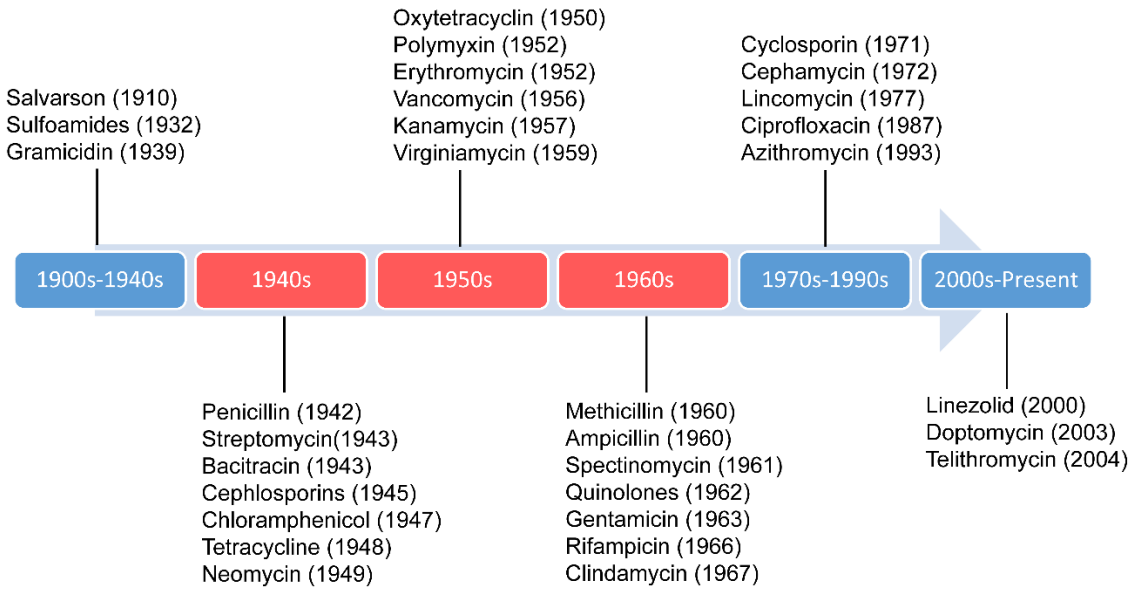


**Figure 1.1.** Timeline of antibiotic discovery. It is known as the "golden era of antibiotic discovery" from the 1940s to the 1960s.

*The emergence of antibiotic resistance in microorganisms and the need for new chemotherapeutics*

Given the success of penicillin and the rapid developments of a vast array of effective antibacterial agents, physicians believed that virtually all bacterial infections were treatable and would be eventually eradicated. Nevertheless, such optimism was sadly abandoned in the early 1970s due to the massive emergence of antibiotic resistant pathogens (18). Misuse of antimicrobial drugs accelerated the frequency of resistance in microorganisms (19). Unfortunately, Alexander Fleming predicted this outcome and stated in his Nobel Prize lecture, "The time may come when penicillin can be bought by anyone in the shops. Then there is the danger that the ignorant man may easily underdose himself and by exposing his microbes to non-lethal quantities of the drug make them resistant" (20). Although the exact mechanism has not been completely understood, four major factors

have been proposed to cause antibiotic resistance: induced drug inactivation, altered target site, modified metabolic pathway, and reduced drug accumulation (21, 22).

While antibiotic resistance is on the rise, discovery of new antibiotics has dramatically slowed down after the 'golden era of antibiotic discovery'. It has become increasingly difficult to develop novel antibacterial agents that are insusceptible to drug resistance. As a consequence, a large number of pharmaceutical companies and biotechnology institutes have left this research area (23). However, there remains an urgent need for new chemotherapeutics as the reemergence of preexisting infectious diseases, which were once considered under total control, have posted a huge threat to the public health. The unpredictable and probably inevitable prevalence of resistant pathogens has urged a new wave of antibiotic development.

One strategy of discovering new antibiotics bases on 'empirical' whole cell screening. Although it is not mechanistically specific, the outcome of screening probes all possible targets in each pathogen and can select active lead compounds from the outset. Another strategy of antibiotic development depends on the validation of relevant targets in pathogens. This approach has become more favored after bacterial genome has been deciphered from *H. influenza* (24). Since then, strenuous efforts have been made to identify potentially important targets and to develop candidates through medicinal chemistry structure-activity relationship (SAR) studies (25-28).

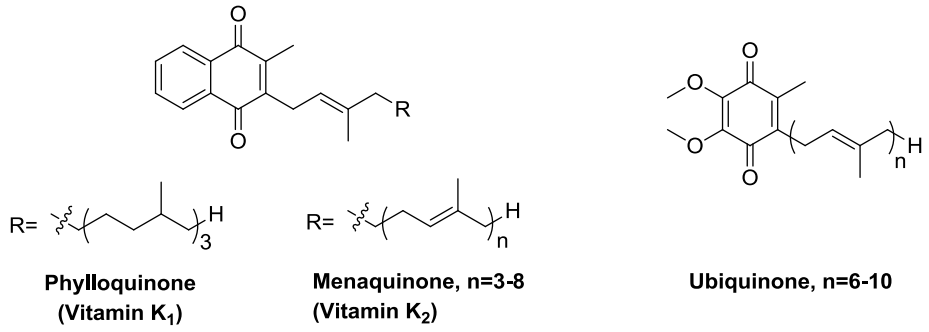


**Figure 1.2.** The structure of phylloquinone, menaquinone and ubiquinone. Phylloquinone is the plant derived quinone form with a 3-phytyl substituent. Menaquinone has a 3-polyisoprenyl side chain, and is utilized primarily by Gram-positive bacteria, anaerobic Gram-negative bacteria and Mycobacteria. Ubiquinone is utilized by human and aerobic Gram-negative bacteria.

Quinones are lipid soluble redox molecules (**Figure 1.2**) with important functions in all living organisms. As a quinone subtype, vitamin K, which includes the plant-derived phylloquinone (PQ, vitamin $K_1$) and the bacteria-derived menaquinone (MK, vitamin $K_2$), is a cofactor of the γ-glutamyl carboxylase in the eukaryotic coagulation system (29). Another important physiological function of quinones is to mediate electron transport between redox protein complexes in the respiratory chain (**Figure 1.3**) (30). The quinone-associated electron movement is coupled to the transport of protons towards the outside space of the membrane. The accumulated electrical gradient forces the exterior protons to flow back into the interior of the cell membrane through the only proton-permeable channel, ATP synthase. The proton motive force is utilized to produce ATP from ADP. It has been demonstrated that eukaryotic cells utilize ubiquinone (UBQ) and phylloquinone as the redox molecules (31), whilst prokaryotes use menaquinone and ubiquinone. In particular,

Gram-positive bacteria, such as *S. aureus* and *B. subtilis*, utilize menaquinone as the electron carrier and Gram-negative organisms use ubiquinone (32, 33).

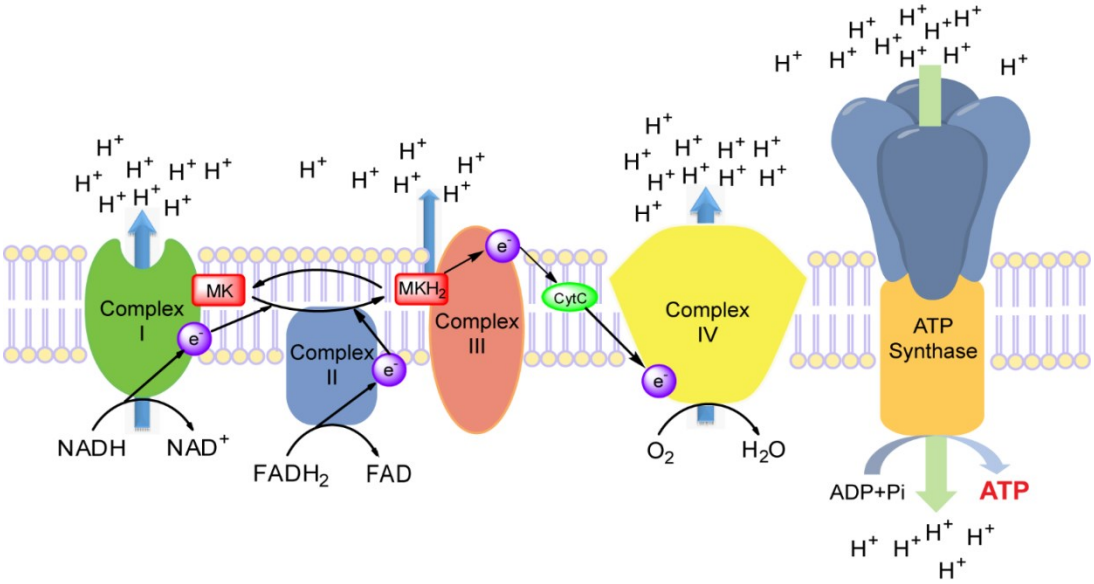


**Figure 1.3.** The function of menaquinone (MK) in the bacterial electron transport chain. Menaquinone plays a central role by mediating the movement of electrons between different redox complexes, and is a critical component in ATP biosynthesis.

The biosynthesis of menaquinone has been extensively studied in *Escherichia coli* (*E. coli*) (34-36). As shown in **Figure 1.4**, menaquinone is synthesized from chorismate through the action of at least 9 enzymes. Chorismate is first converted into isochorismate by isochorismate synthase (MenF) and subsequently into 2-succinyl-6-hydroxy-2,4-cyclohexadiene-1-carboxylate (SEPHCHC) by MenD. The decomposition of SEPHCHC is catalyzed by MenH yielding SHCHC, which is then converted to an aromatic intermediate, *O*-succinylbenzoate (OSB) by MenC. The OSB carboxylate is then activated formation of *O*-succinylbenzoyl-CoA (OSB-CoA) then catalyzed by MenE followed by a ring-closing reaction catalyzed by the 1,4-dihydroxyl-2-naphthoyl-CoA synthase (MenB). The product of the MenB reaction, DHNA-CoA, is hydrolyzed by MenI to give 1,4-

dihydroxy-2-naphthoic acid (DHNA). An isoprenoyl side chain is then attached to DHNA at the C-3 position by the isoprenoyl transferase (MenA), and a methyl group is conjugated to the C-2 position on the naphthoquinone ring by *S*-adenosylmethionine (SAM)-dependent methyl transferase (MenG) to produce menaquinone. Although the exact mechanisms of several steps are still controversial, the menaquinone biosynthestic pathway is thought to be identical in various organims including *Mycobacterium tuberculosis*, *Staphylococcus aureus* and *Bacillus subtilis* (37-39).

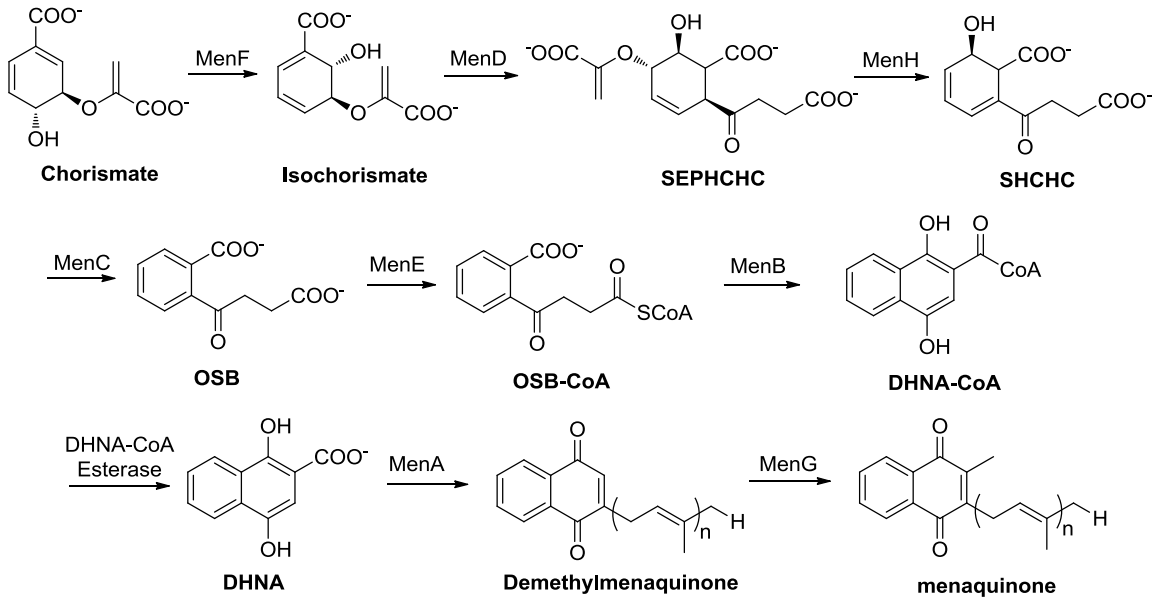


**Figure 1.4.** The bacterial menaquinone biosynthesis pathway. This pathway initiates from chorismate and proceeds throught the action of a series of enzymes named Men proteins. The de novo menaquinone biosynthesis pathway has been discovered only in menaquinone-utilizing prokaryotes but not in human.

Interestingly, although several bacterial species produce and utilize menaquinone, bioinformatic analysis of whole genomes have shown that not all organisms have homologues of *men* genes. This is the case for *Streptomyces ceolicolor A3(2) (40, 41),*

*Campylobacter jujuni (42)* and lactobacilli (43, 44). Recently, an alternative menaquinone biosynthetic pathway has been proposed in *S. coelicolor A3(2)* and is named the futalosine pathway (**Figure 1.5**) (45, 46).

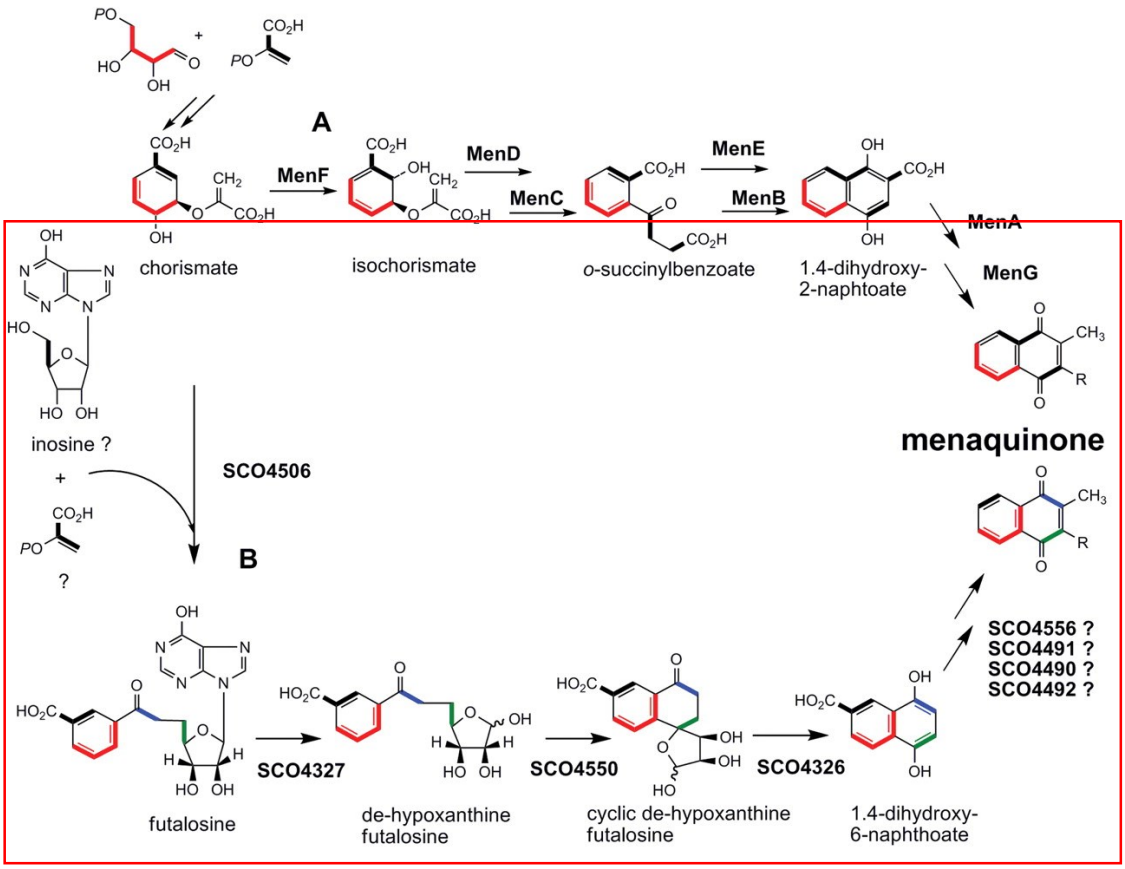


**Figure 1.5.** The alternative menaquinone biosynthetic pathway (the lower branch showed in red square) in *S. coelicolor A3(2).* This figure was adapted from Bentley *et al*. (40).

The biosynthesis of menaquinone has been considered a potential drug target in Gram-positive bacteria due to the critical function of this quinone in respiration (34, 47-49). This idea has been supported by recent transposon site hybridization experiments, which demonstrated that several enzymes in the menaquinone biosynthetic pathway are crucial for the survival of various bacterial species (50-52). Furthermore, although vitamin K also plays an important role in eukaryotic physiology, *de novo* menaquinone biosynthesis

only exists in Gram-positive and anaerobic Gram-negative bacteria. In contrast, humans can only source vitamin K from dietary intake. Therefore, inhibition of menaquinone biosynthesis is a potential strategy to develop drugs that can specifically target bacteria without affecting the host cells. Recently, efforts have been made to identify inhibitors of Men proteins by different research groups (**Figure 1.6, Table 1.1**). For example, a series of animomethanone compounds have been developed as MenA inhibitors and exhibited whole cell inhibition towards various pathogenic bacteria, such as drug resistant *M. tuberculosis* (53, 54). A series of 1,4-benzoxazine derivatives have been selected through high throughput screening (HTS) as inhibitors of MenB from *M. tuberculosis*. SAR modifications of this scaffold resulted in the discovery of potential antimicrobial candidates that are active against live bacteria (55). Oxythiamine derivatives and succinylphosphonate esters have been identified as MenD inhibitors and were reported to have potential antibacterial potency (56). Additionally, a series of vinyl sulfonamides have been demonstrated active against MenE from *E. coli*, *S. aureus* and *M. tuberculosis* (57, 58).

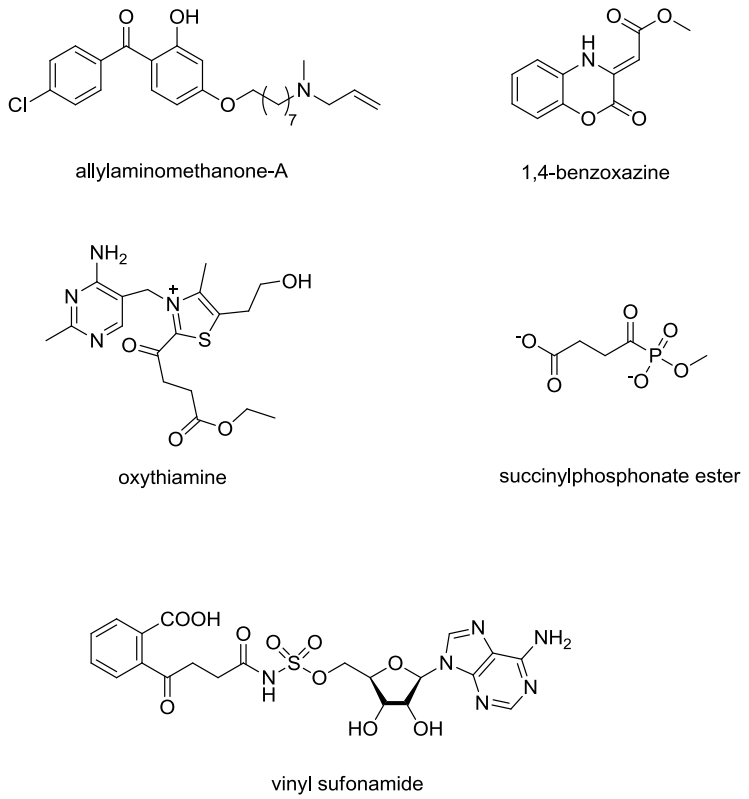


**Figure 1.6.** Representative inhibitors targeting the bacterial menaquinone biosynthesis pathway.

**Table 1.1.** Examples of menaquinone biosynthesis inhibitors.

| Inhibitor | Target | Bacterium | $IC_{50}$ (µM) | MIC (µg/ml) |
|---|---|---|---|---|
| aminomethanone | MenA | *M. tuberculosis* | N/A[a] | 1.5 |
| 1,4-benzoxazine | MenB | *M. tuberculosis* | 10 | 0.6 |
| oxythiamine | MenD | *S. aureus* | 25 | 240 |
| vinyl sulfonamide | MenE | *M. tuberculosis*<br>*S. aureus* | 0.05<br>0.06 | N/A |

[a] N/A: not available

*Fatty acid biosynthesis pathway as a potential antibacterial target*

The cell membrane is responsible for essential aspects of cell physiology. Most importantly, it separates the interior of cells from the outside environment and functions as a semi-permeable barrier to protect the integrity and the viability of cells. Cell membranes are also involved in various cellular processes other than protection, such as molecular transportation, cell mobility and intercellular communication.

The cell membrane is chemically a lipid bilayer composed of phospholipids with embedded proteins. As a principle building block of phospholipids, fatty acids are important metabolic precursors for the construction and function of the cell membrane. In eukaryotes, fatty acid biosynthesis is accomplished by a process known as the Type I fatty acid synthesis (FAS-I), in which all synthetic steps are catalyzed by a single fatty acid synthase protein (59). In prokaryotes, fatty acid biosynthesis is catalyzed by a series of enzymes and is known as the Type II fatty acid biosynthetic pathway (FAS-II) (**Figure 1.7**) (60-62). Since FAS-II has fundamental differences from FAS-I chemically and biologically, it has been considered an attractive antibacterial target. Gene knockouts and knockdown experiments showed that enzymes in FAS-II are essential for the survival of bacteria (61, 63). Subsequent studies suggested that bacteria are not able to scavenge fatty acids from the host (26, 60).

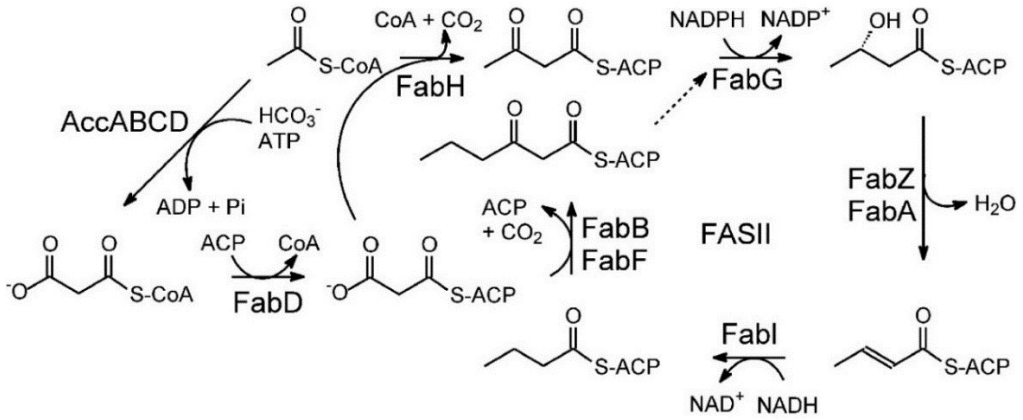


**Figure 1.7.** Fatty acid biosynthesis pathway in *E. coli*. AccABCD is the acetyl-CoA carboxylase; FabH is the malonyl-CoA:ACP transacylase; FabG is the β-ketoacyl-ACP reductase; FabA and FabZ are the β-hydroxyacyl-ACP dehydrases; FabI is the enoyl-ACP reductase; FabH, FabB and FabF are the β-ketoacyl-ACP synthase. The first condensation step is catalyzed by FabH and the further elongations are initiated by FabB/FabF.

In FAS-II, the NADH-dependent enoyl-ACP reductase (FabI) catalyzes the reduction from enoyl-ACP to acyl-ACP, which is the last step in the elongation cycle. The structure and catalytic mechanism of FabI from different organisms, such as *E. coli, M. tuberculosis, S. aureus* and *Burkhoderia mallei*, have been investigated (64-69). Evidence from genetic studies have supported that FabI is essential for the viability of bacteria (70-72). Thus, inhibition of FabI has been proposed an effective way to interfere with bacterial growth. The most noted FabI inhibitor is isoniazid (INH), a first-line antibiotic that has been used for anti-TB treatment for more than 60 years (73, 74). Mechanistic studies revealed that the antibacterial efficacy of INH depends on its activation by the mycobacterial catalase-peroxidase enzyme (KatG) to form an INH-$NAD^+$ adduct (75, 76) (**Figure 1.8** and **Figure 1.9**). The INH-$NAD^+$ adduct is a tight binding inhibitor of InhA, the enoyl-ACP reductase from *Mycobacterium tuberculosis*, with an overall *Ki* of 0.75 nM (77). However, clinical efficacy of INH is eroding because of the rapid emergence of drug

resistant bacteria. Further studies demonstrated that INH resistant *M. tuberculosis* has a mutated KatG protein which can no longer convert INH to the active $NAD^+$ adduct (78).

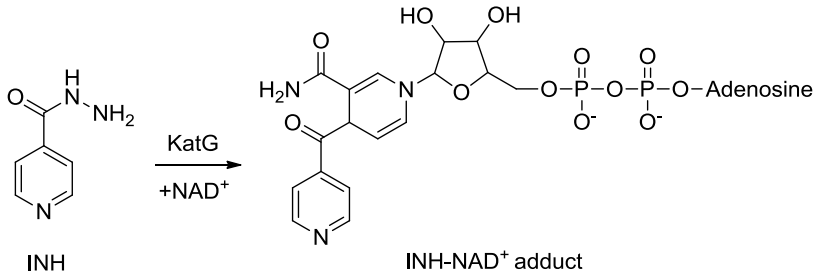


**Figure 1.8.** The mode of action of isoniazid (INH). Isoniazid acts as a prodrug that is activated by KatG in bacteria to form INH-$NAD^+$ adduct. In a drug resistant bacterial strain, a mutated KatG is not able to catalyze this activation.

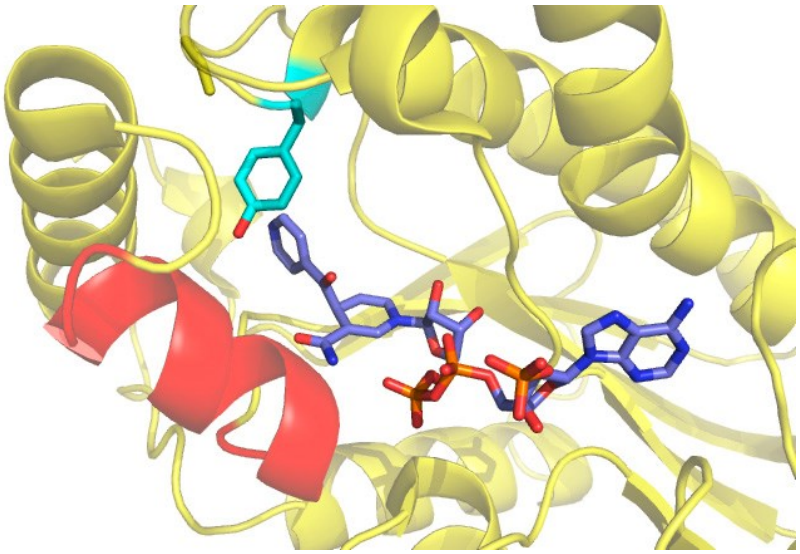

**Figure 1.9.** Structure of the INH-$NAD^+$ adduct binding to InhA (PDB: 2PR2).

Several new series of FabI inhibitors have been discovered based on high throughput screening (HTS) (**Table 1.2**). For example, GlaxoSmithKline screened over 300,000 compounds and identified a benzodiazepine derivative as a lead molecule (79). Following studies resulted in the discovery of four series of FabI inhibitors: imidazoles, indoles, acrylamides, and aminopyrodines (80-82). FabI inhibitors with diverse structures

have also been reported by different research institutes. Indole-piperazines, pyrazole-based compounds and pyrrolidine carboxamides were identified to have sub-micromolar $IC_{50}$ values (83). 2-Pyridone derivatives, developed by CrystalGenomics Inc., showed antibacterial activity against multiple pathogens including drug resistant strains (84). Potential FabI inhibitors have also been discovered during the antibacterial evaluations of natural products (**Table 1.3**). Aquastatin A, cephalochromine, curcumin and branched fatty acids have been reported to be active against *S. aureus* and *E. coli (85-88)*.

**Table 1.2.** Examples of synthetic FabI inhibitors.

| **Inhibitor** | **Structure** | **Bacterium** | **$IC_{50}$ (µM)** | **MIC (µg/ml)** |
|---|---|---|---|---|
| Acrylamides | | *S. aureus* | 0.004 | 0.008 |
| Aminopyridines | | *S. aureus* | 2.4 | 0.5 |
| Imidazoles | | *S. aureus* | 0.36 | 8 |
| Indoles | | *S. aureus* | 0.11 | 0.5 |
| 2-pyridones | | *S. aureus* | N/A[a] | 0.5 |
| Pyrazoles | | *M. tuberculosis* | N/A | 2.5 |

| | | | | |
|---|---|---|---|---|
| 4-pyridones | 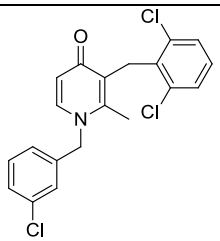 | *S. aureus* | 0.34 | 0.5 |
| Thiopyridines | 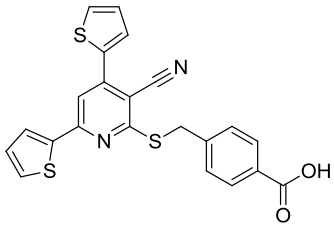 | *S. aureus* | 3 | 0.75 |

[a] N/A: not available.

**Table 1.3.** Examples of natural products as FabI inhibitors.

| Compound/Structure | Bacterium | $IC_{50}$ (μM) | MIC (μg/ml) |
|---|---|---|---|
| 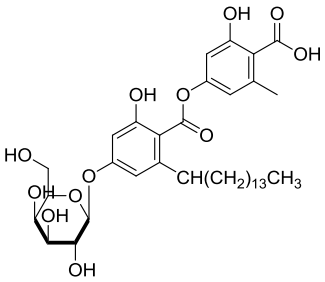 Aquastatin A | *S. aureus* | 3.2 | 32 |
| 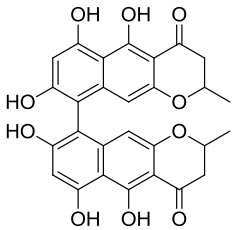 Cephalochromine | *S. aureus* | 1.9 | 8 |
| 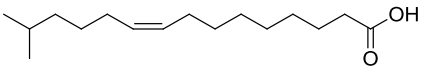 Methy-branched fatty acids | *S. aureus* | 16 | 32 |

| | | | |
|---|---|---|---|
| 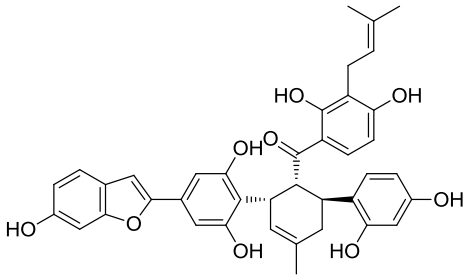 <br>Chalocomoracin | *S. aureus* | 5.5 | 4 |
| 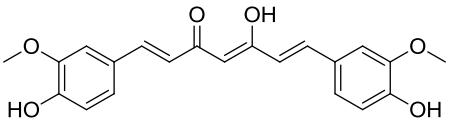 <br>Curcumin | *E. coli* | *Ki* = 15 μM | 74 |

Triclosan is a diphenyl ether-based compound and has been identified as a tight binding inhibitor of FabI from *E. coli* with a *Ki* value of 7 pM (89-92). Triclosan mimics the chemical structure of the INH-$NAD^+$ adduct (**Figure 1.10**). Being able to bypass the KatG-dependent activation, triclosan has been considered a possible alternative to INH toward drug resistant pathogens. Although triclosan was approved by FDA as an antibacterial additive only in soaps, toothpastes and mouth washes, it provides an excellent model to explore the interaction between FabI and small molecule inhibitors. Extensive SAR studies on diphenyl ether derivatives have been conducted in our lab as well as in other groups. Information from the crystal structure of FabI allows further chemical optimization (93, 94). Inhibitors of FabI from various pathogens have identified and showed tight binding affinities and inhibitory activity on bacterial growth (68, 95-97).

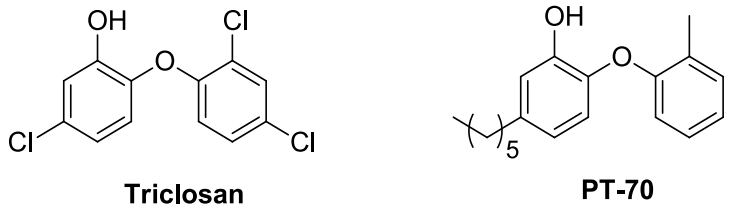


**Figure 1.10.** Structures of triclosan and a representative diphenyl ether-based FabI inhibitor previously synthesized by our group. This diphenyl ether-based scaffold mimics the structure of INH-NAD$^+$ adduct.

*Research project overview*

In this project, we will mainly focus on activity evaluation and mechanism exploration of novel antibacterial agents targeting the menaquinone biosynthesis pathway and the FAS-II pathway. In Chapter II, we will evaluate the *in vitro* and *in vivo* activity of a series MenB inhibitors against methicillin resistant *Staphylococcus aureus* (MRSA). We will also investigate the mode of action of these inhibitors by showing their specific effect on menaquinone biosynthesis. In Chapter III, we will demonstrate the effect of menaquinone on bacterial small colony variants (SCVs) phenotype by identifying a salvage pathway. In Chapter IV, we will evaluate the activity of a series of FabI inhibitors in a mouse model of MRSA. We aim to correlate the *in vivo* efficacy with residence time ($t_R$), and to demonstrate the importance of the kinetics of drug-target interaction in drug development. In Chapter V, we will investigate the *in vivo* biodistribution of FabI inhibitors using positron emission tomography (PET) technique.

**References:**


1. Dobson AP & Carper ER (1996) Infectious diseases and human population history - Throughout history the establishment of disease has been a side effect of the growth of civilization. *Bioscience* 46(2):115-126.
2. Wolfe ND, Dunavan CP, & Diamond J (2007) Origins of major human infectious diseases. *Nature* 447(7142):279-283.
3. Boyden SV & Australian Academy of Science. (1970) *The Impact of civilisation on the biology of man* (Australian National University Press, Canberra)
4. Cockburn TA (1971) Infectious diseases in ancient populations. *Current anthropology* 12:45-62.
5. Haensch S*, et al.* (2010) Distinct clones of Yersinia pestis caused the black death. *PLoS pathogens* 6(10):e1001134.
6. Bryk R, Lima CD, Erdjument-Bromage H, Tempst P, & Nathan C (2002) Metabolic enzymes of mycobacteria linked to antioxidant defense by a thioredoxin-like protein. *Science* 295(5557):1073-1077.
7. Ahmad S (2011) Pathogenesis, immunology, and diagnosis of latent Mycobacterium tuberculosis infection. *Clinical & developmental immunology* 2011:814943.
8. WHO (2014) WHO Global Tuberculosis Report 2013
9. McNeill WH (1978) Disease in history. *Social science & medicine* 12(2B):79-84.

10. Lindblad WJ (2008) Considerations for determining if a natural product is an effective wound-healing agent. *The international journal of lower extremity wounds* 7(2):75-81.

11. Kingston W (2008) Irish contributions to the origins of antibiotics. *Ir J Med Sci* 177(2):87-92.

12. Landsberg E (1949) Cerebral palsy; a public health problem. *Journal of the American Medical Women's Association* 4(8):338-340.

13. Bosch F & Rosich L (2008) The contributions of Paul Ehrlich to pharmacology: a tribute on the occasion of the centenary of his Nobel Prize. *Pharmacology* 82(3):171-179.

14. Fleming A (1955) The story of penicillin. *Bulletin. Georgetown University. Medical Center* 8(4):128-132.

15. Sykes R (2001) Penicillin: from discovery to product. *Bulletin of the World Health Organization* 79(8):778-779.

16. Pelaez F (2006) The historical delivery of antibiotics from microbial natural products--can history repeat? *Biochemical pharmacology* 71(7):981-990.

17. Wright GD (2007) The antibiotic resistome: the nexus of chemical and genetic diversity. *Nature reviews. Microbiology* 5(3):175-186.

18. Lowy FD (2003) Antimicrobial resistance: the example of Staphylococcus aureus. *The Journal of clinical investigation* 111(9):1265-1273.

19. WHO (2004) Use of antimicrobials outside human medicine and resultant antimicrobial resistance in humans.

20. Fleming A (1945) Penicillin. (Nobel Lecture).

21. Cohen ML (1992) Epidemiology of drug resistance: implications for a post-antimicrobial era. *Science* 257(5073):1050-1055.

22. Levy SB & Marshall B (2004) Antibacterial resistance worldwide: causes, challenges and responses. *Nature medicine* 10(12 Suppl):S122-129.

23. Payne DJ, Gwynn MN, Holmes DJ, & Pompliano DL (2007) Drugs for bad bugs: confronting the challenges of antibacterial discovery. *Nature reviews. Drug discovery* 6(1):29-40.

24. Fleischmann RD*, et al.* (1995) Whole-genome random sequencing and assembly of Haemophilus influenzae Rd. *Science* 269(5223):496-512.

25. Walsh C (2000) Molecular mechanisms that confer antibacterial drug resistance. *Nature* 406(6797):775-781.

26. McDevitt D & Rosenberg M (2001) Exploiting genomics to discover new antibiotics. *Trends in microbiology* 9(12):611-617.

27. Becker D*, et al.* (2006) Robust Salmonella metabolism limits possibilities for new antimicrobials. *Nature* 440(7082):303-307.

28. Wenzel RP (2004) The antibiotic pipeline--challenges, costs, and values. *N Engl J Med* 351(6):523-526.

29. Suttie JW (1985) Vitamin K-dependent carboxylase. *Annual review of biochemistry* 54:459-477.

30. Truglio JJ*, et al.* (2003) Crystal structure of Mycobacterium tuberculosis MenB, a key enzyme in vitamin K2 biosynthesis. *The Journal of biological chemistry* 278(43):42352-42360.

31. Bentinger M, Tekle M, & Dallner G (2010) Coenzyme Q--biosynthesis and functions. *Biochemical and biophysical research communications* 396(1):74-79.

32. Bishop DH, Pandya KP, & King HK (1962) Ubiquinone and vitamin K in bacteria. *The Biochemical journal* 83:606-614.

33. Haddock BA & Jones CW (1977) Bacterial respiration. *Bacteriological reviews* 41(1):47-99.

34. Bentley R & Meganathan R (1982) Biosynthesis of vitamin K (menaquinone) in bacteria. *Microbiological reviews* 46(3):241-280.

35. Meganathan R & Bentley R (1981) Biosynthesis of o-succinylbenzoic acid in a men- Escherichia coli mutant requires decarboxylation of L-glutamate at the C-1 position. *Biochemistry* 20(18):5336-5340.

36. Widhalm JR, van Oostende C, Furt F, & Basset GJ (2009) A dedicated thioesterase of the Hotdog-fold family is required for the biosynthesis of the naphthoquinone ring of vitamin K1. *Proceedings of the National Academy of Sciences of the United States of America* 106(14):5599-5603.

37. Shineberg B & Young IG (1976) Biosynthesis of bacterial menaquinones: the membrane-associated 1,4-dihydroxy-2-naphthoate octaprenyltransferase of Escherichia coli. *Biochemistry* 15(13):2754-2758.

38. Meganathan R (2001) Biosynthesis of menaquinone (vitamin K2) and ubiquinone (coenzyme Q): a perspective on enzymatic mechanisms. *Vitamins and hormones* 61:173-218.

39. Chen M, *et al.* (2013) Identification of a hotdog fold thioesterase involved in the biosynthesis of menaquinone in Escherichia coli. *J Bacteriol* 195(12):2768-2775.

40. Bentley SD, *et al.* (2002) Complete genome sequence of the model actinomycete Streptomyces coelicolor A3(2). *Nature* 417(6885):141-147.

41. Borodina I, Krabben P, & Nielsen J (2005) Genome-scale analysis of Streptomyces coelicolor A3(2) metabolism. *Genome research* 15(6):820-829.

42. Parkhill J, *et al.* (2000) The genome sequence of the food-borne pathogen Campylobacter jejuni reveals hypervariable sequences. *Nature* 403(6770):665-668.

43. Tomb JF, *et al.* (1997) The complete genome sequence of the gastric pathogen Helicobacter pylori. *Nature* 388(6642):539-547.

44. Marcelli SW, *et al.* (1996) The respiratory chain of Helicobacter pylori: identification of cytochromes and the effects of oxygen on cytochrome and menaquinone levels. *FEMS microbiology letters* 138(1):59-64.

45. Hiratsuka T, *et al.* (2008) An alternative menaquinone biosynthetic pathway operating in microorganisms. *Science* 321(5896):1670-1673.

46. Seto H, *et al.* (2008) Studies on a new biosynthetic pathway for menaquinone. *Journal of the American Chemical Society* 130(17):5614-5615.

47. Collins MD & Jones D (1981) Distribution of isoprenoid quinone structural types in bacteria and their taxonomic implication. *Microbiological reviews* 45(2):316-354.

48. Kobayashi K*, et al.* (2003) Essential Bacillus subtilis genes. *Proceedings of the National Academy of Sciences of the United States of America* 100(8):4678-4683.

49. Guest JR (1977) Menaquinone biosynthesis: mutants of Escherichia coli K-12 requiring 2-succinylbenzoate. *Journal of bacteriology* 130(3):1038-1046.

50. Dhiman RK*, et al.* (2009) Menaquinone synthesis is critical for maintaining mycobacterial viability during exponential growth and recovery from non-replicating persistence. *Molecular microbiology* 72(1):85-97.

51. Sassetti CM, Boyd DH, & Rubin EJ (2003) Genes required for mycobacterial growth defined by high density mutagenesis. *Molecular microbiology* 48(1):77-84.

52. Kurosu M & Begari E (2010) Vitamin K2 in electron transport system: are enzymes involved in vitamin K2 biosynthesis promising drug targets? *Molecules* 15(3):1531-1553.

53. Debnath J*, et al.* (2012) Discovery of selective menaquinone biosynthesis inhibitors against Mycobacterium tuberculosis. *Journal of medicinal chemistry* 55(8):3739-3755.

54. Kurosu M, Narayanasamy P, Biswas K, Dhiman R, & Crick DC (2007) Discovery of 1,4-dihydroxy-2-naphthoate [corrected] prenyltransferase

inhibitors: new drug leads for multidrug-resistant gram-positive pathogens. *Journal of medicinal chemistry* 50(17):3973-3975.

55. Li X*, et al.* (2010) Synthesis and SAR studies of 1,4-benzoxazine MenB inhibitors: novel antibacterial agents against Mycobacterium tuberculosis. *Bioorganic & medicinal chemistry letters* 20(21):6306-6309.

56. Fang M*, et al.* (2010) Succinylphosphonate esters are competitive inhibitors of MenD that show active-site discrimination between homologous alpha-ketoglutarate-decarboxylating enzymes. *Biochemistry* 49(12):2672-2679.

57. Lu X, Zhang H, Tonge PJ, & Tan DS (2008) Mechanism-based inhibitors of MenE, an acyl-CoA synthetase involved in bacterial menaquinone biosynthesis. *Bioorganic & medicinal chemistry letters* 18(22):5963-5966.

58. Lu X*, et al.* (2012) Stable analogues of OSB-AMP: potent inhibitors of MenE, the o-succinylbenzoate-CoA synthetase from bacterial menaquinone biosynthesis. *Chembiochem : a European journal of chemical biology* 13(1):129-136.

59. Chirala SS, Huang WY, Jayakumar A, Sakai K, & Wakil SJ (1997) Animal fatty acid synthase: functional mapping and cloning and expression of the domain I constituent activities. *Proceedings of the National Academy of Sciences of the United States of America* 94(11):5588-5593.

60. Payne DJ, Warren PV, Holmes DJ, Ji Y, & Lonsdale JT (2001) Bacterial fatty-acid biosynthesis: a genomics-driven target for antibacterial drug discovery. *Drug discovery today* 6(10):537-544.

61. Campbell JW & Cronan JE, Jr. (2001) Bacterial fatty acid biosynthesis: targets for antibacterial drug discovery. *Annual review of microbiology* 55:305-332.

62. White SW, Zheng J, Zhang YM, & Rock (2005) The structural biology of type II fatty acid biosynthesis. *Annual review of biochemistry* 74:791-831.

63. Heath RJ, White SW, & Rock CO (2001) Lipid biosynthesis as a target for antibacterial agents. *Progress in lipid research* 40(6):467-497.

64. Baldock C*, et al.* (1996) A mechanism of drug action revealed by structural studies of enoyl reductase. *Science* 274(5295):2107-2110.

65. Baldock C, Rafferty JB, Stuitje AR, Slabas AR, & Rice DW (1998) The X-ray structure of Escherichia coli enoyl reductase with bound NAD+ at 2.1 A resolution. *Journal of molecular biology* 284(5):1529-1546.

66. Roujeinikova A*, et al.* (1999) Inhibitor binding studies on enoyl reductase reveal conformational changes related to substrate recognition. *The Journal of biological chemistry* 274(43):30811-30817.

67. Rozwarski DA, Vilcheze C, Sugantino M, Bittman R, & Sacchettini JC (1999) Crystal structure of the Mycobacterium tuberculosis enoyl-ACP reductase, InhA, in complex with NAD+ and a C16 fatty acyl substrate. *The Journal of biological chemistry* 274(22):15582-15589.

68. Xu H*, et al.* (2008) Mechanism and inhibition of saFabI, the enoyl reductase from Staphylococcus aureus. *Biochemistry* 47(14):4228-4236.

69. Rozwarski DA, Grant GA, Barton DH, Jacobs WR, Jr., & Sacchettini JC (1998) Modification of the NADH of the isoniazid target (InhA) from Mycobacterium tuberculosis. *Science* 279(5347):98-102.

70. Zhang YM, White SW, & Rock CO (2006) Inhibiting bacterial fatty acid synthesis. *The Journal of biological chemistry* 281(26):17541-17544.

71. Heath RJ & Rock CO (1995) Enoyl-acyl carrier protein reductase (fabI) plays a determinant role in completing cycles of fatty acid elongation in Escherichia coli. *The Journal of biological chemistry* 270(44):26538-26542.

72. Bergler H, Fuchsbichler S, Hogenauer G, & Turnowsky F (1996) The enoyl-[acyl-carrier-protein] reductase (FabI) of Escherichia coli, which catalyzes a key regulatory step in fatty acid biosynthesis, accepts NADH and NADPH as cofactors and is inhibited by palmitoyl-CoA. *European journal of biochemistry / FEBS* 242(3):689-694.

73. Slayden RA, Lee RE, & Barry CE, 3rd (2000) Isoniazid affects multiple components of the type II fatty acid synthase system of Mycobacterium tuberculosis. *Molecular microbiology* 38(3):514-525.

74. Cohn DL (2000) Treatment of latent tuberculosis infection: renewed opportunity for tuberculosis control. *Clinical infectious diseases : an official publication of the Infectious Diseases Society of America* 31(1):120-124.

75. Suarez J*, et al.* (2009) An oxyferrous heme/protein-based radical intermediate is catalytically competent in the catalase reaction of

Mycobacterium tuberculosis catalase-peroxidase (KatG). *The Journal of biological chemistry* 284(11):7017-7029.

76. Zhang Y, Heym B, Allen B, Young D, & Cole S (1992) The catalase-peroxidase gene and isoniazid resistance of Mycobacterium tuberculosis. *Nature* 358(6387):591-593.

77. Rawat R, Whitty A, & Tonge PJ (2003) The isoniazid-NAD adduct is a slow, tight-binding inhibitor of InhA, the Mycobacterium tuberculosis enoyl reductase: adduct affinity and drug resistance. *Proceedings of the National Academy of Sciences of the United States of America* 100(24):13881-13886.

78. Ramaswamy SV*, et al.* (2003) Single nucleotide polymorphisms in genes associated with isoniazid resistance in Mycobacterium tuberculosis. *Antimicrobial agents and chemotherapy* 47(4):1241-1250.

79. Payne DJ*, et al.* (2002) Discovery of a novel and potent class of FabI-directed antibacterial agents. *Antimicrobial agents and chemotherapy* 46(10):3118-3124.

80. Heerding DA*, et al.* (2001) 1,4-Disubstituted imidazoles are potential antibacterial agents functioning as inhibitors of enoyl acyl carrier protein reductase (FabI). *Bioorganic & medicinal chemistry letters* 11(16):2061-2065.

81. Seefeld MA*, et al.* (2001) Inhibitors of bacterial enoyl acyl carrier protein reductase (FabI): 2,9-disubstituted 1,2,3,4-tetrahydropyrido[3,4-b]indoles

as potential antibacterial agents. *Bioorganic & medicinal chemistry letters* 11(17):2241-2244.

82. Miller WH*, et al.* (2002) Discovery of aminopyridine-based inhibitors of bacterial enoyl-ACP reductase (FabI). *Journal of medicinal chemistry* 45(15):3246-3256.

83. Kuo MR*, et al.* (2003) Targeting tuberculosis and malaria through inhibition of Enoyl reductase: compound activity and structural data. *The Journal of biological chemistry* 278(23):20851-20859.

84. Yum JH*, et al.* (2007) In vitro activities of CG400549, a novel FabI inhibitor, against recently isolated clinical staphylococcal strains in Korea. *Antimicrobial agents and chemotherapy* 51(7):2591-2593.

85. Wehrli W (1977) Kinetic Studies of Interaction between Rifampicin and DNA-Dependent Rna-Polymerase of Escherichia-Coli. *European Journal of Biochemistry* 80(2):325-330.

86. Wehrli W, Knusel F, & Staeheli.M (1968) Action of Rifamycin on Rna-Polymerase from Sensitive and Resistant Bacteria. *Biochemical and biophysical research communications* 32(2):284-8.

87. Stubbings W, Bostock J, Ingham E, & Chopra I (2006) Mechanisms of the post-antibiotic effects induced by rifampicin and gentamicin in Escherichia coli. *The Journal of antimicrobial chemotherapy* 58(2):444-448.

88. Yao J, Zhang Q, Min J, He J, & Yu Z (2010) Novel enoyl-ACP reductase (FabI) potential inhibitors of Escherichia coli from Chinese medicine monomers. *Bioorganic & medicinal chemistry letters* 20(1):56-59.

89. McMurry LM, Oethinger M, & Levy SB (1998) Triclosan targets lipid synthesis. *Nature* 394(6693):531-532.

90. Levy CW, *et al.* (1999) Molecular basis of triclosan activity. *Nature* 398(6726):383-384.

91. Sivaraman S, *et al.* (2004) Inhibition of the bacterial enoyl reductase FabI by triclosan: a structure-reactivity analysis of FabI inhibition by triclosan analogues. *Journal of medicinal chemistry* 47(3):509-518.

92. Ward WH, *et al.* (1999) Kinetic and structural characteristics of the inhibition of enoyl (acyl carrier protein) reductase by triclosan. *Biochemistry* 38(38):12514-12525.

93. Li HJ, *et al.* (2014) A Structural and Energetic Model for the Slow-Onset Inhibition of the Mycobacterium tuberculosis Enoyl-ACP Reductase InhA. *ACS chemical biology* 9(4):986-93.

94. Qiu X, *et al.* (1999) Molecular basis for triclosan activity involves a flipping loop in the active site. *Protein science : a publication of the Protein Society* 8(11):2529-2532.

95. Lu H, *et al.* (2009) Slow-onset inhibition of the FabI enoyl reductase from francisella tularensis: residence time and in vivo activity. *ACS chemical biology* 4(3):221-231.

96. am Ende CW, *et al.* (2008) Synthesis and in vitro antimycobacterial activity of B-ring modified diaryl ether InhA inhibitors. *Bioorganic & medicinal chemistry letters* 18(10):3029-3033.

97. Luckner SR, Liu N, am Ende CW, Tonge PJ, & Kisker C (2010) A slow, tight binding inhibitor of InhA, the enoyl-acyl carrier protein reductase from Mycobacterium tuberculosis. *The Journal of biological chemistry* 285(19):14330-14337.

## Chapter II. *In vitro* Activity, Cellular Mechanism, and *in vivo* Efficacy of 4-Oxo-4-Phenylbut-2-Enoate Compounds against *Staphylococcus aureus*

### Background

*Staphylococcus aureus and MRSA*

*Staphycoloccus aureus* (*S. aureus*) first identified in 1880 by a British surgeon Alexander Ogston, has been one of the prominent causative agents of infectious diseases (1-3). *S. aureus* is a Gram-positive bacterium that appears as grape-like clusters under a microscope. Although it is estimated that about 30% of people carry *S. aureus* as a commensal microorganism without developing symptoms, *S. aureus* is responsible for a variety of infections (staph infection) (4, 5). The most common staph infections are usually not life threatening, such as dermatitis, folliculitis and moderate surgical site infections (SSI). However, *S. aureus* is also the etiological agent of some serious, even fatal conditions including staph pneumonia, endocarditis, osteomyelitis and bacteremia (3, 6, 7). Transmission of this pathogen is primarily caused by direct skin-to-skin contact, and individuals with abnormal skin barrier or deficient immune system are at higher risk of being infected, such as long-term hospitalized patients. Each year, more than 1 million patients in the US healthcare facilities contract staph infection (8).

Treatment of staph infections with antibiotics was greatly successful because *S. aureus* was originally susceptible to most antibiotics that have been used in clinical practice (4, 9). This high susceptibility contributed to Alexander Fleming's fortunate discovery of penicillin (10). However, resistance to penicillin emerged only a few years after the introduction of this miracle drug into clinical practice (4, 11, 12). By the mid-

1950s, penicillin resistant *S. aureus* (PRSA) became prevalent in Europe and the US. To solve this problem, methicillin, an alternative to penicillin, was developed and was used to treat PRSA associated infections. In 1962, less than two years after the first clinical use of methicillin, methicillin resistant *S. aureus* (MRSA) was isolated in hospitals (13, 14). Currently, MRSA associated infection has become a surging problem worldwide. It is estimated that approximately 50% of the total *S. aureus* clinical isolates are resistant to methicillin (15, 16). Notably, MRSA is an iconic name and does not mean that the resistance is restricted to methicillin. In fact, most MRSA strains are impervious to multiple first-line antibiotics (**Figure 2.1**).

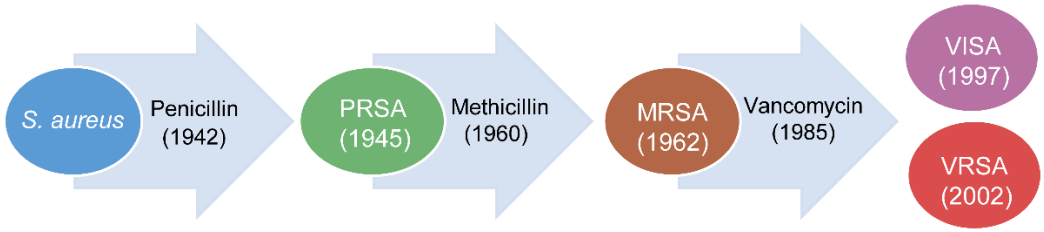


**Figure 2.1.** Evolution of drug resistance in *S. aureus*. The emergence of penicillin resistant *S. aureus* (PRSA), methicillin resistant *S. aureus* (MRSA) and vancomycin reisistant *S. aureus* (VRSA) occurs shortly after the clinical use of each antibiotic.

To treat life threatening MRSA infections, some second-line antibiotics are currently used including vancomycin, which is known as 'the drug of last resort' (16, 17). However, vancomycin has some limitations such as high nephrotoxicity / ototoxicity and requirement for intravenous administration (18, 19). Moreover, by the late 1990s, strains of vancomycin intermediate / resistant *S. aureus* (VISA / VRSA) were discovered, and were shown to be extensively drug resistant (**Figure 2.1**) (20-22).

Discovery of novel antibiotics has been completely outpaced by the emergence of drug resistance in *S. aureus* since the 'golden era of antibiotics' (23). Linezolid, one of few antibiotics approved by the FDA since 2000, was reported to be active against MRSA and VRSA (24-26). However, there is a huge gap between clinical needs and availability of chemotherapeutic options. Moreover, MRSA infection was originally considered an issue only in hospitals, but increasing evidence has suggested that MRSA has become the primary causative agent for both hospital acquired and community acquired infections (4, 27-29). Although staph infections are normally treatable in most cases, MRSA associated illnesses significantly raise the difficulty and the cost of treatment. According to an annual report from the Centers for Disease Control and Prevention (CDC), direct cost of treatments against MRSA infections in long-term hospitalized patients ranges from $10,500 to $111,000 per case (30). The widespread occurrence of MRSA has posted a potential danger for public health all over the world, and has generated great pressure to validate novel antibacterial targets.

*Previous work: discovery of a series of 4-oxo-4-phenylbut-2-enoate compounds as MenB inhibitors.*

As discussed in Chapter I, the menaquinone biosynthetic pathway in Gram-positive bacteria is thought to be a promising target for intervention. Previously, our lab worked on an enzyme in this pathway named 1, 4-dihydroxyl-2-naphthoyl-CoA synthase, or MenB (**Figure 2.2**). Extensive studies on MenB, such as mechanistic enzymology, structural analyses, and inhibitor developments, have been performed by former lab members (31-33).

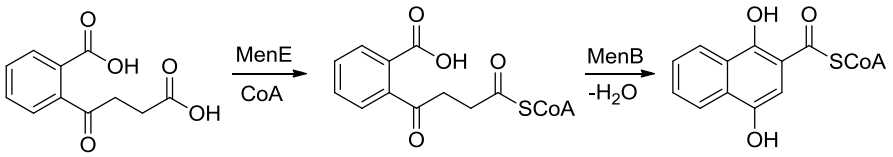


**Figure 2.2.** The MenB reaction in menaquinone biosynthesis pathway.

An effort to identify MenB inhibitors using high throughput screening (HTS) was carried out by Dr. Huaning Zhang and Dr. Xiaokai Li. After screening about 100,000 drug-like small molecules from a library of known bioactives and commercial compounds at the ICCB-Longwood Screening Facility at Harvard University Medical School, 455 hits were selected with at least 30% enzyme inhibition (34). A series of compounds, including 1548L21, were particularly attractive as they contain an *O*-succinylbenzoate (OSB) backbone and were considered potential leads to develop MenB inhibitors (**Figure 2.3**).

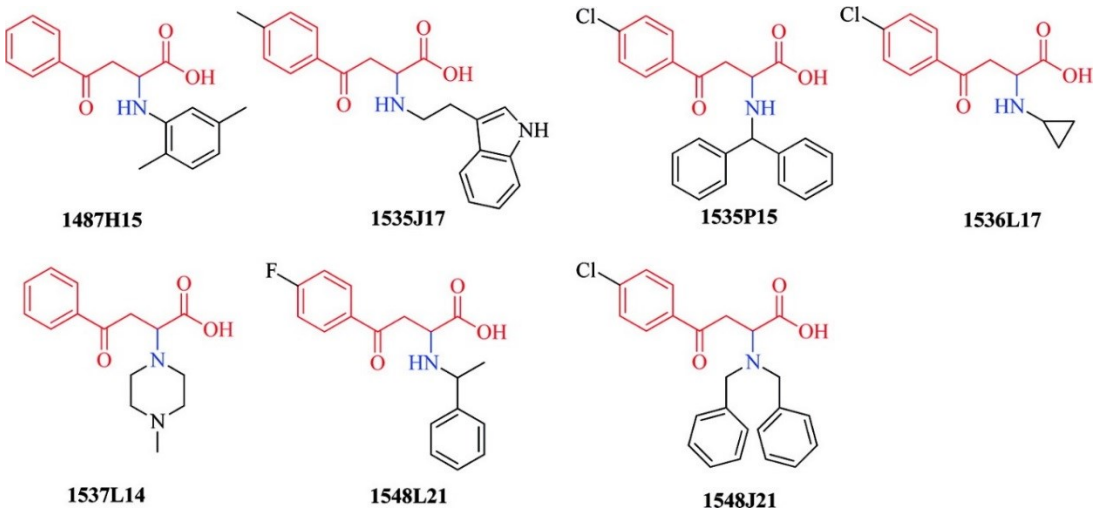


**Figure 2.3.** Representative structures of MenB hits identified by HTS. The OSB backbone shared by these molecules is highlighted in red.

Analogues of 1548L21 were subsequently synthesized, and were evaluated for inhibitory activity against MenB as well as for their whole cell antibacterial activity against *M. tuberculosis*. Several compounds showed good MenB inhibition with $IC_{50}$ values under 10 μM (**Table 2.1**). However, subsequent studies revealed that these MenB inhibitors are not stable in solution and can undergo a retro-Michael addition, yielding the corresponding (*E*)-benzoylacrylic acids (**Figure 2.4**). The observed decomposition weakened the potential of 1548L21 and its analogues as antibacterial candidates due to poor stability. However, the whole cell activity suggested that the resulting enoates, which have a Michael acceptor $C_2$=$C_3$ double bond inhibited bacterial growth. We hypothesized that the reactive $C_2$=$C_3$ double bond can form a Coenzyme A (CoA) adduct, which has a similar structure to OSB-CoA, and functions as a MenB inhibitor. Hence, a series of CoA adduct derivatives were synthesized and their $IC_{50}$ against MenB was determined by Dr. Nina Liu (**Table 2.2**). Consistent with our hypothesis, the CoA adducts were active MenB inhibitors with $IC_{50}$ values at μM or sub-μM levels (34). However, these adducts were not active against bacterial cells. This result was expected as the CoA structure made these compounds too hydrophilic to penetrate the bacterial membrane. In contrast, a series of 4-oxo-4-phenylbut-2-enoyl methyl esters exhibited whole cell activity against *M. tuberculosis* (34). This demonstrated that the butenoate compounds were able to penetrate into bacterial cells where they form adducts with CoA, and ultimately intervene with menaquinone biosynthesis and bacterial growth.

**Table 2.1**. *In vitro* activity of 1548L21 analogues.*

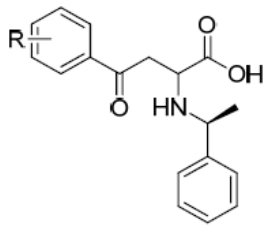


| Compound | R | $IC_{50}$ (μM) | MIC (μg/mL) |
|---|---|---|---|
| **1** | H | 112.1±10.6 | 6.25 |
| **2** | 4-F | 13.2±0.75 | 12.5 |
| **3** | 4-Cl | 8.54±0.80 | 50.0 |
| **4** | 4-Br | 105.4±15.0 | 12.5 |
| **5** | 4-$NO_2$ | >150 | 100 |
| **6** | 4-OMe | >150 | 12.5 |
| **7** | 2-F | 8.70±0.80 | 25.0 |
| **8** | 2-Cl | 8.50±0.80 | 50.0 |
| **9** | 2-Br | 0.60±0.07 | 12.5 |
| **10** | 2-I | 0.63±0.03 | 6.25 |
| **11** | 2-$NO_2$ | 2.10±0.22 | 12.5 |
| **12** | 2-$CF_3$ | 2.10±0.19 | 25.0 |
| **13** | 2-OMe | >150 | 12.5 |
| **14** | 3-Cl | >150 | 12.5 |
| **15** | 3-$NO_2$ | >150 | 100 |
| **16** | 2,4-diF | 1.40±0.18 | 6.25 |
| **17** | 2-Cl, 4-F | 1.10±0.08 | 12.5 |
| **18** | 2-Br, 4-F | 0.43±0.32 | 12.5 |
| **19** | 2-$CF_3$, 4-F | 0.82±0.09 | 12.5 |
| **20** | 2,4-diCl | 0.26±0.02 | 25.0 |
| **21** | 2,6-diCl | 7.11±0.11 | 1.56 |

* This work was performed by Dr. Nina Liu.

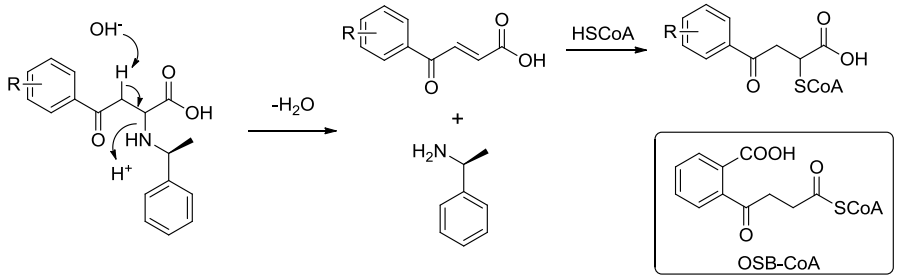


**Figure 2.4.** Mechanism of decomposition of the 1548L21 analogues. These compounds are unstable in solution and undergo a retro-Michael addition.

**Table 2.2.** MenB inhibition by the 2-CoA-4-oxo-4-phenylbutanoic acids.

| Compound | Structure | R | $IC_{50}$ (μM) |
|---|---|---|---|
| **7** | | 4-Cl | 0.47 |
| **8** | | 4-OMe | 33.5 |
| **9** | | 2-F | 0.20 |
| **10** | | 2-Cl | 0.10 |
| **11** | 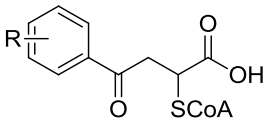 | 2-Br | 0.14 |
| **12** | | 2-I | 0.42 |
| **13** | | 2-$NO_2$ | 0.15 |
| **14** | | 2-OMe | 12.1 |
| **15** | | 3-Cl | 14.1 |
| **16** | | 2,4-Cl | 0.11 |

*Project overview*

The 4-oxo-4-phenylbut-2-enoate compounds were hypothesized to form CoA adducts in bacterial cells and subsequently inhibit MenB as a mechanism of their antibacterial activity. In this project, we first determined whole cell activity of the 4-oxo-

phenylbut-2-enoates against *S. aureus* and MRSA. Additionally, the spectrum of activity of the most potent compound was identified against various Gram-positive and Gram-negative pathogens by determining MIC values. We then explored the mode of action of the 4-oxo-phenylbut-2-enoates, especially the butenoyl methyl esters, by identifying whether the proposed CoA adduct forms in treated bacterial cells. We further validated the *in situ* mechanism of the 4-oxo-phenylbut-2-enoate compounds by determining menaquinone biosynthesis levels in *S. aureus* before and after drug treatments. To achieve this goal, an MS/MS-based method was applied. Finally, we evaluated the *in vivo* activity of the most potent 4-oxo-phenylbut-2-enoate compound in a mouse model of MRSA to explore its potential as an anti-MRSA candidate.

## Result and discussion

*In vitro activity of* the *4-oxo-4-phenylbut-2-enoate compounds against S. aureus and MRSA*

The activity of the butenoic acids and the corresponding butenoyl methyl esters were evaluated. *In vitro* activity was determined against MSSA (RN 4220) and MRSA (BAA 1762 and BAA 44) strains using a conventional microbroth dilution assay (35). The results are summarized in **Table 2.3** and **Table 2.4.** Several 4-oxo-4-phenylbut-2-enoyl methyl esters inhibited growth of *S. aureus* with MIC values under 8 µg/mL. Among the active compounds, M-8 was the most potent with an MIC of 0.35 µg/mL against MSSA. This is significant because the antibacterial activity of M-8 was comparable to some first-line antibiotics (**Table 2.5**). Moreover, the compounds exhibited similar activity against MRSA strains which are resistant to multiple antibiotics including oxacillin and erythromycin (**Table 2.5**). MIC values of M-8 against BAA 1762 and BAA 44 were found to be 0.75 and 1 µg/mL, respectively. This is important not only because MRSA accounts for more than 50% of total clinical isolates of *S. aureus* strains, but also because new chemotherapeutics against MRSA are urgently needed (36, 37). Significantly, several 4-oxo-4-phenylbut-2-enoyl methyl esters exhibited even better whole cell inhibition than vancomycin, which gave an MIC of 4 µg/mL. These data suggest that M-8 has potential to be developed as a novel anti-MRSA agent. Additionally, we observed that the 4-oxo-4-phenylbut-2-enoyl methyl esters have evidently better antibacterial activity than the corresponding butenoic acids. For example, the MIC of **A-8** against MSSA (16 µg/mL) was 32 fold higher than that of **M-8**. We propose that this was because the butenoyl methyl esters penetrate cell membranes better than their free acid counterparts.

**Table 2.3.** Antibacterial activity of the butenoyl methyl esters.

| Compound | Structure | R | MIC (μg/mL)[a] | | |
|---|---|---|---|---|---|
| | | | RN 4220[b] | BAA 44[c] | BAA 1762[c] |
| M-1 | | H | 32 | NA[d] | NA |
| M-2 | | 2-OMe | 128 | NA | NA |
| M-3 | | 4-OMe | NA | NA | NA |
| M-4 | | 2-F | 4 | 8 | 8 |
| M-5 | | 4-F | 8 | 8 | 12 |
| M-6 | | 2-Cl | 2 | 4 | 8 |
| M-7 | | 3-Cl | 16 | 24 | 16 |
| M-8 | | 4-Cl | 0.35 | 1 | 0.75 |
| M-9 | | 2-Br | 8 | 8 | 8 |
| M-10 | | 4-Br | 8 | 16 | 16 |
| M-11 | | 2-I | 8 | 16 | 24 |
| M-12 | | 2-$CF_3$ | 4 | 8 | 8 |
| M-13 | | 2-$NO_2$ | 4 | 4 | 8 |
| M-14 | | 3-$NO_2$ | 12 | 16 | 32 |
| M-15 | | 4-$NO_2$ | 4 | 8 | 4 |
| M-16 | | 2,4-F | 4 | 4 | 4 |
| M-17 | | 2,4-Cl | 1 | 3 | 2 |
| M-18 | | 2-Cl, 4-F | 2 | 2 | 4 |
| M-19 | | 2-Br, 4-F | 4 | 4 | 4 |

[a] The MIC values were tested in duplicate and were presented as mean values.

[b] MSSA strain

[c] MRSA strain

[d] not active, MIC>128 μg/mL

**Table 2.4**. Antibacterial activity of the butenoic acids.

| Compound | Structure | R | MIC (μg/mL)[a] | | |
|---|---|---|---|---|---|
| | | | RN 4220[b] | BAA 44[c] | BAA 1762[c] |
| A-1 | | H | NA[d] | NA | NA |
| A-2 | | 2-OMe | NA | NA | NA |
| A-3 | | 4-OMe | NA | NA | NA |
| A-4 | | 2-F | 24 | 32 | 32 |
| A-5 | | 4-F | 16 | 24 | 32 |
| A-6 | | 2-Cl | 16 | 16 | 32 |
| A-7 | | 3-Cl | 64 | 64 | 64 |
| A-8 | | 4-Cl | 16 | 32 | 24 |
| A-9 | | 2-Br | 24 | 32 | 32 |
| A-10 | | 4-Br | 32 | 32 | 32 |
| A-11 | | 2-I | 32 | 64 | 48 |
| A-12 | | 2-$CF_3$ | 32 | 32 | 32 |
| A-13 | | 2-$NO_2$ | 16 | 32 | 32 |
| A-14 | | 3-$NO_2$ | 32 | 64 | 32 |
| A-15 | | 4-$NO_2$ | 32 | 32 | 32 |
| A-16 | | 2,4-F | 24 | 32 | 32 |
| A-17 | | 2,4-Cl | 12 | 24 | 16 |
| A-18 | | 2-Cl, 4-F | 12 | 16 | 32 |
| A-19 | | 2-Br, 4-F | 16 | 16 | 24 |

[a] The MIC values were tested in duplicate and were presented as mean values.
[b] MSSA strain
[c] MRSA strain
[d] not active, MIC>128 μg/mL

**Table 2.5.** Comparative *in vitro* antibacterial efficacy of M-8 and several first-line antibiotics against MSSA and MRSA.

| Antibiotic | MIC (μg/mL)[a] | | |
|---|---|---|---|
| | RN 4220[b] | BAA 44[c] | BAA 1762[c] |
| 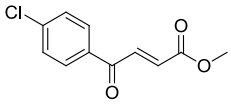 M-8 | 0.35 | 1 | 0.75 |
| Penicillin | 0.1 | NA[d] | NA |
| Oxacillin | 0.1 | NA | NA |
| Erythromycin | 0.15 | NA | NA |
| Vancomycin | 2 | 4 | 4 |

[a] The MIC values were tested in duplicate and were presented as mean values.
[b] MSSA strain
[c] MRSA strain
[d] not active, MIC>128 μg/mL

*Antibacterial spectrum of M-8*

In the previous section, we demonstrated that the 4-oxo-4-phenylbut-2-enoates were active against *S. aureus*, with compound M-8 being the most potent. We then determined the spectrum of activity of M-8 towards other microorganisms. In order to explore the mechanism of action of this compound, we evaluated its activity against bacteria which differ in whether they use menaquinone or ubiquinone for respiration. This included the menaquinone utilizing bacteria *Enterococcous faecalis* (*E. faecalis*), *Enterococcus faecium* (*E. faecium*) and *Mycobacterium smegmatis*, and the ubiquinone utilizing Gram-negative bacteria *Klebseilla pneumoniae* (*K. pneumoniae*), *Pseudomonas aeruginosa* (*P. aeruginosa*) and *Proteus mirabilis* (*P. mirabilis*) *(38, 39)*. As shown in **Table 2.6**, M-8 was active against all Gram-positive bacteria with better activity than several first line antibiotics. For example, the MIC of M-8 for *E. faecalis* was 16 fold and

6 fold lower than that of oxacillin and vancomycin. This is important because *Enterococci*, although usually considered commensal in human intestine, are known for their intrinsic resistance and can cause severe infections such as endocarditis or septicemia (40-42). Additionally, M-8 was active against *M. smegmatis* with an MIC of 1 μg/mL. This is consistent with our previous study in which the MIC of M-8 against *M. tuberculosis* was observed to be 0.64 μg/mL (34). Although not typically categorized as Gram-positive bacteria, *Mycobacterial species*, which also synthesize and use menaquinone, were inhibited by our MenB inhibitors. In contrast, **M-8** showed no activity towards Gram-negative bacteria up to a concentration of 128 μg/mL, suggesting that this compound is only active against menaquinone-utilizing organisms. Taken together, the spectrum of activity is consistent with our hypothesis that menaquinone biosynthesis is essential for the viability of Gram-positive bacteria and Mycobacterial species, and menaquinone biosynthesis is a promising antibacterial target in multiple pathogens.

**Table 2.6.** MIC values of M-8 and clinical antibiotics against various bacteria.

| | Type of quinone | MIC (μg/mL)[a] | | | | |
|---|---|---|---|---|---|---|
| | | M-8 | Penicillin | Oxacillin | Vancomycin | Polymyxin B |
| MSSA | menaquinone | 0.5 | 0.1 | NA | 4 | |
| MRSA | | 0.75 | NA | NA | 4 | |
| *E. faesalis* | | 4 | 48 | 64 | 24 | |
| *E. faecium* | | 6 | 48 | 48 | 16 | |
| *M. smegmatis* | | 1 | | | | |
| *K. pneumoniae* | ubiquinone | NA[b] | NA | NA | 24 | 4 |
| *P. aeruginosa* | | NA | NA | NA | 32 | 2 |
| *P. mirabilis* | | NA | | | | |

[a] The MIC values were tested in duplicate and were presented as mean values.
[b] not active, MIC>128 μg/mL

*Mode of action of **M-8**: hydrolysis and CoA adduct formation in S. aureus cells*

Although the 4-oxo-4-phenylbut-2-enoate compounds were shown to be active against whole bacteria, their mode of action has not been clarified. As mentioned previously, these Michael acceptor molecules were proposed to form CoA adducts in bacterial cells, which subsequently inhibit MenB enzyme and interfere with bacterial growth (**Figure 2.5**). In this section, efforts to probe our 'prodrug' hypothesis will be discussed.

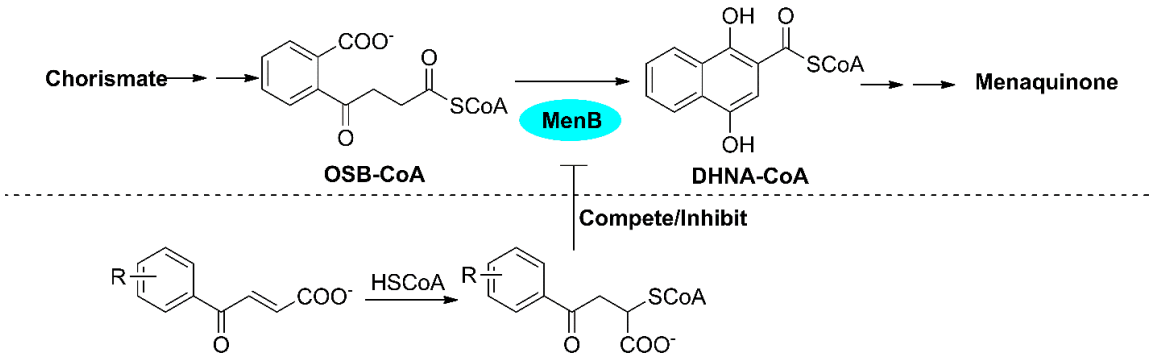


**Figure 2.5.** The proposed mode of action of 4-oxo-4-phenylbut-2-enoates. The a 4-oxo-4-phenylbut-2-enoyl methyl ester is hypothesized to penetrate into bacterial cells where it is hydrolyzed and forms adduct with coenzyme A.

The Michael acceptor double bond, which provides the reaction site for CoA addition, is critical for the proposed antibacterial activity of the 4-oxo-4-phenylbut-2-enoates. Thus, we first tested the MIC value of M-8-$H_2$ against MSSA and MRSA. M-8-$H_2$ is an analogue of the most potent butenoyl methyl ester M-8 in which the key $C_2$-$C_3$ bond is saturated. Consistent with our hypothesis, M-8-$H_2$ had no activity against *S. aureus*

up to a concentration of 256 µg/mL (**Figure 2.6**), indicating the importance of the $C_2$=$C_3$ double bond for antibacterial activity.

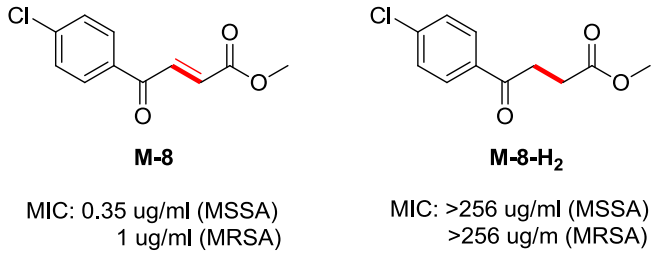


**Figure 2.6.** The structure of M-8 and its analogue M-8-$H_2$. The key $C_2$-$C_3$ bonds were highlighted. The MIC values against MSSA and MRSA were shown.

To directly approach the mode of action of the 4-oxo-4-phenylbut-2-enoates, we subsequently used a MALDI-based method to investigate the fate of M-8 in bacterial cells. Briefly, pre-cultured *S. aureus* cells were co-incubated with M-8 and the cell pellets were subsequently collected and disrupted. MALDI-TOF was then applied to analyze cell extracts for the presence of metabolites derived from M-8. To get a better insight, this experiment was performed using a 50:50 mixture of M-8 and a [2,3,5,6-D4] isotopologue, M-8-$d_4$. The result is shown in **Figure 2.7.** While no peaks were observed between 960-1000 Da in the mass spectrum of samples obtained from untreated cells, a pair of peaks was detected at 978 / 982 Da following treatment with M-8 / M-8-$d_4$. This species was clearly derived from M-8 as not only were two peaks observed differing by 4 Da which is a result of using the D4-isotopologue, but the parent ions also had a second peak at +2 Da that has an intensity equaled to 1/3 of that of the major peak, consistent with the presence of Cl that has two major isotopes ($^{35}$Cl and $^{37}$Cl) in the molecule. Our conclusion was confirmed by comparing the spectrum to that acquired from CoA adduct synthesized in solution (**Figure 2.7**).

Interestingly, this mass corresponded to that expected for the CoA adduct formed from M-8 in which the methyl ester has been hydrolyzed. In contrast, the methyl ester addition product (theoretical M+1= 992 Da) was not detected. Such a result is reasonable given that the conversion of carboxylates to esters is a widely used prodrug strategy to improve drug stability and cell penetration (43, 44). A similar experiment was then conducted in *S. aureus* with the butenoic acid compound A-8. Although the addition between CoA and A-8 occurred rapidly in solution, no CoA adduct was detected in cell extracts from treated bacteria, suggesting that the butenoic acid compounds had limited cell penetration. This also explained why the MIC values of the butenoic acids were at least 16 fold higher in comparison to the corresponding methyl esters. Taken together, we determined the importance of the Michael acceptor double bond for the antibacterial activity of the 4-oxo-4-phenylbut-2-enoates. We further probed the *in situ* mode of action of M-8 and demonstrated that this compound penetrated into *S. aureus* cells where it hydrolyzed and formed an adduct with CoA.

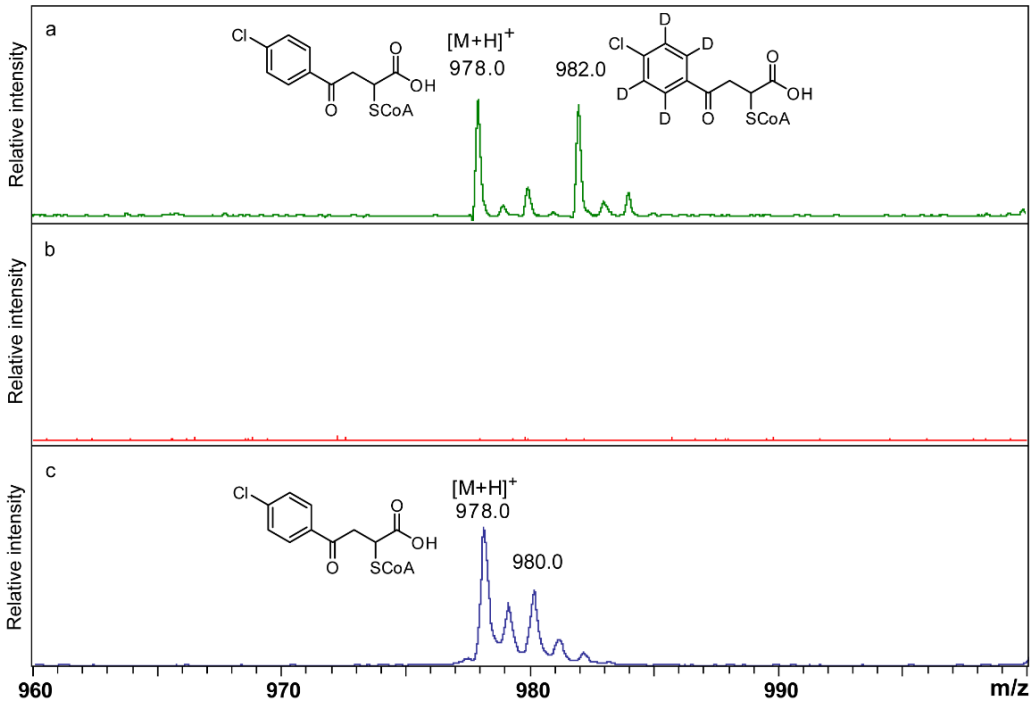


**Figure 2.7.** The MALDI-TOF spectra acquired from treated bacteria (a), untreated bacteria (b) and CoA adduct standard (c). The spectrum of the treated bacteria was shown in additive mode due to low signal response.

*Cellular inhibitory mechanism of the 4-oxo-4-phenylbut-2-enoates: the effect on menaquinone biosynthesis in S. aureus*

Although canonical antibacterial assay data (MIC) can demonstrate drug activity on a whole cell level, it does not provide information regarding cellular inhibitory mechanism of the tested agents, which is very important for drug evaluation and further optimization. To confirm a specific effect on menaquinone biosynthesis, we determined menaquinone levels in *S. aureus* cells using an APCI-MS/MS-based method before and after drug treatment. In this section, the identification / quantification of menaquinone will be discussed.

We first conducted a complementation experiment that is commonly used to demonstrate on-target activity. In brief, we determined the susceptibility of *S. aureus* to several 4-oxo-4-phenylbut-2-enoyl methyl esters with or without dihydroxyl naphthoic acid (DHNA) supplementation. DHNA is a downstream product of MenB and has been previously used to rescue bacteria treated with drugs targeting menaquinone biosynthesis (45, 46). The result is summarized in **Table 2.7.** Activity of the control drug (oxacillin) was not affected by the addition of DHNA. In contrast, bacteria treated with M-4, M-8 and M-17 at 5 × MIC were viable after DHNA complementation. This suggests that menaquinone biosynthesis was the target of the butenoyl methyl esters.

**Table 2.7.** Viability of drug treated *S. aureus* before and after DNHA complementation

| Compound | MIC (μg/mL) | Complement | Viability at 5×MIC (DHNA-) | Viability at 5×MIC (DHNA 50 μg/mL) |
|---|---|---|---|---|
| M-4 | 4 | | -[a] | +[b] |
| M-8 | 0.5 | 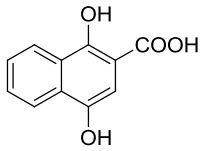 | - | + |
| M-17 | 1 | | - | + |
| Oxacillin | 0.1 | | -[c] | -[c] |

[a] $OD_{600}$ value < 0.3
[b] $OD_{600}$ value > 0.3
[c] bacteria were not viable at 2×MIC with or without DHNA

In order to validate the cellular mechanism of the 4-oxo-4-phenylbut-2-enoyl methyl esters, we used a MS/MS-based method to investigate menaquinone biosynthesis levels in *S. aureus* before and after drug treatment. Although mass spectrometry (MS) has been extensively used to identify cellular metabolites (47-49), it was thought to be challenging to analyze cellular menaquinone levels using this method since MS is usually

used in combination with HPLC and bacteria synthesize a series of menaquinone species differing in length of isoprenyl chain. Separation of these extremely hydrophobic molecules is difficult and potential overlap between the different species could cause problems quantifying menaquinone levels. Therefore, we applied an APCI-MS/MS-based method in which menaquinone identification is performed using a secondary ionization (50, 51).

The parent ion and daughter ion of MK-4, which formed during primary ionization and secondary ionization, respectively, were identified (**Figure 2.8).** The result suggested that the 'M+1' ion further fragmented into a fragment ion with a mass of 187. The daughter ion was rationalized as a protonated dimethyl naphthoquinone. As summarized in **Table 2.8**, each menaquinone species formed a specific 'M+1' parent ion and a same 187 daughter ion, which allowed species identification by monitoring separate ion transitions. MS/MS also provided an approach to quantitate menaquinone levels. A calibration curve was generated by plotting the intensity of ion transitions as a function of menaquinone concentration (**Figure 2.9**). The result showed a linear correlation ($R^2 > 0.99$), indicating the reliability of this method. When analyzing cell extracts, the intensity of the ion transition signals was compared with the calibration curve and the corresponding menaquinone concentration was subsequently calculated.

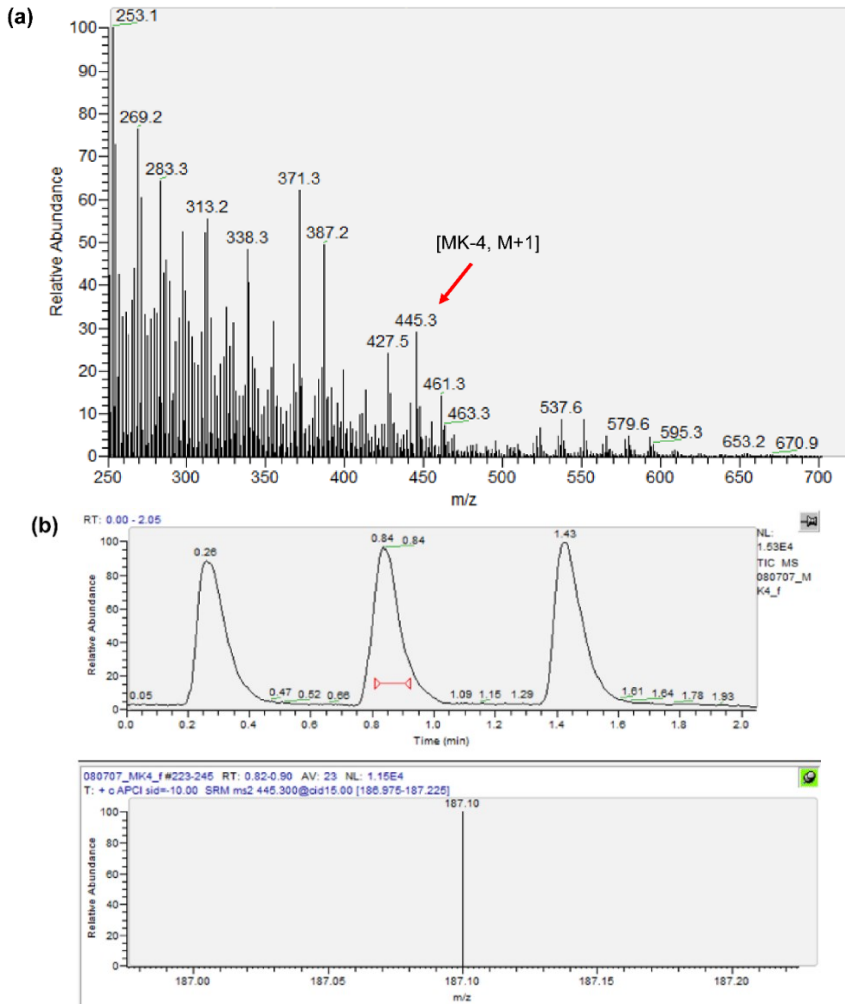


**Figure 2.8**. Mass spectra from (a) the primary ionization and (b) the secondary ionization of MK-4.

**Table 2.8.** Primary and secondary ionization of different menaquinone species (MK-n).

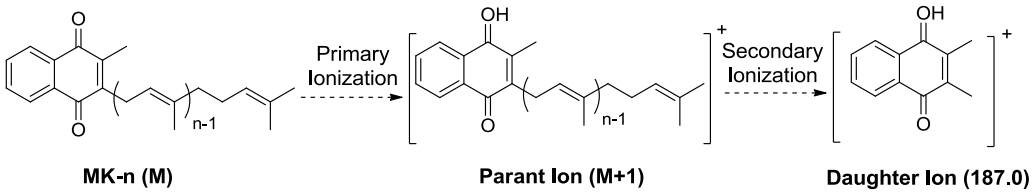


| Compound | Parent ion (M+1) | Daughter ion |
|---|---|---|
| MK-4 | 445 | 187 |
| MK-5 | 513 | 187 |
| MK-6 | 581 | 187 |

| | | |
|---|---|---|
| MK-7 | 649 | 187 |
| MK-8 | 717 | 187 |
| MK-9 | 785 | 187 |

The primary ion and the daughter ion of menaquinone species are rationalized as a protonated menaquinone and a protonated 2,3-dimehtyl-1,4-naphthoquinone. The corresponding ions of each menaquinone species are shown in the table.

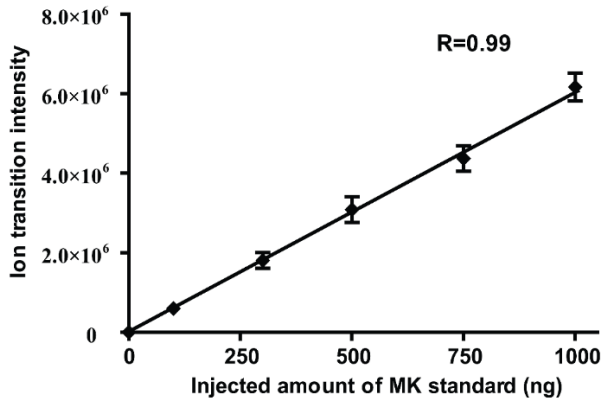


**Figure 2.9.** Quantitation of menaquinone. Menaquinone calibration curve is generated with MK-4 standard. The error bars represent the SEM (n=5).

To investigate menaquinone biosynthesis levels in bacterial cells, we used a liquid-liquid extraction method. (52, 53). As a control, extraction efficiency was determined by spiking menaquinone standard into a buffer solution and cell culture, respectively. The result suggested that 91 ± 4% of menaquinone can be recovered from buffer while 80 ± 5% can be extracted from bacterial cells.

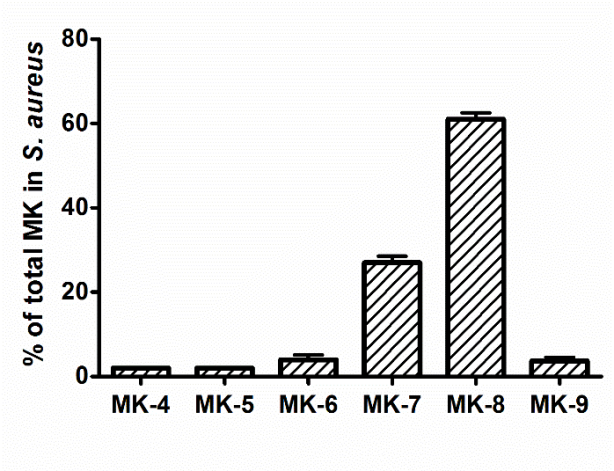


**Figure 2.10**. Distribution of menaquinone (MK-n) in *S. aureus*. Each MK species is shown as a percentage of the total MK content. The Error bars represent SEM.

We first identified the distribution of menaquinone in untreated *S. aureus*. As shown in **Figure 2.10**, a series of menaquinone species, from MK-4 to MK-9, were detected. This observation is consistent with previously reported MK composition in this organism (54). We noted that MK-8 was the most abundant species, which comprised over 60% of the total menaquinone in *S. aureus*. Thus, when investigating menaquinone levels in treated cells, we compared MK-8 concentration with that observed in untreated bacteria. RN4220 cells were then co-incubated with different antibacterial agents, including two butenoyl methyl ester MenB inhibitors M-8 and M-17, and two clinical antibiotics oxacillin and vancomycin. As shown in **Figure 2.11**, MK-8 concentration was significantly reduced 76 ± 4.6 % ($P < 0.005$) and 65 ± 6.5 % ($P < 0.005$) in *S. aureus* treated with M-8 and M-17 at 1/2 MIC concentrations, respectively. In contrast, although this MSSA strain (RN4220) is susceptible to oxacillin and vancomycin, menaquinone biosynthesis was not significantly affected by treatments of these two drugs, which only reduced MK-8 concentration by 8% and 2% ($P > 0.1$). This result was expected since these antibiotics do not target menaquinone biosynthesis in bacteria. Moreover, we observed that M-8 and M-

17 inhibited the biosynthesis of all menaquinone species and the proportion of each component remained the same as in wild type *S. aureus* (**Figure 2.12**). These data further support our hypothesis that menaquinone biosynthesis is the antibacterial target of the 4-oxo-4-phenyl-2-butenoyl esters. We then extended this experiment to MRSA. Consistently, MK-8 concentration decreased 81% and 67% in M-8 and M-17 treated bacteria, respectively, whereas vancomycin exhibited only a minimal effect on menaquinone levels (**Figure 2.13**).

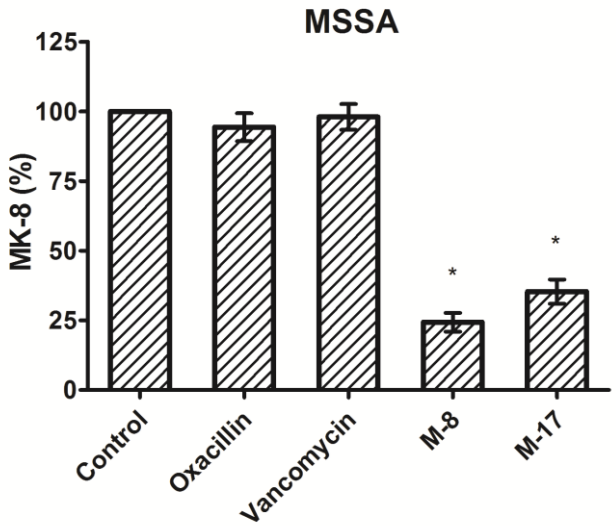


**Figure 2.11**. MK-8 concentration in drug treated *S. aureus* (MSSA, RN4220), in comparison to that in untreated bacteria. Decrease of menaquinone biosynthesis in M-8 and M-17 treated bacteria is significant. *P value < 0.005.

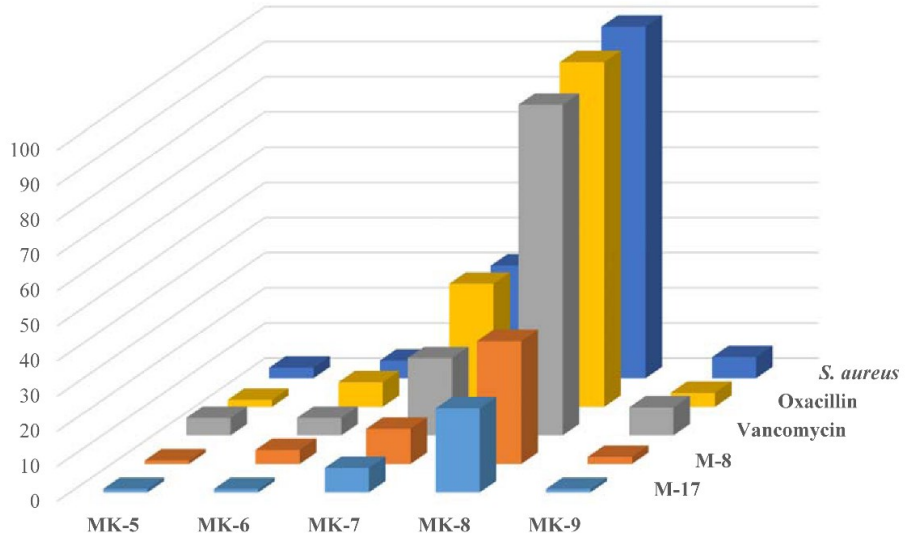


**Figure 2.12**. Inhibition of all menaquinone species in drug treated bacteria (MSSA, RN4220). Each component was shown as a percentage of MK-8 concentration in control. The distribution of menaquinone species in treated *S. aureus* cells remains the same.

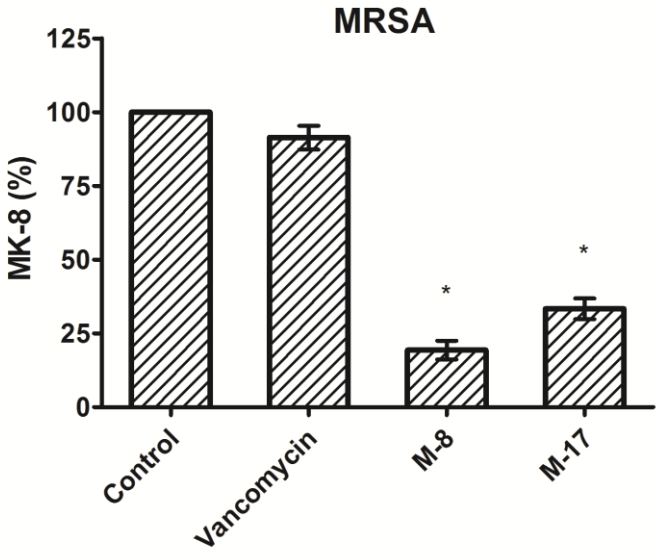


**Figure 2.13**. MK-8 concentration in drug treated MRSA cells, in comparison to that in untreated bacteria. Decrease of menaquinone biosynthesis in M-8 and M-17 treated bacteria is significant. * P value < 0.005.

To explore the correlation between the antibacterial activity and menaquinone biosynthesis inhibition, we determined menaquinone levels in bacterial cells treated with escalating concentrations of M-8. As shown in **Figure 2.14**, MK-8 level decreased 27%, 61% and 76% in *S. aureus* cells treated with M-8 at concentrations of 1/5, 1/3 and 1/2 the MIC. This dose dependent change supports the notion that menaquinone biosynthesis is the cellular target of M-8 in *S. aureus*. Taken together, although we cannot completely eliminate the possibility of off-target effects, our results suggest that the 4-oxo-4-phenylbut-2-enoates inhibit bacterial growth *via* a specific on-target cellular mechanism.

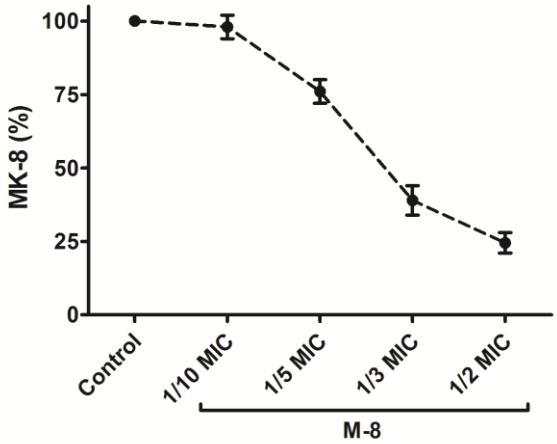


**Figure 2.14**. Decrease of MK-8 concentration in treated bacteria (MSSA, RN4220) cells in response to escalating doses of M-8 treatment.

*In vivo antibacterial activity of M-8 in a mouse model of MRSA*

The excellent antibacterial activity of the 4-oxo-4-phenylbut-2-enoyl methyl esters against MRSA indicated the potential of these compounds, especially M-8, as novel antibacterial agents. Consequently, we evaluated the *in vivo* efficacy of M-8 in two mouse models of MRSA: a systemic infection model and a thigh infection model. Previously, the cytotoxicity of M-8 has been determined with Vero cells and the selective index (SI) of

this compounds against *S. aureus* over mammalian cells was demonstrated to be greater than 30 (34). This suggested that M-8 is a suitable candidate for *in vivo* studies.

Systemic infection. A systemic infection model is widely used in preclinical studies to evaluate antibacterial agents (55, 56). We first determined the lethal dose of BAA 1762 (MRSA) strain in Swiss Webster mice. As shown in **Figure 2.15**, we selected $2\times10^7$ CFU/mouse as the inoculum size in this study because it was the lowest dose to kill 100% of the infected mice.

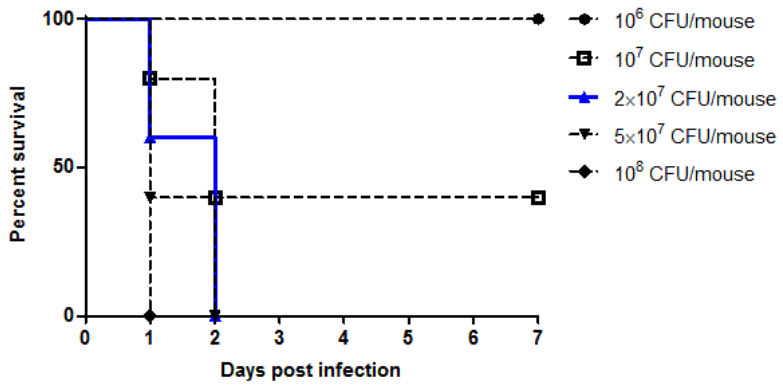


**Figure 2.15**. systemic infection with different doses of *S. aureus* BAA 1762 in Swiss Webster mice.

The infected mice were treated with oxacillin, vancomycin and M-8. Notably, M-8 has poor solubility in aqueous solution due to its lipophilicity. Thus, a vehicle comprising saline, ethanol and PEG-400 (40:40:20) was used for drug administration. The infected animals were monitored for seven days after treatment and the survival is depicted in **Figure 2.16**. All MRSA infected mice that received vehicle alone died within two days resulting in an average survival time of 1.4 ± 0.25 days (± standard error of the mean, SEM). As expected, oxacillin treatment failed to rescue the infected mice, given an average survival time of 1.6 ± 0.25 days. In contrast, 70% of mice treated with M-8 survived at

least two days after infection and the overall mortality at the end of the seven-day experiment was reduced from 100% to 50%. Additionally, the average survival time of M-8 treated mice significantly increased to 4.6 ± 0.87 days, demonstrating the *in vivo* efficacy of this compound. However, although M-8 exhibited better *in vitro* activity against MRSA than vancomycin, it was not as effective as vancomycin against this lethal MRSA infection in mice. As the positive control, vancomycin treatment led to a mortality of 20% and an average survival time of 5.8 ± 0.81 days.

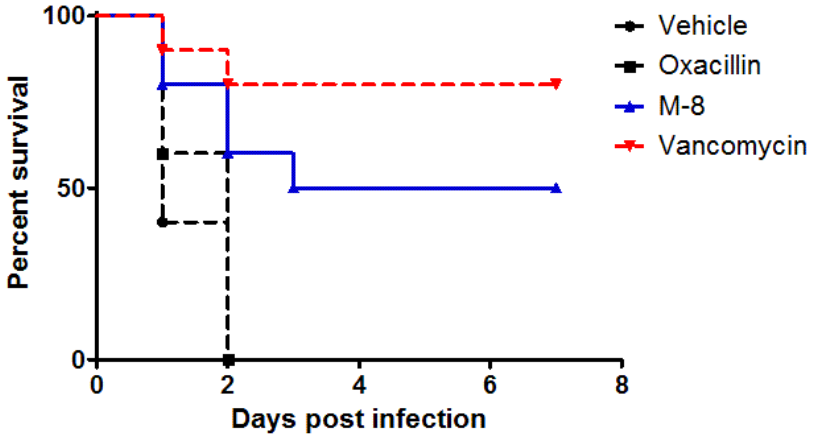


**Figure 2.16**. Survival of infected mice after received treatments of vehicle (n=5), oxacillin (n=5), M-8 (n=10) and vancomycin (n=10).

Thigh infection. We further investigated the antibacterial activity of M-8 using a thigh infection model. The thigh infection model has been widely used to evaluate *in vivo* antibacterial activity of drugs against *S. aureus*, which is the primary causative agent of soft tissue infections (57-59). In previous reports, animals were rendered neutropenic by injecting cyclophosphamide (CPA). This was because a relatively small inoculation dose was used in this model, and immunocompetent mice could protect themselves from this moderate infection, causing errors when evaluating drug efficacy. Thus, pre-treatment with

CPA is used to compromise the mouse immune system (60, 61). We first tested the effect of CPA treatment on *in vivo* MRSA growth. As shown in **Figure 2.17**, bacteria grew significantly faster in neutropenic mice than in healthy mice. In addition, bacterial growth rate varied significantly in mice that were not rendered neutropenic with CPA.

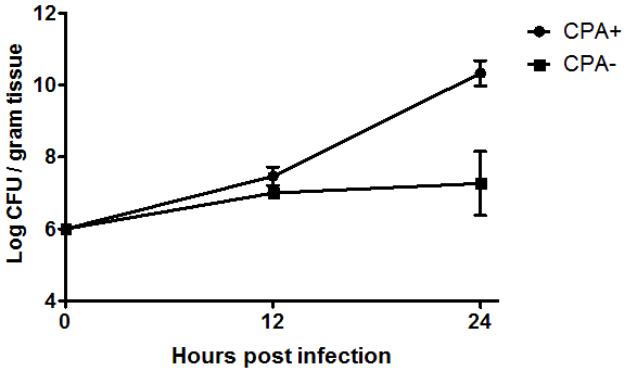


**Figure 2.17**. Bacterial growth in thigh muscle in neutropenic mice (CPA+, n=3) and immune competent mice (CPA-, n=3).

To evaluate the antibacterial activity of the MenB inhibitors, neutropenic mice were infected with MRSA, followed by dosing with M-8 (100 mg/kg, SC) and control antibiotics. Bacterial burden in the thigh muscle was determined 24 hours post infection by CFU counting. The result is shown in **Figure 2.18**. In comparison to the vehicle control group, oxacillin demonstrated only minimal activity, reducing bacterial load by 0.29 log CFU / gram tissue. In contrast, M-8 exhibited significant anti-MRSA activity, resulting in a decrease of bacterial burden of 3.1 log CFU/gram tissue. Such a reduction of bacterial burden is significantly as the P value, which is calculated by one tail T test, is less than 0.005. We then performed a dose escalating study on this compound. As depicted in **Figure 2.18**, a dose dependent effect was observed in M-8 treated mice, in which efficacy was seen with doses as low as 25 mg/kg. Compared to the vehicle control, bacterial load was

reduced 0.9, 1.5 and 3.1 log CFU/gram tissue in mice treated with 25, 50 and 100 mg/kg of M-8. Consistent with the result from systemic infection model, vancomycin exhibited the best *in vivo* activity against MRSA in the thigh infection model that resulted in a decrease of bacterial burden of 4.2 log CFU/gram tissue. Nevertheless, our data provide strong support that menaquinone biosynthesis is a potential target for antibiotic development.

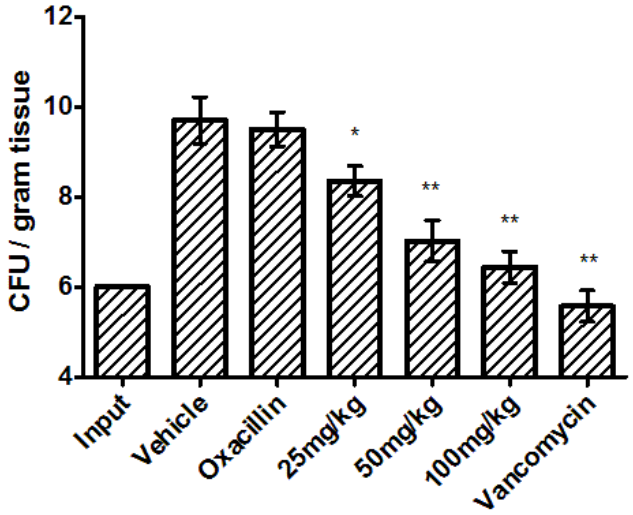


**Figure 2.18**. Thigh muscle bacterial load in infected mice treated with vehicle (n=5), oxacillin (n=5), M-8 (n=10 for each dose), and vancomycin (n=5). * $P < 0.02$. ** $P < 0.005$.

**Summary**

The emergence of methicillin resistant *Staphylococcus aureus* (MRSA), which is the primary causative agent of both hospital and community acquired infections, exemplifies the eroding clinical efficacy of first-line antibiotics and emphasizes the need to identify novel antibacterial targets. We have previously reported the discovery of a series of 4-oxo-4-phenylbut-2-enoates that inhibite the 1,4-dihydroxyl-2-naphthoyl-CoA synthase (MenB) in the bacterial menaquinone (MK) biosynthesis pathway through the formation of an adduct with CoA. We observed that the butenoyl methyl esters had promising MIC values against both drug sensitive and resistant *S. aureus*, suggesting that MenB is a potential target for antibiotic discovery. To support this hypothesis, we have now conducted studies to investigate their mechanism of action. Here we demonstrate that the butenoyl methyl esters penetrate into bacterial cells where they are hydrolyzed and converted into the corresponding CoA adducts. This observation substantiates our 'prodrug' hypothesis. We also showed using MS/MS quantification that the butenoyl methyl esters reduced menaquinone levels in *S. aureus*. Our data suggest that the compounds act through a specific effect on the menaquinone biosynthesis pathway, confirming the on-target inhibition that is important for further drug modification. Based on their promising *in vitro* activity, we evaluated the butenoyl methyl esters in a mouse model of MRSA infection. We found that the most potent molecule was active *in vivo* exhibiting comparable efficacy to vancomycin. Our results suggest the potential of these agents as new anti-MRSA candidates.

## Experimental Procedures

*Compound synthesis*

Synthesis of all 4-oxo-4-phenylbut-2-enoate derivatives was performed by Dr. Xiaokai Li (34). 2-CoA-4-(4-chloro)-phenyl-4-oxo-butanoic acid (CoA adduct standard) was synthesized from 4-oxo-4-(4-chloro)-phenylbut-2-enoic acid (A-8) (**Figure 2.19**). Compound A-8 (1 mmol) was added to a round bottom flask (RBF) with a magnetic stir bar. CoA (1.1 mmol) was dissolved in 10 mL DDI-$H_2O$ and transferred into the RBF. The reaction was stirred at room temperature for 1 hour. The product was purified with HPLC using 20 mM $NH_4OAc$ in water as solvent A and acetonitrile as solvent B. The HPLC gradient was: 0-30 minutes, B% 0-40%; 30-45 minutes, B% 40-100%.

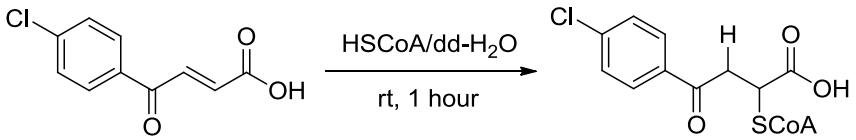


**Figure 2.19**. Synthesis of 2-CoA-4-(4-chloro)-phenyl-4-oxo-butanoic acid.

*Determination of MIC values*

Bacterial strains used in the present study include MSSA (RN4220), MRSA (BAA44 and BAA1762), *Enterococuss faecalis* (ATCC19433), *Enterococcus faecium* (ATCC19434), *Klebsiella pneumoniae* (ATCC13883), *Proteus mirabilis* (ATCC35659) and *Pseudomonas aeruginosa* (ATCC27853). All antibacterial assays were conducted at Stony Brook University, department of oral biology and pathology under biosafety level-2 (BSL-2) condition. MIC values were determined with the microbroth dilution assay according to the clinical and laboratory standards institutes methods for antimicrobial

susceptibility testes for aerobically growing bacteria (35). In brief, a starting bacterial culture was incubated to mid-log phase ($OD_{600}$ = 0.6, $10^8$ CFU/mL) in Mueller Hinton II (MH-II, BD) broth. Bacterial culture was diluted with sterile MH-II broth to a concentration of $5\times10^5$ CFU/mL and was pipetted onto a plastic 96-well plate. Compounds were dissolved in DMSO and were added to wells with 2-fold dilutions. The final drug concentration ranged from 0.05 to 256 µg/mL. The plates were incubated at 37 °C for 24 hours. Visible bacterial growth was examined and the lowest drug concentration that resulted in no cell growth was used as the MIC. MIC values of all compounds were tested in duplicate.

*Hydrolysis and CoA addition of the butenoyl methyl esters in S. aureus cells*

MSSA (RN4220) was incubated in 50 mL of Mueller Hinton (MH) broth at 37 °C to log phase (OD600 = 1.0). Bacterial cells were collected by centrifugation (5,000 rpm, 30 minutes). Cell pellets were subsequently suspended in 50 mL of phosphate buffer (50 mM, pH 7.0). M-8 and its isotopologue M-8-$d_4$ were added to the bacterial suspension which was then incubated at 25 °C for 12 h. Bacterial cells were collected by centrifugation and the cell pellets were resuspended in 5 mL of phosphate buffer (50 mM, pH 7.0). Cells were disrupted using a French press and the suspension centrifuged at 33,000 rpm, 1 h. The resulting supernatant was collected and dried on a lyophilizer. The residue was dissolved in 250 µL of DDI-water. MALDI samples were prepared using 2, 5-dihydroxy benzoic acid (DHB) as the matrix.

Mass spectra were acquired using a Bruker Autoflex II MALDI-TOF mass spectrometer (Bruker Dalbtonic, Billerica, MA), operated in reflectron mode. A nitrogen

UV laser (337 nm, 1-5 ns pulse of max energy 140 mJ, 10 Hz) was used to accomplish desorption/ionization. The positive ions were subjected to an accelerating potential of 19.0 kV and 16.9 kV from ion source 1 and ion source 2 respectively, 8.35 kV for the optical lens, reflected by reflectron electrodes (20 kV and 9.52 kV), and detected by a microchannel plate (MCP) detector using 4X voltage gain. The pulsed ion extraction time was 135 ns. Matrix ions were suppressed using low mass (m/z<400) cutoff. Due to low signal intensity, the spectra were acquired from multiple laser shots and were shown in additive mode. As a control, a spectrum was acquired from standard HSCoA in which the free CoA was detected with a correct molecular mass at 781.

*MK extraction from S. aureus cells*

A liquid-liquid lipid extraction protocol was used to extract MK from bacteria. In general, a starting culture of *S. aureus* was co-incubated with one of the test drugs at a sub-MIC concentration (1/3 to 1/2 MIC), in 100 mL of MH broth at 37 °C. At log phase ($OD_{600}$ = 1.0 - 1.2), cell cultures from each study group were diluted with fresh MH broth, to an identical concentration ($OD_{600}$ = 1.0, $10^9$ cells /mL). 100 mL of each diluted cell culture was centrifuged (5,000 rpm, 30 minutes) and the resulting cell pellets were suspended in 30 mL of phosphate buffer (50 mM $KH_2PO_3$, pH 7.0) and transferred to a separatory funnel. 20 mL of methanol and 15 mL of chloroform were added and the mixture was shaken vigorously for 3 minutes. After standing for 2h, 15 mL of chloroform was added and the mixture was shaken again for 2 minutes. The lower organic layer was collected, washed with brine (30 mL), and dehydrated by treating with $MgSO_4$ anhydrate for 4 hours. Organic solvent was then removed using a rotary evaporator and the residue was dissolved in 500 µL of methanol/chloroform (1/2, v/v) prior to MS/MS analysis. To compare MK

concentrations between different experimental groups, strict parallel extraction protocols were executed.

Extraction efficiently of this protocol was confirmed by spiking MK standards in buffer solution and in cell culture. After applying the above protocol, extracted MK was quantitated using APCI-MS/MS and the percentage of MK recovery was calculated (62).

*MK identification and quantification using MS/MS*

MK identification was conducted using a flow injection analysis (FIA)-APCI-MS/MS system comprised of a Dionex Ultimate 3000 HPLC system (Sunnyvale, CA) and a Thermo-Fisher TSQ Quantum Access triple Quadruple mass spectrometer (San Jose, CA). Briefly, 5 μL of sample was loop injected and the flow was directed to APCI source mounted on the instrument. Mass spectrometry was performed in positive ion mode with the high voltage set to 3.5 kV, a sheath gas pressure at 30 psi, and a capillary temperature of 350 °C. The collision cell was set to 1.5 mTorr Argon and the collision energy was 30 volts. Multiple Reaction Monitoring (MRM) transitions were detected at a 100 ms dwell times during the course of the experiment (**Figure 2.20**). Each MK component was identified by detecting a specific ion transition (parent ion to daughter ion). Multiple injections were performed over a 5-minute time frame. MK quantification was achieved by monitoring intensity of ion transition. As mentioned in previous section, a calibration curve was generated in prior to sample analysis using MK standards. After injecting cell extract to mass spectrometer, ion transition of each MK specie was detected and recorded. Signal intensity was subsequently fitted into the calibration curve to calculate MK concentrations in each sample.

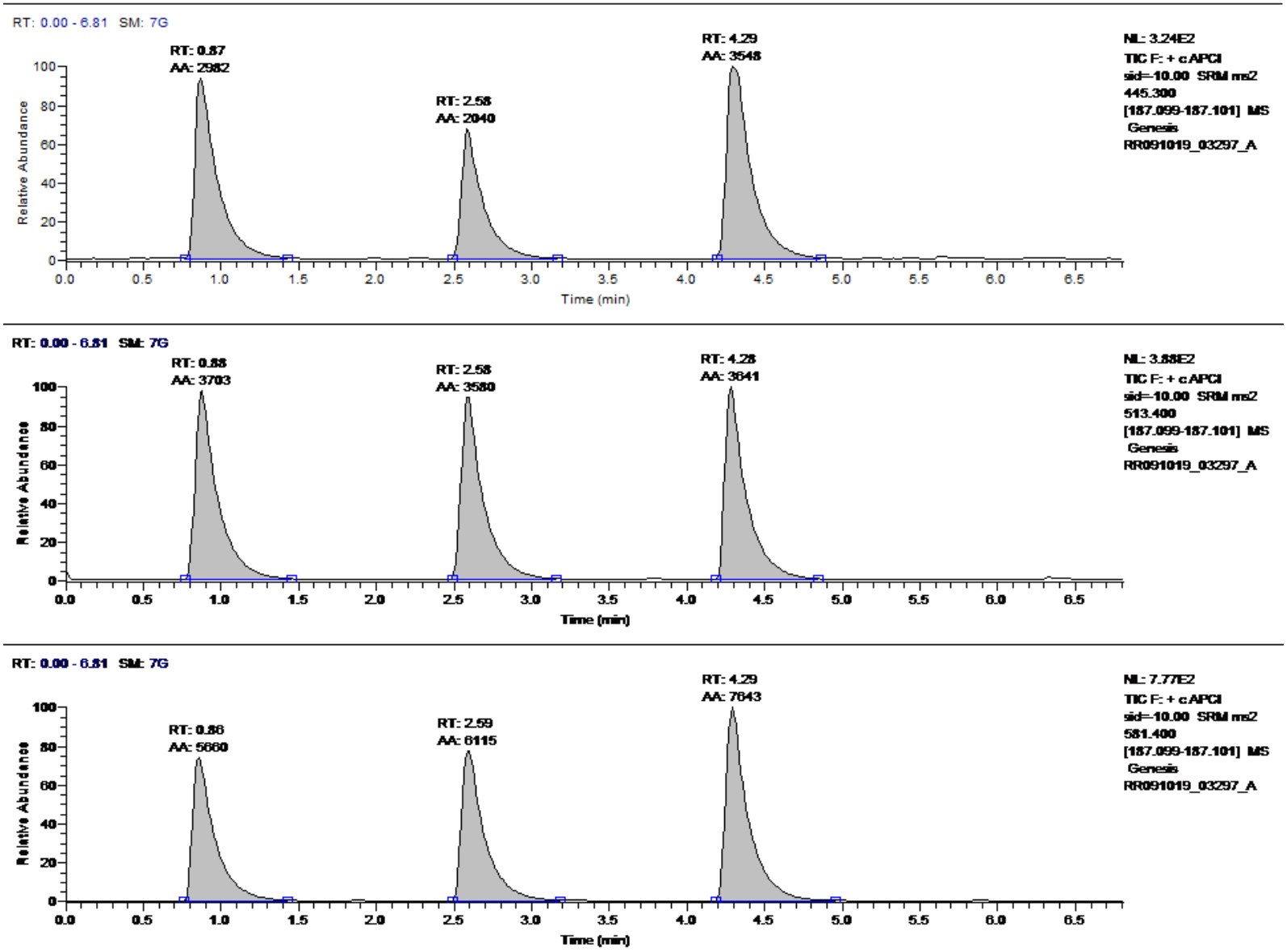
RT: 0.00 - 6.81 SM: 7G
RT: 0.87
AA: 2982
RT: 2.58
AA: 2040
RT: 4.29
AA: 3548
NL: 3.24E2
TIC F: + c APCI
sid=-10.00 SRM ms2
445.300
[187.099-187.101] MS
Genesis
RR091019_03297_A
Relative Abundance
Time (min)
RT: 0.00 - 6.81 SM: 7G
RT: 0.88
AA: 3703
RT: 2.58
AA: 3580
RT: 4.28
AA: 3641
NL: 3.88E2
TIC F: + c APCI
sid=-10.00 SRM ms2
513.400
[187.099-187.101] MS
Genesis
RR091019_03297_A
Relative Abundance
Time (min)
RT: 0.00 - 6.81 SM: 7G
RT: 0.86
AA: 5660
RT: 2.59
AA: 6115
RT: 4.29
AA: 7643
NL: 7.77E2
TIC F: + c APCI
sid=-10.00 SRM ms2
581.400
[187.099-187.101] MS
Genesis
RR091019_03297_A
Relative Abundance
Time (min)

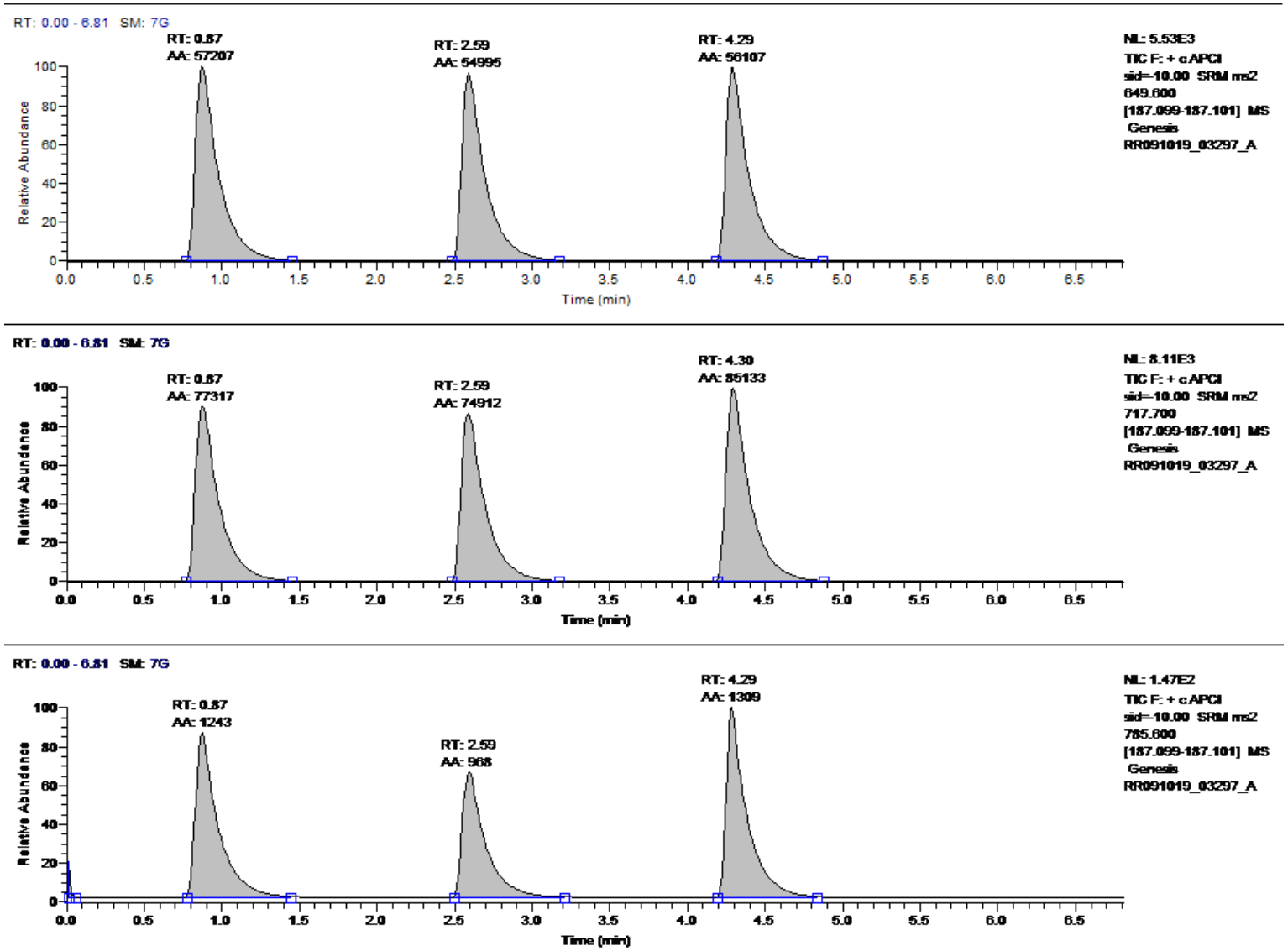


**Figure 2.20**. MRM signals of all MK species from cell extract. MK quantification was performed in triplet.

*In vivo activity of M-8 in mouse models with MRSA*

Studies involving animals were performed following approval from the Institutional Animal Care and Use Committee (IACUC) at Stony Brook University. All animals were maintained in accordance with the American Association for Accreditation of Laboratory Animal Care criteria. Experiments were conducted under BSL-2 conditions in the Division of Laboratory Animal Resource (DLAR) at Stony Brook University. Six-week old, specific pathogen free, male Swiss Webster mice weighing 27g to 32g (Taconic) were used in this study. Mice were provided *ad libitum* access to food and water through the entire experimental course.

Systemic infection. To induce a systemic infection, $2\times10^7$ CFU of MRSA (in 200 μL of saline) were administered by intraperitoneal injection (IP). Drugs doses were prepared in a vehicle consisting of 40% saline, 40% ethanol, 20% PEG-400, and were delivered by subcutaneous injection (SC) at 1 hour, 12 hours and 24 hours post infection with a dosage of 100 mg/kg. Mortality of infected mice were checked every 12 hours for 7 days. Dead mice were removed from the study immediately. Animals surviving at the end of the experiment were euthanized by $CO_2$ inhalation as recommended by the American Veterinary Medical Association (AVMA) Guidelines on Euthanasia.

Thigh infection. Mice were rendered neutropenic by injecting cyclophosphamide (CPA) 4 days (IP, 150 mg/kg) and 1 day (IP, 100 mg/kg) before infection. Previous studies have shown that this treatment could produce neutropenia for 5 days. To induce thigh infection, MRSA cells ($10^6$ CFU in 50 μl of saline) were injected into left thigh muscle (IM). Drug administration was performed by subcutaneous injection (SC) at 1 hour and 12 hours post infection with a dose of 100 mg/kg. No death was observed until 24 hours after

infection and all mice were euthanized by $CO_2$ inhalation. Infected thigh muscles were collected, weighed and homogenized in 2 mL of saline. Serial dilutions of each homogenized sample were plated on Mueller Hinton agar with sheep blood. The number of viable bacteria was then counted following overnight incubation of plates at 37 °C. Bacterial burdens were subsequently calculated.

**References**


1. Massey RC, Horsburgh MJ, Lina G, Hook M, & Recker M (2006) The evolution and maintenance of virulence in Staphylococcus aureus: a role for host-to-host transmission? *Nature reviews. Microbiology* 4(12):953-958.
2. Kluytmans J, van Belkum A, & Verbrugh H (1997) Nasal carriage of Staphylococcus aureus: epidemiology, underlying mechanisms, and associated risks. *Clinical microbiology reviews* 10(3):505-520.
3. Lowy FD (1998) Staphylococcus aureus infections. *The New England journal of medicine* 339(8):520-532.
4. Chambers HF & Deleo FR (2009) Waves of resistance: Staphylococcus aureus in the antibiotic era. *Nature reviews. Microbiology* 7(9):629-641.
5. Gorwitz RJ*, et al.* (2008) Changes in the prevalence of nasal colonization with Staphylococcus aureus in the United States, 2001-2004. *The Journal of infectious diseases* 197(9):1226-1234.
6. CDC (2004) Staphylococcus aureus in Healthcare Settings.
7. Mylotte JM, McDermott C, & Spooner JA (1987) Prospective study of 114 consecutive episodes of Staphylococcus aureus bacteremia. *Reviews of infectious diseases* 9(5):891-907.
8. NIH (2012) Staph infections - hospital.
9. Gill SR*, et al.* (2005) Insights on evolution of virulence and resistance from the complete genome analysis of an early methicillin-resistant Staphylococcus aureus strain and a biofilm-producing methicillin-resistant Staphylococcus epidermidis strain. *J Bacteriol* 187(7):2426-2438.

10. Fleming A (1955) The story of penicillin. *Bulletin. Georgetown University. Medical Center* 8(4):128-132.

11. Chambers HF (2001) The changing epidemiology of Staphylococcus aureus? *Emerging infectious diseases* 7(2):178-182.

12. Kirby WM (1944) Extraction of a Highly Potent Penicillin Inactivator from Penicillin Resistant Staphylococci. *Science* 99(2579):452-453.

13. Cosgrove SE*, et al.* (2003) Comparison of mortality associated with methicillin-resistant and methicillin-susceptible Staphylococcus aureus bacteremia: a meta-analysis. *Clinical infectious diseases : an official publication of the Infectious Diseases Society of America* 36(1):53-59.

14. Parker MT & Hewitt JH (1970) Methicillin resistance in Staphylococcus aureus. *Lancet* 1(7651):800-804.

15. Lowy FD (2003) Antimicrobial resistance: the example of Staphylococcus aureus. *The Journal of clinical investigation* 111(9):1265-1273.

16. Small PM & Chambers HF (1990) Vancomycin for Staphylococcus aureus endocarditis in intravenous drug users. *Antimicrob Agents Chemother* 34(6):1227-1231.

17. Pantosti A & Venditti M (2009) What is MRSA? *The European respiratory journal* 34(5):1190-1196.

18. Edlund C, Barkholt L, Olsson-Liljequist B, & Nord CE (1997) Effect of vancomycin on intestinal flora of patients who previously received antimicrobial therapy. *Clinical infectious diseases : an official publication of the Infectious Diseases Society of America* 25(3):729-732.

19. Cantu TG, Yamanaka-Yuen NA, & Lietman PS (1994) Serum vancomycin concentrations: reappraisal of their clinical value. *Clinical infectious diseases : an official publication of the Infectious Diseases Society of America* 18(4):533-543.

20. Smith TL*, et al.* (1999) Emergence of vancomycin resistance in Staphylococcus aureus. Glycopeptide-Intermediate Staphylococcus aureus Working Group. *The New England journal of medicine* 340(7):493-501.

21. Walsh TR & Howe RA (2002) The prevalence and mechanisms of vancomycin resistance in Staphylococcus aureus. *Annual review of microbiology* 56:657-675.

22. Sievert DM*, et al.* (2008) Vancomycin-resistant Staphylococcus aureus in the United States, 2002-2006. *Clinical infectious diseases : an official publication of the Infectious Diseases Society of America* 46(5):668-674.

23. Pelaez F (2006) The historical delivery of antibiotics from microbial natural products--can history repeat? *Biochemical pharmacology* 71(7):981-990.

24. Brickner SJ*, et al.* (1996) Synthesis and antibacterial activity of U-100592 and U-100766, two oxazolidinone antibacterial agents for the potential treatment of multidrug-resistant gram-positive bacterial infections. *J Med Chem* 39(3):673-679.

25. Ford CW*, et al.* (1996) In vivo activities of U-100592 and U-100766, novel oxazolidinone antimicrobial agents, against experimental bacterial infections. *Antimicrob Agents Chemother* 40(6):1508-1513.

26. Swaney SM, Aoki H, Ganoza MC, & Shinabarger DL (1998) The oxazolidinone linezolid inhibits initiation of protein synthesis in bacteria. *Antimicrob Agents Chemother* 42(12):3251-3255.

27. Kaplan SL, *et al.* (2005) Three-year surveillance of community-acquired Staphylococcus aureus infections in children. *Clinical infectious diseases : an official publication of the Infectious Diseases Society of America* 40(12):1785-1791.

28. Klevens RM, *et al.* (2007) Invasive methicillin-resistant Staphylococcus aureus infections in the United States. *JAMA : the journal of the American Medical Association* 298(15):1763-1771.

29. Diep BA, *et al.* (2006) Complete genome sequence of USA300, an epidemic clone of community-acquired meticillin-resistant Staphylococcus aureus. *Lancet* 367(9512):731-739.

30. Hidron AI, *et al.* (2008) NHSN annual update: antimicrobial-resistant pathogens associated with healthcare-associated infections: annual summary of data reported to the National Healthcare Safety Network at the Centers for Disease Control and Prevention, 2006-2007. *Infection control and hospital epidemiology : the official journal of the Society of Hospital Epidemiologists of America* 29(11):996-1011.

31. Truglio JJ, *et al.* (2003) Crystal structure of Mycobacterium tuberculosis MenB, a key enzyme in vitamin K2 biosynthesis. *The Journal of biological chemistry* 278(43):42352-42360.

32. Li HJ, *et al.* (2011) Mechanism of the intramolecular Claisen condensation reaction catalyzed by MenB, a crotonase superfamily member. *Biochemistry* 50(44):9532-9544.

33. Li X, *et al.* (2010) Synthesis and SAR studies of 1,4-benzoxazine MenB inhibitors: novel antibacterial agents against Mycobacterium tuberculosis. *Bioorganic & medicinal chemistry letters* 20(21):6306-6309.

34. Li X, *et al.* (2011) CoA Adducts of 4-Oxo-4-Phenylbut-2-enoates: Inhibitors of MenB from the M. tuberculosis Menaquinone Biosynthesis Pathway. *ACS Med Chem Lett* 2(11):818-823.

35. Institute CaLS (2012) Methods for Dilution Antimicrobial Susceptibility Tests for Bacteria That Grow Aerobically; Approved Standard M7-A9.

36. Hiramatsu K, *et al.* (2013) Genomic Basis for Methicillin Resistance in Staphylococcus aureus. *Infect Chemother* 45(2):117-136.

37. Kurosu M, Siricilla S, & Mitachi K (2013) Advances in MRSA drug discovery: where are we and where do we need to be? *Expert Opin Drug Discov* 8(9):1095-1116.

38. Whistance GR, Brown BS, & Threlfall DR (1970) Biosynthesis of ubiquinone in non-photosynthetic gram-negative bacteria. *Biochem J* 117(1):119-128.

39. Pandya KP & King HK (1966) Ubiquinone and menaquinone in bacteria: a comparative study of some bacterial respiratory systems. *Arch Biochem Biophys* 114(1):154-157.

40. Fisher K & Phillips C (2009) The ecology, epidemiology and virulence of Enterococcus. *Microbiology* 155(Pt 6):1749-1757.

41. Orsi GB & Ciorba V (2013) Vancomycin resistant enterococci healthcare associated infections. *Ann Ig* 25(6):485-492.

42. Molton JS, Tambyah PA, Ang BS, Ling ML, & Fisher DA (2013) The global spread of healthcare-associated multidrug-resistant bacteria: a perspective from Asia. *Clin Infect Dis* 56(9):1310-1318.

43. Paternotte I, *et al.* (2001) Syntheses and hydrolysis of basic and dibasic ampicillin esters tailored for intracellular accumulation. *Bioorganic & medicinal chemistry* 9(2):493-502.

44. Moreira R, *et al.* (1996) Acyloxymethyl as a drug protecting group. Part 3. Tertiary O-amidomethyl esters of penicillin G: chemical hydrolysis and anti-bacterial activity. *Pharmaceutical research* 13(1):70-75.

45. Meganathan R, Bentley R, & Taber H (1981) Identification of Bacillus subtilis men mutants which lack O-succinylbenzoyl-coenzyme A synthetase and dihydroxynaphthoate synthase. *Journal of bacteriology* 145(1):328-332.

46. Taber HW, Dellers EA, & Lombardo LR (1981) Menaquinone biosynthesis in Bacillus subtilis: isolation of men mutants and evidence for clustering of men genes. *Journal of bacteriology* 145(1):321-327.

47. Chen C, Gonzalez FJ, & Idle JR (2007) LC-MS-based metabolomics in drug metabolism. *Drug Metab Rev* 39(2-3):581-597.

48. Reaves ML & Rabinowitz JD (2011) Metabolomics in systems microbiology. *Curr Opin Biotechnol* 22(1):17-25.

49. Honoré AH, Thorsen M, & Skov T (2013) Liquid chromatography-mass spectrometry for metabolic footprinting of co-cultures of lactic and propionic acid bacteria. *Anal Bioanal Chem* 405(25):8151-8170.

50. Nakagawa K, *et al.* (2010) Identification of UBIAD1 as a novel human menaquinone-4 biosynthetic enzyme. *Nature* 468(7320):117-121.

51. Okano T, *et al.* (2008) Conversion of phylloquinone (Vitamin K1) into menaquinone-4 (Vitamin K2) in mice: two possible routes for menaquinone-4 accumulation in cerebra of mice. *J Biol Chem* 283(17):11270-11279.

52. Geyer R, Peacock AD, White DC, Lytle C, & Van Berkel GJ (2004) Atmospheric pressure chemical ionization and atmospheric pressure photoionization for simultaneous mass spectrometric analysis of microbial respiratory ubiquinones and menaquinones. *J Mass Spectrom* 39(8):922-929.

53. White DC & Frerman FE (1967) Extraction, characterization, and cellular localization of the lipids of Staphylococcus aureus. *J Bacteriol* 94(6):1854-1867.

54. Bentley R & Meganathan R (1982) Biosynthesis of vitamin K (menaquinone) in bacteria. *Microbiol Rev* 46(3):241-280.

55. Osborne CS, *et al.* (2009) In vivo characterization of the peptide deformylase inhibitor LBM415 in murine infection models. *Antimicrob Agents Chemother* 53(9):3777-3781.

56. Reyes N, Aggen JB, & Kostrub CF (2011) In vivo efficacy of the novel aminoglycoside ACHN-490 in murine infection models. *Antimicrob Agents Chemother* 55(4):1728-1733.

57. Keel RA, Tessier PR, Crandon JL, & Nicolau DP (2012) Comparative efficacies of human simulated exposures of tedizolid and linezolid against Staphylococcus aureus in the murine thigh infection model. *Antimicrob Agents Chemother* 56(8):4403-4407.

58. Banevicius MA, Kaplan N, Hafkin B, & Nicolau DP (2013) Pharmacokinetics, pharmacodynamics and efficacy of novel FabI inhibitor AFN-1252 against MSSA and MRSA in the murine thigh infection model. *J Chemother* 25(1):26-31.

59. Louie A, Liu W, Kulawy R, & Drusano GL (2011) In vivo pharmacodynamics of torezolid phosphate (TR-701), a new oxazolidinone antibiotic, against methicillin-susceptible and methicillin-resistant Staphylococcus aureus strains in a mouse thigh infection model. *Antimicrob Agents Chemother* 55(7):3453-3460.

60. Andes D & Craig WA (2006) Pharmacodynamics of a new cephalosporin, PPI-0903 (TAK-599), active against methicillin-resistant Staphylococcus aureus in murine thigh and lung infection models: identification of an in vivo pharmacokinetic-pharmacodynamic target. *Antimicrob Agents Chemother* 50(4):1376-1383.

61. Craig WA & Andes DR (2008) In vivo pharmacodynamics of ceftobiprole against multiple bacterial pathogens in murine thigh and lung infection models. *Antimicrob Agents Chemother* 52(10):3492-3496.

62. Schiebel J*, et al.* (2014) Rational Design of Broad-Spectrum Antibacterial Activity based on a Clinically Relevant Enoyl-ACP Reductase Inhibitor. *J Biol Chem*.

# Chapter III. Demonstration of Cellular MK Conversion from Various Quinone-Based Molecules in *S. aureus*, and Identification of MenA as a Candidate Catalyzing the Reaction

## Introduction

*Small colony variants in S. aureus*

Small colony variants (SCVs) represent a naturally existing subpopulation of bacteria with distinctive phenotypes. The most characteristic feature of SCVs is the formation of smaller colonies having only 1/10 of the normal size (**Figure 3.1**). Bacterial SCVs was first identified in 1910 as an aberrant form of bacteria (1, 2) and has been observed in various bacterial genera and species thereafter such as *Escherichia coli* (3), *Pseudomonas aeruginosa* (4), and *Brucella melitensis* (5). *Staphylococcus aureus* is one of the bacterial species in which SCVs was originally identified (6, 7). In addition to forming smaller colonies and significant growth rate reduction, *S. aureus* SCVs also show altered biochemical characteristics such as lack of pigmentation, non-hemolytic variants and reduced production of virulence factors, making them more difficult to be detected by routine laboratory testing (8, 9). In light of the advancements of clinical diagnostic methods, *S. aureus* SCVs have been recovered from clinical specimens and have been correlated with a wide range of infectious diseases including cystic fibrosis, osteomyelitis and endocarditis (1, 10, 11). Furthermore, epidemiological surveys suggest that the frequency of SCVs from human infections is surprisingly high; >40% in patients with repeating osteomyelitis and >70% in patients suffering from cystic fibrosis (12, 13). Another hallmark clinical feature of *S. aureus* SCVs is that they can persist in hosts evading

aggressive antibiotic treatments (1, 14). While the mechanism of lower susceptibility in SCVs is still unclear, it has been hypothesized to arise from three major factors: reduced bacterial growth rate that causes limited susceptibility to cell-wall-targeting drugs; decreased physiological activity that results in reduced drug uptake; persistence within host cells that confers resistance to antibiotics that cannot penetrate host cells (1, 15). Recently, there has been a great interest in *S. aureus* SCVs. In addition to being the causative agent of many illnesses, a detail study of SCVs can provide new insights into drug resistance in staphylococcal infections.

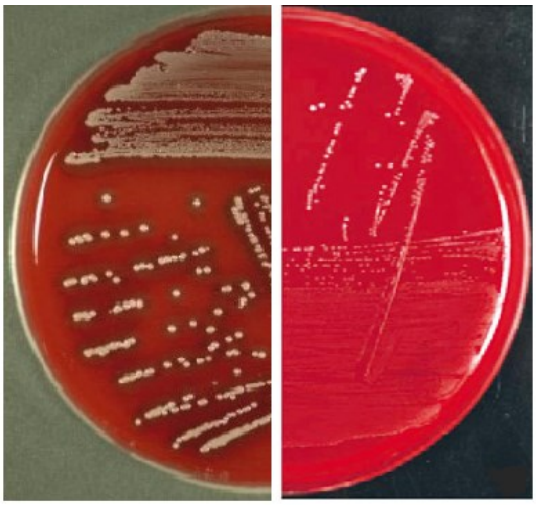

**Figure 3.1.** Sheep blood-agar plates that show the normal (left) and the small colony variant phenotype (right) of *S. aureus*. The clinical SCV strains form smaller colonies on agar plate (1/10 of the normal size) and do not show hemolysis on blood agar.

*S. aureus SCVs and menaquinone biosynthesis*

Although bacterial SCVs were discovered more than a century ago, the mechanism of how this distinctive phenotype emerged has not been thoroughly addressed. Initial research mainly focused on understanding the slower growth rate in SCVs and on identifying conditions that can restore wild type-like growth. Early studies found that

compounds, such as menadione, heme, thiamine and $CO_2$, could stimulate growth of SCVs (1, 16-18). Subsequent studies shed light on metabolism in bacterial SCVs and demonstrated that the auxotrophic character correlates to deficiency in electron transport (menadione and heme) (1, 19). In particular, menadione, which is an analogue of menaquinone (MK), and heme, which functions in the biosynthesis of cytochromes in the electron transport chain, are both critical factors for ATP biosynthesis in bacteria (**Figure 3.2**). Although the exact mechanism of menadione or heme auxotrophy has not been elucidated, an effect on respiration is consistent with multiple phenotypic changes observed in clinical SCVs. For example, an inhibition of ATP biosynthesis causes a slower growth rate, and reduces production of bacterial virulence factors such as α-toxin. Defects in electron transport yield a decreased electrochemical gradient (ΔΨ) which leads to a reduced uptake of cationic antibiotics such as aminoglycosides, explaining why SCVs are less susceptible to these antibiotics (20).

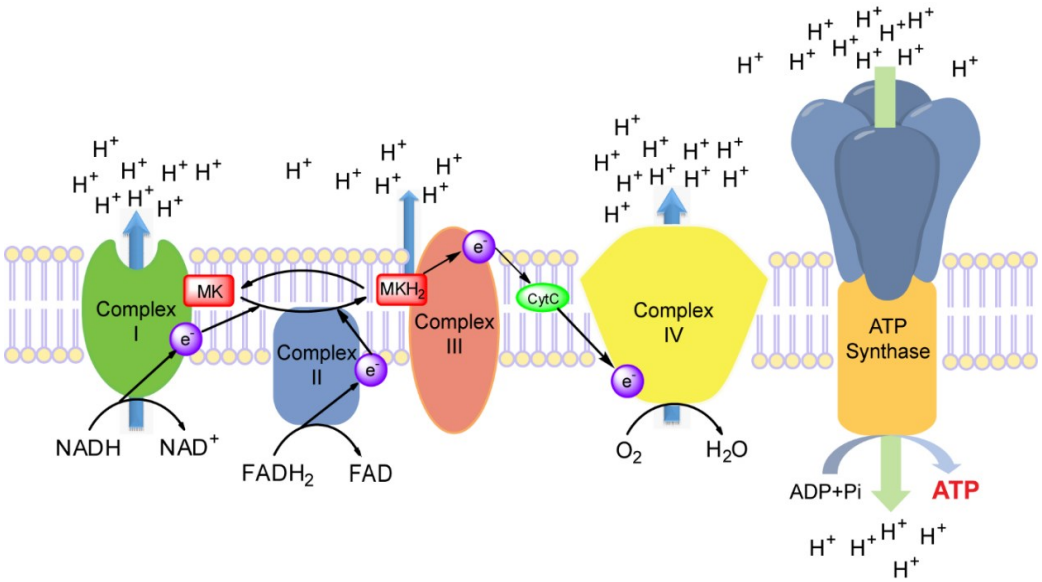


**Figure 3.2.** Bacterial electron transport chain. Menaquinone and heme are involved in this physiological process. Heme forms cytochrome in complex with membrane proteins; menaquinone transfers electrons between different redox complexes.

While mapping the precise genetic changes in *S. aureus* SCVs has proven to be a challenge (1), potential targets that are responsible for SCV phenotype have been proposed by different complementation studies. For example, a menadione-auxotrophic strain could be recovered by supplying bacteria with *O*-succinylbenzoate (OSB) but not with isochorismate, suggesting that a step between these two intermediates in the menaquinone biosynthesis pathway was disrupted (**Figure 3.3.)** (21). Subsequent studies demonstrated that interruption of the *menD* gene in normal *S. aureus* could reproduce an SCV-like phenotype that showed identical features to clinical isolates (22, 23). Meanwhile, the *menD* disrupted strains were restored to the wild type phenotype by complementing the bacteria with menadione. Similar results have also been observed in heme auxotroph SCVs (24).

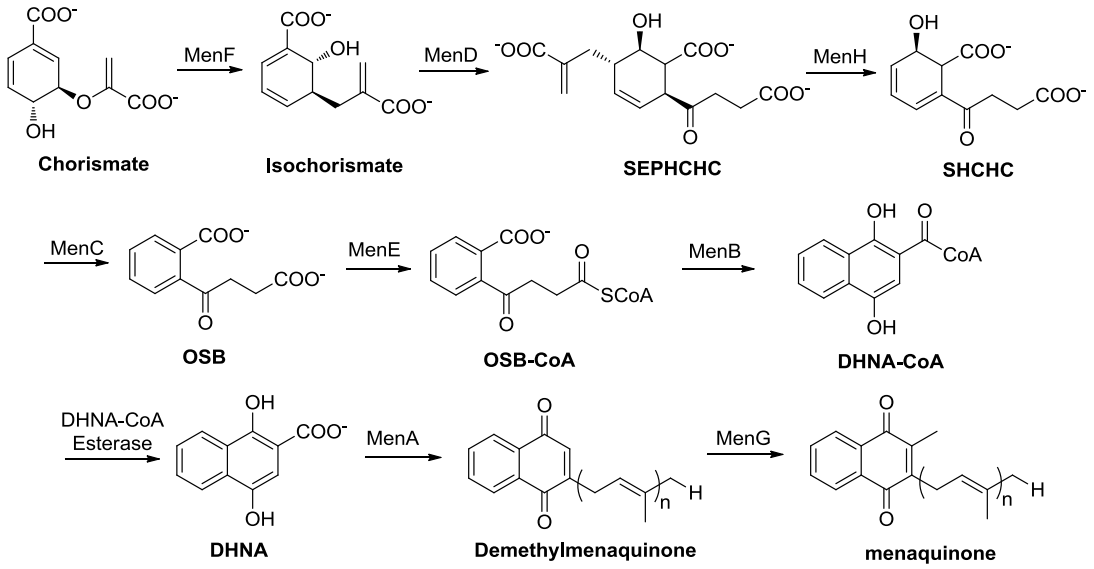


**Figure 3.3.** The bacterial menaquinone biosynthesis pathway.

Given that an effect on menaquinone biosynthesis has been implicated as a potential causative mechanism of SCVs, there is now a debate about the utility of menaquinone biosynthetic enzymes as drug targets. The major concern is that inhibition of Men proteins,

such as MenD, does not cause bacterial death but leads to formation of SCVs which are more persistent. This hypothesis has been supported by studies showing that *menD* and *hemB* disrupted *S. aureus* strains are viable *in vitro* and are infective in animal models (23, 25). However, little is known about menadione auxotrophic SCVs mechanistically. Some critical questions need to be addressed such as which molecule functions as the substitute for menaquinone in the electron transport chain in defect bacteria. In addition, it is unclear how menadione, which is not a natural intermediate in menaquinone biosynthesis, can restore the wild type-like physiology.

*Project overview*

The mechanism(s) leading to the SCV phenotype in *S. aureus* remains inconclusive. In this study, we focus on understanding the viability and biochemistry of a menadione auxotrophic *S. aureus* strain (*menD*$^-$). Here, we first evaluated the viability of this mutant in various growth media with or without menadione supplementation. We then tested the ability of other compounds, which are chemically similar to menaquinone / menadione, to restore growth of the *menD*$^-$ strain. Additionally, we investigated the mechanism of menadione auxotrophy in the *menD*$^-$ *S. aureus* strain by examining the recovery of menaquinone biosynthesis in bacteria. Finally, we proposed a conversion mechanism in *S. aureus*, and identified a potential candidate that catalyzes this conversion.

## Results and Discussion

*Viability of the menD⁻ S. aureus*

To investigate the correlation between the SCV phenotype in *S. aureus* and menaquinone biosynthesis, experiments were conducted using a menaquinone deficient *S. aureus* strain, in which an *erm*C cassette had been inserted into the chromosomal copy of *menD* from RN4220. This *menD* disrupted mutant (*menD*$^-$) has been demonstrated to reproduce an SCV phenotype (23).

We first determined the viability of the *menD*$^-$ strain in comparison to the wild type (WT) bacteria in liquid media. By monitoring the optical density at 600 nm ($OD_{600}$) of the bacterial culture, we observed that the *menD*$^-$ *S. aureus* strain grew significantly slower than the wild type in rich media such as Tryptic soy broth (TSB) and Mueller Hinton II broth (MH-II) (**Figure 3.4**). Quantitatively, the doubling time of the *menD*$^-$ strain at log phase (58 minutes) was more than two fold longer than that of the wild type strain (26 minutes). Additionally, the *menD*$^-$ strain failed to reach the same final density as the wild type did. These data are consistent with reduced growth being one of the characteristic features of *S. aureus* SCVs (1, 12). Moreover, growth of the *menD*$^-$ strain was stimulated by adding menadione into media (**Figure 3.4**). This result supports the previous conclusion on the *menD*$^-$ strain that the genetic disruption caused SCVs-like phenotype in *S. aureus* which was menadione auxotrophic (1).

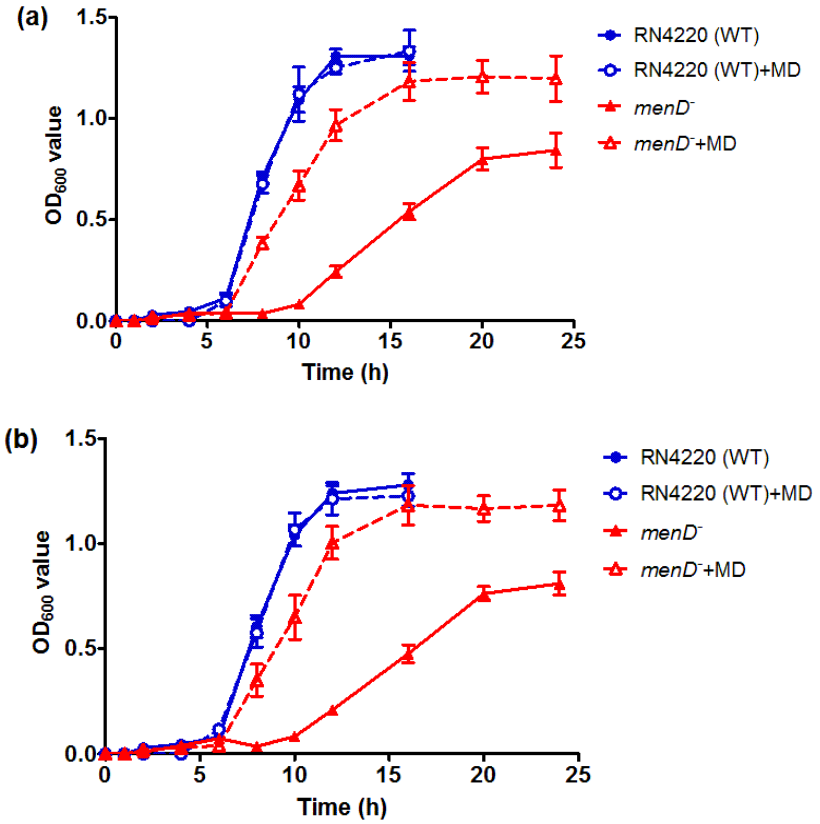


**Figure 3.4.** Growth of RN4220 and the *menD*$^-$ strain in (a) Tryptic Soy broth (TSB) and (b) Mueller Hinton II broth (MH-II). Both strains are viable in rich media and growth of the disrupted strain can be stimulated by menadione supplement.

Subsequently, similar growth experiments were conducted using a minimal media, AOAC synthetic broth (or chemically defined media, CDM). As shown in **Figure 3.5**, wild type *S. aureus* cells were viable in CDM though, as expected, grew slower than in rich media. The addition of menadione into CDM did not result in a faster growth of the wild type, suggesting that the reduced growth rate was not caused by menaquinone deficiency. However, in a parallel experiment, the *menD*$^-$ strain was not able to survive in CDM at all (**Figure 3.5a**). The bacterial culture was incubated for as long as 7 days (not shown in the figure) and still did not grow ($OD_{600}$ value < 0.05). Furthermore, the mutant strain did not

form any colonies on minimal agar plates while the wild type strain did (**Figure 3.5b**). Significantly, growth of the *menD*$^-$ *S. aureus* in CDM was restored by complementing with menadione (**Figure 3.5a**). This observation further suggests that disruption of *menD* in *S. aureus* can transform the bacteria into a menadione auxotroph similar to clinical SCVs. However, our data also demonstrate that inhibition of menaquinone biosynthesis does not only result in formation of smaller colonies, but also causes bacterial growth inhibition in the absence of menadione supplements.

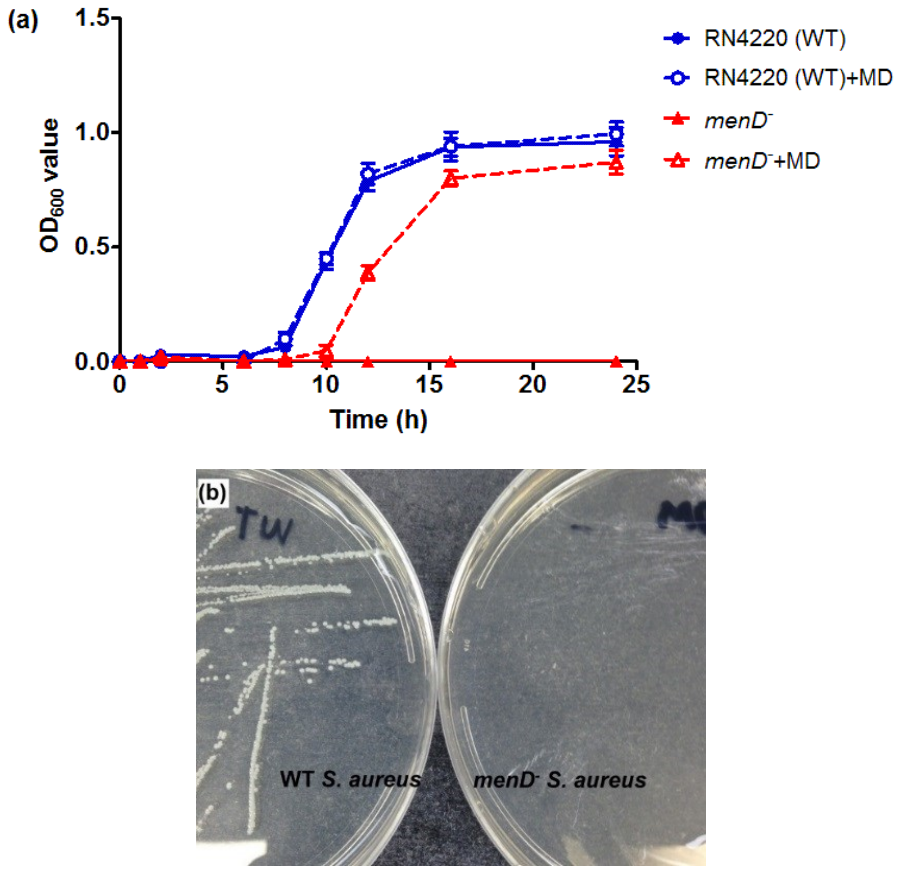


**Figure 3.5.** Viability of the *menD*$^-$ *S. aureus* (a) in chemically defined media (CDM) with or without of menadione (MD) supplementation. (b) on minimal agar plates. The disrupted strain is not viable in minimal media or on minimal agar. The growth can be recovered by the supplementation of menadione.

*Growth recovery of the menD⁻ strain in CDM by supplementing with various quinone-based molecules*

We have observed that survival of *S. aureus* cells in minimal media required either a competent menaquinone biosynthesis or an exogenous supplement of menadione, suggesting that interruption of menaquinone biosynthesis was lethal for bacteria in the absence of supplements. However, we also observed that the *menD⁻* strain was able to grow in rich media without menadione, suggesting that some nutrients in these broths could complement the growth defect of these cells. Notably, menadione is not a natural molecule but a synthetic analogue of menaquinone (26), making it an unlikely component of MH-II and TSB media. We investigated both media using Gas Chromatography-mass spectrometry (GC-MS) and did not observe menadione (**Figure 3.6**) in media extracts. Our data suggest the presence of another compound in rich media that can restore the growth of the menaquinone deficient *S. aureus* strain. This result also demonstrates that recovery of the auxotrophic phenotype of the *menD⁻* mutant is not limited to menadione.

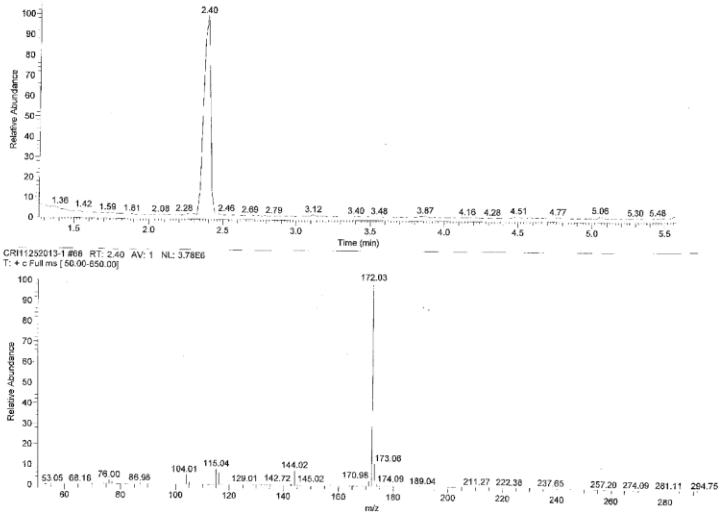


**Figure 3.6**. GC-MS spectra of menadione. Detection of menadione in the GC spectrum (top); molecular mass of menadione in mass spectrum (bottom).

Therefore, we conducted a series of experiments to identify quinone-based supplements that can restore the growth of the *menD*$^-$ strain in CDM. Compounds used in this study included menaquinone-4 (MK-4), phylloquinone (Vitamin $K_1$, PQ), ubiquinone-10 (Ubq-10), naphthoquinone (NQ), and 2,3-dimethyl naphthoquinone (2,3-diMe) (**Figure 3.7**). MK-4 is a menaquinone sub-species, though not the most abundant component in *S. aureus*. Phylloquinone is the plant-derived Vitamin K species with a C-3 phytyl side chain (27, 28). Ubiquinone functions in the electron transport chain in Gram-negative bacteria and in mammalian cells (29-31), and is the only molecule studied that does not have a 1,4-naphthoquinone backbone. Naphthoquinone and 2,3-dimethyl- naphthoquinone are both analogues of menaquinone.

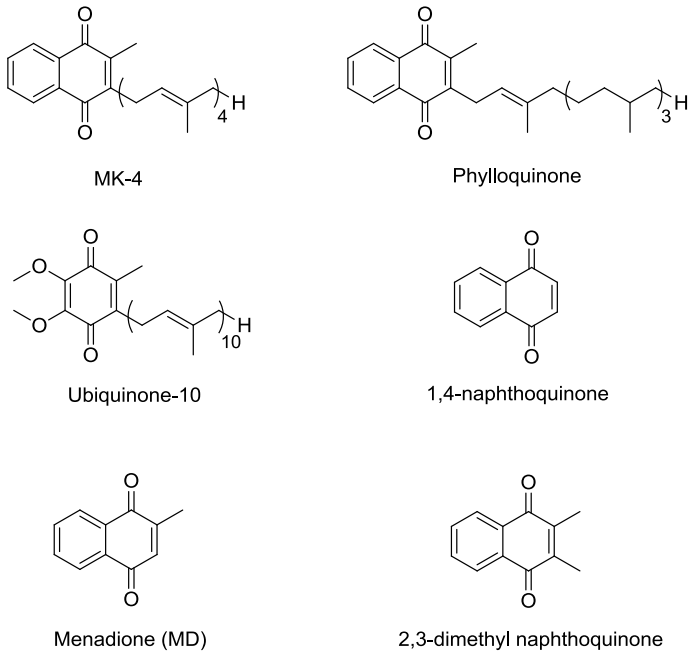


**Figure 3.7.** Structure of quinone-based supplements. All studied molecules, except for ubiquinone-10, have the same 1,4-naphthoquinone scaffold.

As shown in **Figure 3.8**, all compounds tested, apart from ubiquinone-10, recovered the growth of the *menD*$^-$ strain in CDM, substantiating our hypothesis that the

*menD*$^-$ *S. aureus* is not only auxotrophic to menadione. As a final product of the menaquinone biosynthesis pathway, MK-4 was expected to be able to rescue bacteria from menaquinone deficiency. However, it is interesting that phylloquinone, which has not been reported to be utilized by Gram-positive bacteria in the past, also restored the growth of the mutant cells. Significantly, although being more menaquinone-like from a chemical standpoint, MK-4 and phylloquinone were less efficient than menadione in terms of cell growth recovery. In addition, ubiquinone-10 was the only molecule that failed to restore bacterial growth, suggesting the importance of the 1,4-naphthoquinone structure in the complements.

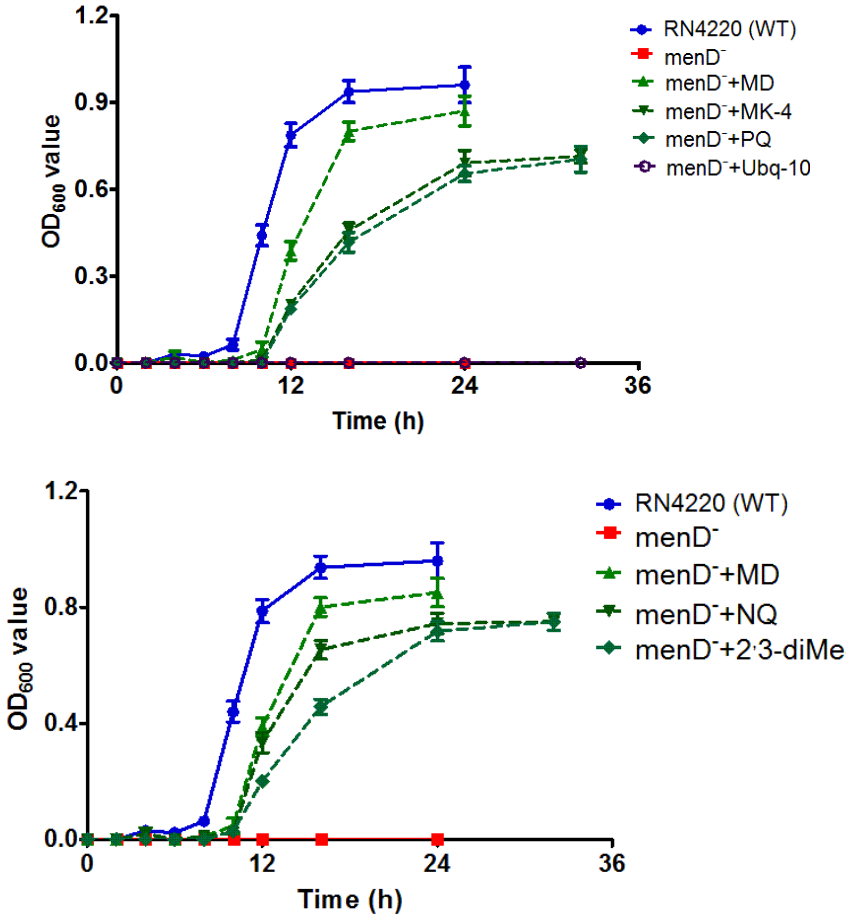


**Figure 3.8.** Recovery of the growth of the *menD*$^-$ strain in chemically defined media (CDM) by supplementing with different quinone-based molecules.

*Recovery of menaquinone biosynthesis in the menD⁻ S. aureus*

So far, we have demonstrated that the growth of the *menD⁻ S. aureus* in CDM could be recovered by supplying the bacteria with menadione and a series of quinone-based molecules. However, the mechanism of this phenotype has not been clarified. Considering the structural similarity between the complements and menaquinone, we proposed two hypotheses: 1) The quinone-based molecules can replace the function of menaquinone in *S. aureus* by directly participating in the bacterial electron transport chain; or 2) *S. aureus* cells can take up these menaquinone analogues and convert them into menaquinone to counteract the effects of *menD* disruption.

To explore the mechanism involved, we performed an experiment using MS/MS to examine whether menaquinone biosynthesis was restored in the *menD⁻* mutant supplemented with quinone molecules. The *menD⁻* cells were incubated in CDM and were complemented with one of the quinones. The cell pellets were collected at log phase and were subsequently extracted with organic solvent. The presence of menaquinone was then identified using a MS/MS-based method as discussed in Chapter II. As shown in **Figure 3.9**, we observed recovery of menaquinone biosynthesis in mutant cells co-incubated with all supplements including menadione, MK-4, phylloquinone, naphthoquinone and 2,3-dimethyl-naphthoquinone. These data suggest that all the quinone-based molecules rescued the growth of the *menD⁻* strain by restoring menaquinone biosynthesis, substantiating our second hypothesis of menaquinone conversion. This observation also demonstrates that *S. aureus* has a second pathway of synthesizing menaquinone other than the *de novo* biosynthesis. It also explains how menadione could stimulate growth of clinical SCVs

isolates. It is especially significant that *S. aureus* cells are able to utilize the plant-derived vitamin $K_1$ as a substrate for menaquinone biosynthesis.

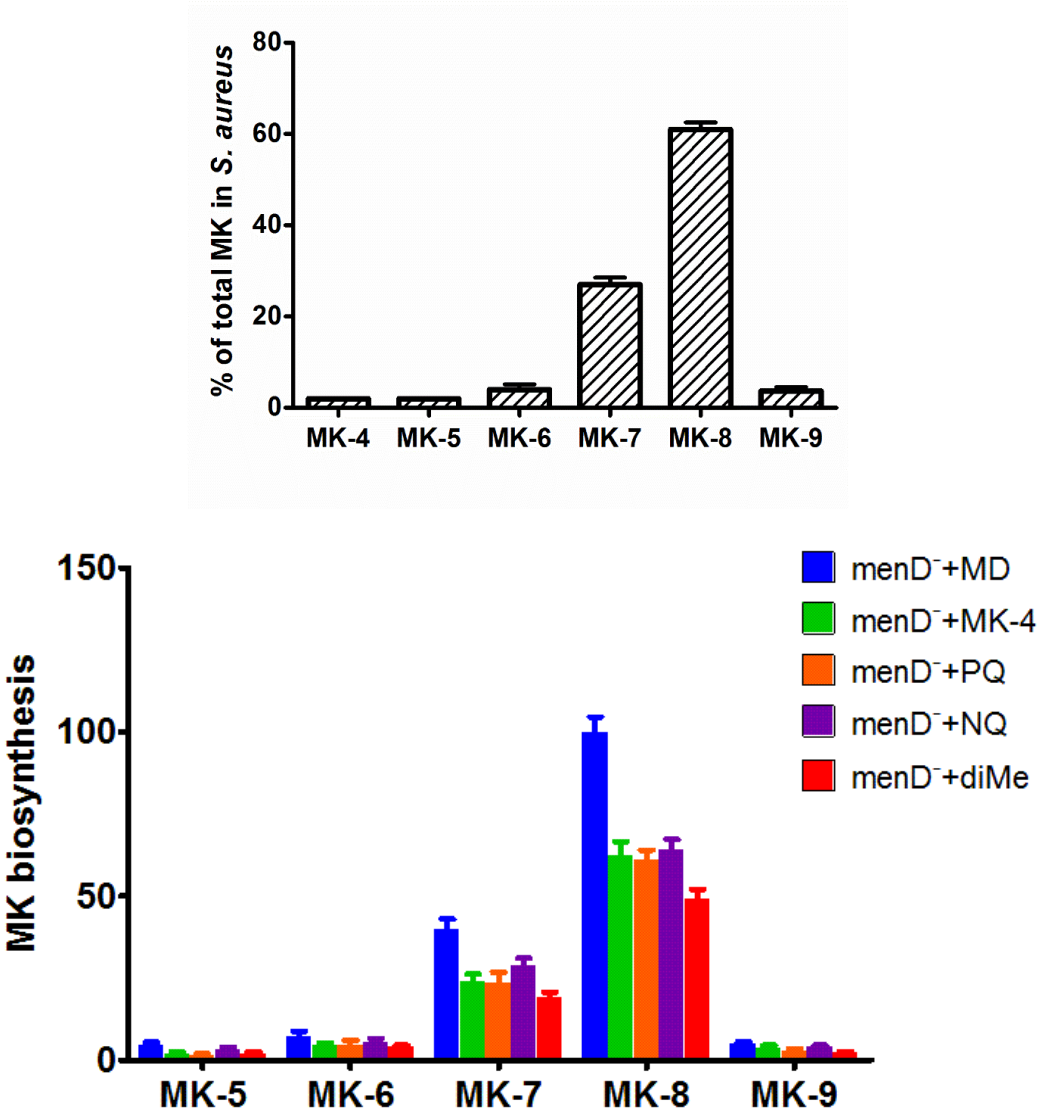


**Figure 3.9.** Recovery of menaquinone (MK) biosynthesis in the *menD*$^-$ *S. aureus* complemented by all 1,4-naphthoquinone-based compounds. Same menaquinone profiles were observed from WT (top) and rescued mutant (bottom). The error bars represent the standard error of the means (SEM).

In addition, we observed that the proportion of each menaquinone component in the complemented bacteria remained consistent with that in the WT *S. aureus* wherein MK-

8 is the most abundant species (**Figure 3.9**). Significantly, the supplement of MK-4 was further modified to other menaquinone species with longer isoprenoyl side chains, suggesting the conversion between different menaquinone species. We subsequently executed a parallel experiment using MK-7, a longer and the second most abundant manaquinone species in *S. aureus*, to restore growth of the *menD*$^-$ strain and menaquinone biosynthesis. As expected, bacterial growth was recovered, and MK-7 was converted into other menaquinone species (**Figure 3.10**). Unfortunately, we could not perform a similar study using MK-8 as the complement, since this compound is not commercially available. This experiment would have told us whether *S. aureus* needs a complete menaquinone series to survive or whether the presence of the most abundant component is sufficient. Nevertheless, our data demonstrate that growth inhibition in *menD*$^-$ *S. aureus* can be restored by complementing with a series of 1,4-naphthoquinone-based molecules *via* an menaquinone conversion mechanism.

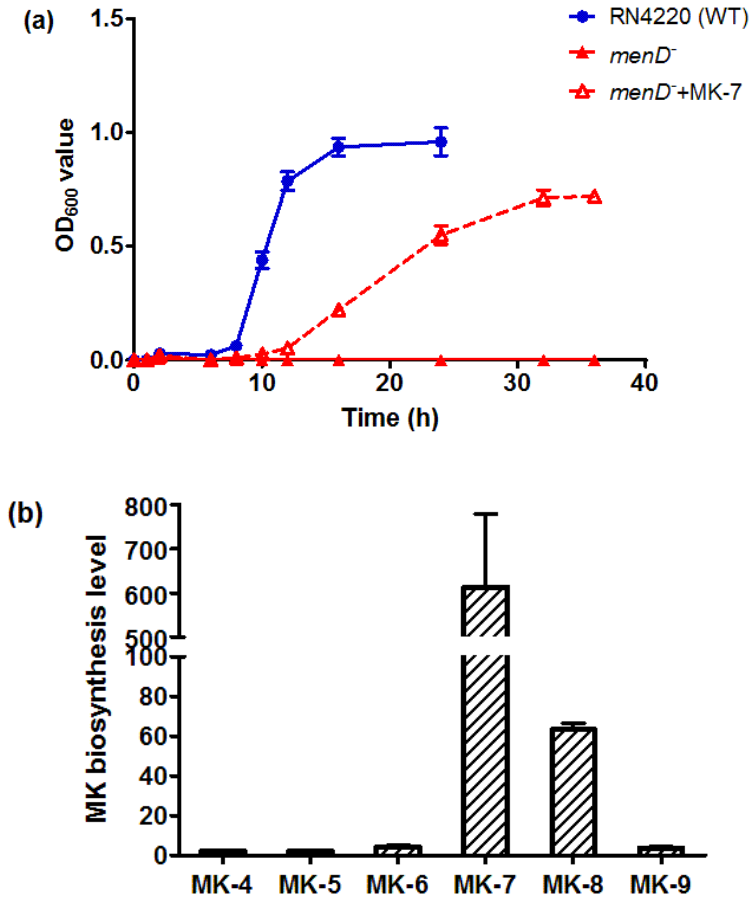


**Figure 3.10.** Recovery of bacterial growth and cellular menaquinone biosynthesis in *menD*$^-$ *S. aureus s*upplemented with MK-7.

To further confirm our conclusion, two deuterium labeled compounds, menadione-$d_3$ (MD-$d_3$) and 2,3-dimethyl-1,4-naphthoquinone-$d_3$ (diMe-$d_3$), were synthesized (**Figure 3.11**) to track the source of menaquinone in the rescued *menD*$^-$ cells. As shown in **Figure 3.12**, derivatives with molecular masses matching menaquinone-$d_3$ isotopologues (MK-n-$d_3$) were detected in cell extracts. These data are consistent with our previous experiments, substantiating the existence of a cellular menaquinone conversion in *S. aureus*. Meanwhile, natural menaquinone species were not observed in the supplemented bacteria, suggesting that the *de novo* menaquinone biosynthesis pathway was completely disrupted in the *menD*$^-$

mutant; and conversion from quinone complements was the only source of menaquinone. We also observed that the methyl group in menadione was intact during the conversion into menaquinone. This suggests that menadione was not oxidized to DHNA and fed into the *de novo* biosynthesis pathway downstream of the interrupted *menD* reaction, which would have resulted in the disappearance of the deuterium labeling (**Figure 3.13**).

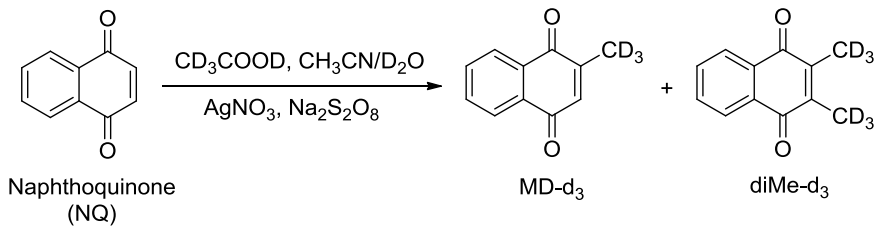


**Figure 3.11.** Synthetic route of MD-$d_3$ and diMe-$d_3$ from 1,4-naphthoquinone.

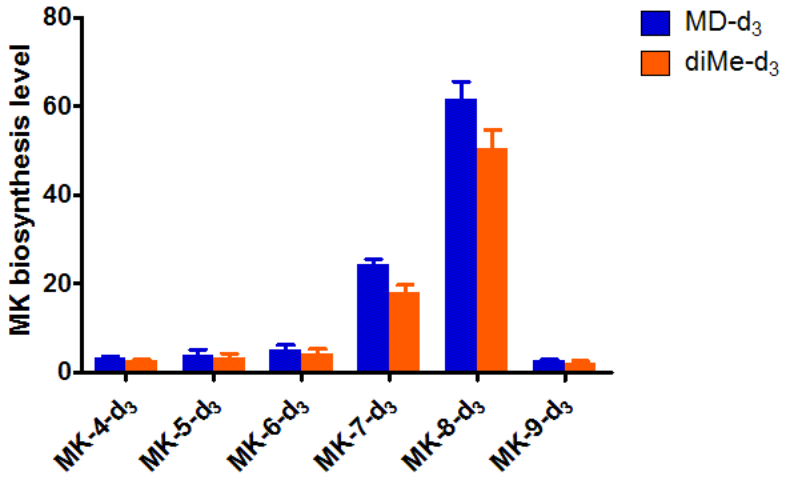


**Figure 3.12.** The biosynthesis of menaquinone in *menD*$^-$ *S. aureus* complemented with MD-$d_3$ and diMe-$d_3$. A complete set of menauqinone species was observed in a deuterium labeled form. No natural MKs was detected, suggesting that the supplyment is the substrate of menaquinone species.

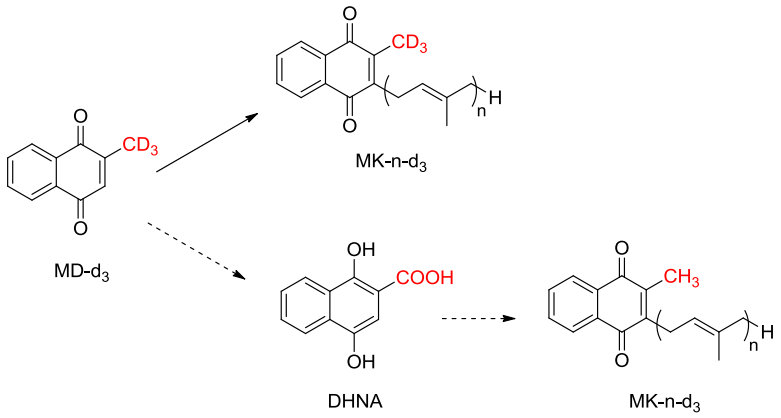


**Figure 3.13.** Proposed mechanism of menaquinone conversion. Substitution at C-2 position was labeled red. Dashed arrows represent a hypothetic mechanism *via* DHNA.

Based on the observation that MK-4 or phylloquinone yielded the entire series of menaquinone derivatives in the wild type *S. aureus*, we proposed that this conversion occurs in two steps: removal of C-3 substituent and subsequent attachment of the poly-isoprenoyl side chains. Our data suggested that menadione was the most effective compound in restoring bacterial growth and menaquinone biosynthesis in the *menD*$^-$ mutant cells. These results were consistent with our proposed mechanism: menadione is a better substrate for menaquinone conversion as it only requires the attachment of a side chain. The observation led to another hypothesis that menadione is an intermediate of menaquinone conversion from quinone-based molecules such as MK-4 and phylloquinone (**Figure 3.14**). This idea was based on a previous study by Hirota *et al*., in which menadione was reported to be detected in urine samples of patients who had taken MK-4 supplements (32). However, we failed to identify menadione in *S. aureus* cells supplemented with MK-4 and phylloquinone. A possible reason is that the removal and the attachment of C-3 substituent were consecutive steps during which free menadione could not be released.

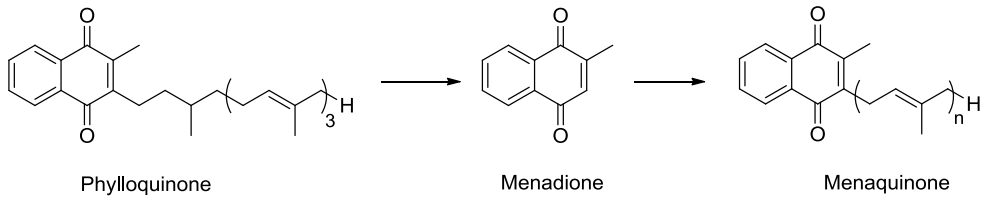


**Figure 3.14.** The hypothetic mechanism of menaquinone conversion with (menadione) MD as an intermediate.

Taken together, we demonstrated that *S. aureus* could take up various naphthoquinone-based molecules and convert them into other menaquinone species which are necessary for bacterial survival. Our results provided evidence explaining the mechanism of the menadione auxotrophic phenotype observed in clinical SCVs and in constructed menaquinone deficient strains. Furthermore, although menadione could stimulate cell growth of the mutant strains, it did not directly replace the function of menaquinone which is the ultimate electron carrier in Gram-positive bacteria.

*Identification of a candidate enzyme catalyzing menaquinone conversion in S. aureus*

Identification of the menaquinone salvage pathway suggested that the *de novo* menaquinone biosynthesis pathway is not the unique way for bacteria to synthesize menaquinone. Further explorations about the mechanism of menaquinone conversion can facilitate our understanding on the auxotrophic phenotype in *S. aureus*. A starting point is to identify the enzyme, or group of enzymes, that catalyze this reaction. We hypothesized that 1,4-dihydroxy-2-naphthoate prenyltransferase (MenA) is a potential candidate based on the following observations: 1. from a chemical standpoint, menaquinone conversion from MD or other quinone molecules would involve a prenylation step that is known to be catalyzed by MenA in the bacterial menaquinone biosynthesis; 2. it has been reported that

a *menA* knockout is fatal in menaquinone-utilizing bacteria (35, 36), consistent with our hypothesis that this key enzyme is indispensable for both *de novo* biosynthesis and the conversion from quinones into menaquinone.

While little is currently known about bacteria utilizing exogenous supplements to generate menaquinone species, human UbiA prenyltransferase containing domain 1 (hUBIAD1) has been reported to catalyze a similar menaquinone conversion (33, 34). UBIAD1 is the first identified mammalian homolog of *E. coli* MenA and has been demonstrated to be responsible for the conversion of vitamin $K_1$ to vitamin $K_2$ in mice. Further studies have shown that UBIAD1 converted other quinone-based molecules such as MD into menaquinone both *in vitro* and *in vivo* (**Figure3.15**) (37, 38).

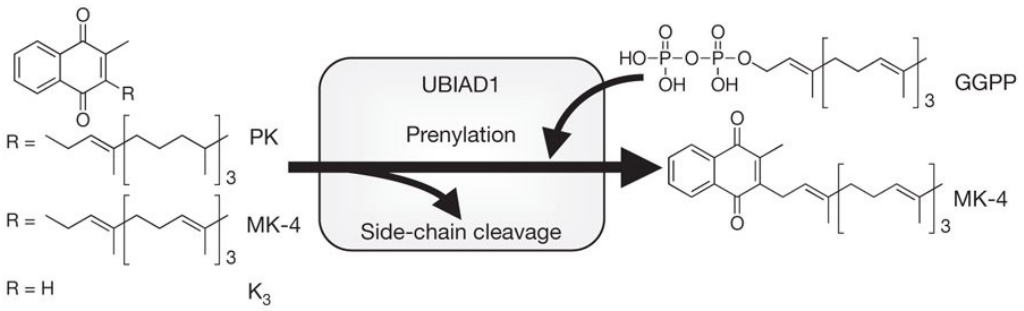


**Figure 3.15.** The conversion of different Vitamin K into MK-4 catalyzed by UBIAD1. This figure was adapted from Nakagawa *et al*. (34).

To investigate our hypothesis, we first tested the antibacterial activity of a MenA inhibitor, CSU-20 (39) (**Table 3.1**), with or without added quinones in the growth media. As shown in **Table 3.1**, supplementation with menadione, phylloquinone or MK-4 did not significantly affect the activity of CSU-20 against *S. aureus*. In contrast, the bacterial survived from exposure to several MenB inhibitor (3-6 × MIC) after the growth media was supplemented with menadione. Our results suggest that menadione could not be converted

into menaquinone in *S. aureus* cells treated with CSU-20. Furthermore, we conducted a parallel experiment in which we tested the MIC of CSU-20 in two growth media, MH-II and CDM. As expected, the same MIC was observed from both groups, further suggesting that not only the *de novo* biosynthesis but also the menaquinone conversion were inhibited by this MenA inhibitor. Although we cannot eliminate the possibility of off-target inhibition, our data demonstrate that MenA is likely involved in this salvage pathway. In future work, more potent MenA inhibitors will be tested to confirm our observation.

**Table 3.1.** Antibacterial activity of CSU-20 and several MenB inhibitors with or without exogenous quinones.

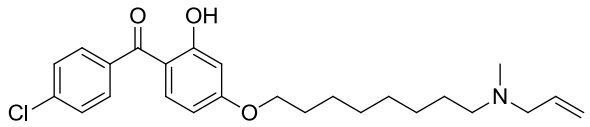


CSU-20

| Compound | Complement | Media | MIC (µg/ml) | MIC increase |
|---|---|---|---|---|
| CSU-20 | None | | 32 | |
| | MD (50 µg/ml) | | 36 | |
| | PQ (50 µg/ml) | | 32 | |
| | MK-4 ( 50µg/ml) | | 32 | |
| M-8 | None | | 0.35 | |
| | MD ( 50µg/ml) | | 2 | 6 fold |
| M-17 | None | | 1 | |
| | MD ( 50µg/ml) | | 4 | 4 fold |
| M-4 | None | | 4 | |
| | MD ( 50µg/ml) | | 12 | 3 fold |
| CSU-20 | | MH II | 32 | |
| | | CDM | 32 | |

To explore whether MenA catalyzes the formation of menaquinone from exogenous quinone-based molecules, we subsequently focused on performing the MenA reaction *in vitro*. However, although MenA has been studied as a potential antibacterial target for years, purification of this trans-membrane protein has proven challenging. To achieve our research goal, two previously reported experimental strategies provided approaches to investigate the function of MenA. The first approach involved transformation of the *menA* gene into a host that does not have menaquinone biosynthesis pathway nor MenA homologs, similar to the method used by Nakagawa *et al.* to elucidate the function of UBIAD1 in sf9 cells (34). A second method, which was used during the discovery of MenA inhibitors, involved the use of a lipid fraction containing the MenA protein (39, 40). We conducted our experiments using the second method. The genomic DNA from *S. aureus* (RN4220) was extracted and the *menA* sequence was cloned into a plasmid pET15b. The target gene was overexpressed in *E. coli* and the MenA containing lipid fraction was separated (39). As shown in **Figure 3.17**, *sa*MenA was successfully overexpressed in *E. coli* after IPTG induction (IPTG+). In contrast, a similar procedure in which the lipid fraction from *E. coli* that was not treated with IPTG did not give a corresponding band on sodium dodecyl sulfate-polyacrylamide gel electrophoresis (SDS-PAGE) (IPTG- in **Figure 3.16**).

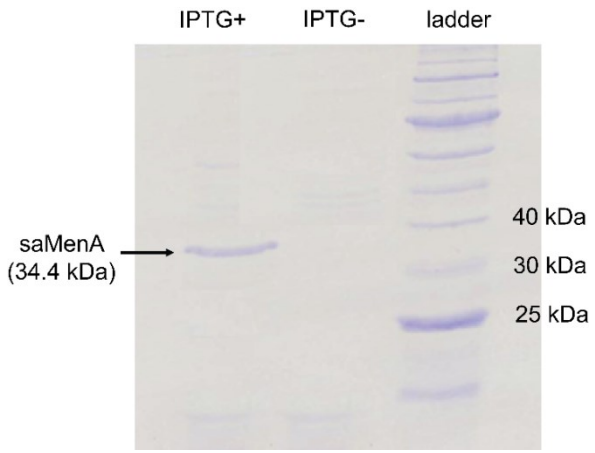


**Figure 3.16.** Identification of *sa*MenA in lipid fraction. A clear band with a molecular mass corresponding to that of *sa*MenA is observed in the MenA enriched lipid fraction from *E. coli*.

Subsequently, we performed an *in vitro* MenA reaction as previously reported by Kurosu *et al* (39). To measure *sa*MenA activity in the lipid fraction, we first used DHNA and geranylgeranyl pyrophosphate (GGPPi) as the substrates and identified the reaction product, demethylmenaquinone-4 (DMMK-4), using MS/MS. As shown in **Figure 3.17**, the condensation reaction did not occur spontaneously in the buffer, nor could it be catalyzed by the lipid fraction collected from IPTG- *E. coli*. In contrast, DMMK-4 was detected from the reaction initiated with the lipid fraction containing *sa*MenA, supporting that the MenA enzyme remained active. In addition, menadione and phylloquinone were used to react with GGPPi to identify whether *sa*MenA utilize these quinones as substrates for menaquinone synthesis. As shown in **Figure 3.18**, formation of MK-4 was observed from the MD + GGPPi reaction. This result demonstrates that MenA is the enzyme responsible for menaquinone conversion from menadione. This is significant because menadione has not been identified as a substrate for menaquinone biosynthesis in the past. However, no MK-4 was detected from the phylloquinone + GGPPi reaction, suggesting

that *sa*MenA cannot convert quinone molecules with substituents on both C-2 and C-3 position. A similar result was observed in a parallel experiment using 2,3-dimethyl-naphthoquinone (diMe) as a substrate. In contrast, UBIAD1 has been reported to catalyze menaquinone conversion from both menadione and phylloquinone, suggesting that this sole enzyme is responsible for both removal and attachment of the polyisoprenyl side chain. But the same study also showed that UBIAD1 had significantly higher activity in the conversion of menadione rather than phylloquinone into MK-4 (>1,000 fold) (34). This observation demonstrates that the removal of the C-3 side chain was evidently slower than the corresponding prenylation step. With respect to our findings, it is possible that the conversion from phylloquinone to MK-4 occurred very slowly and was below the detection limit of the assay. Nevertheless, we cannot rule out the possibility that a separate enzyme in *S. aureus* is responsible for cleaving the side chain. In summary, we have demonstrated that *sa*MenA utilizes menadione as a substrate and converts it into menaquinone by attaching a polyisoprenyl side chain. This observation supports our hypothesis that MenA is responsible for the menaquinone salvage pathway in the *menD*$^{-}$ strain, which complemented the disruption of the *de novo* biosynthesis.

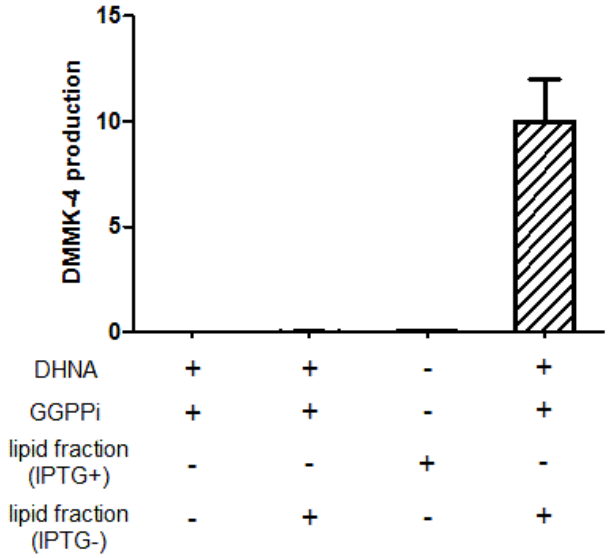


**Figure 3.17.** *In vitro* MenA reaction of DHNA and GGPPi. This reaction does not occur spontaneously (lipid fraction -) and can be catalyzed by the MenA enriched lipid fraction (IPTG+). The product is identified by APCI-MS/MS.

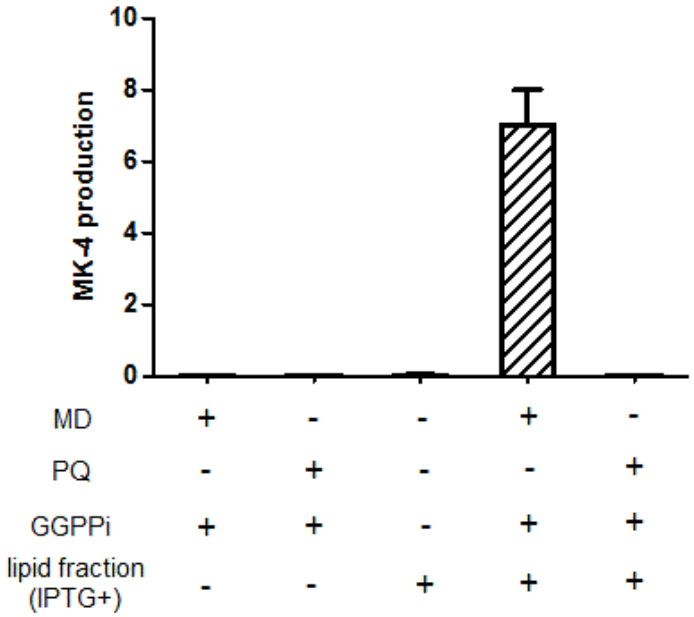


**Figure 3.18.** *In vitro* MenA reaction of GGPPi and menadione (MD) or phylloquinone (PQ). The reactions do not occur spontaneously and the conversion from menadione to menaquinone-4 can be catalyzed by the MenA enriched lipid fraction. The product is identified by APCI-MS/MS.

**Summary**

In this study, we examined the viability of a menaquinone defect *S. aureus* strain (*menD*$^-$) under different conditions. We observed slower growth of this mutant in rich media, which is consistent with previous knowledge of bacterial SCVs. Furthermore, we demonstrated that the *menD*$^-$ strain could not survive in minimal media, suggesting that disruption of menaquinone biosynthesis is fatal for *S. aureus* in the absence of exogenous supplements. We subsequently identified a series of 1,4-naphthoquinone-based molecules, in addition to menadione (MD), that could restore bacterial growth of the *menD*$^-$ strain in chemically defined media (CDM). Using an MS/MS-based quantification method, we demonstrated that menaquinone biosynthesis was restored in the complemented mutant cells. Thus, we proposed a conversion mechanism, which was then supported by complementation experiments using deuterium labeled quinone isotopologues to restore bacterial menaquinone biosynthesis and hence cell growth. Based on our knowledge of the human Ubi prenyltransferase (UBIAD1) that has been showed to catalyze a similar menaquinone conversion in mammalian cells, we propose that 1,4-dihydroxy-2-naphtoate prenyltransferase (MenA) is a candidate that catalyzes the salvage conversion from diverse quinone molecules. We subsequently showed that the antibacterial activity of a MenA inhibitor (CSU-20) did not change in the presence of quinone supplements, supporting our hypothesis that MenA functions in both the *de novo* biosynthesis pathway and cellular conversion of menaquinone. Moreover, we conducted an *in vitro* reaction using a MenA-enriched lipid fraction, and demonstrated that this candidate enzyme can utilize menadione as a substrate for menaquinone synthesis.

Our study demonstrates that menaquinone deficiency caused by a disruption of the *menD* gene is fatal for bacteria in the absence of quinone supplements. The hallmark of this sub-set of SCVs is an auxotrohphy for menadione. Complementation studies reveal that other quinone-based molecules can also lead to growth recovery. However, in each case it is found that this occurs by conversion of the added quinones to a complete set of menaquinone species as observed in the wild type *S. aureus.* The *in vitro* reaction suggests that MenA functions in a key step in this salvage pathway by prenylating the naphthoquinone nucleus. Although studies with the human homolog of MenA suggest that this protein can also remove the prenyl side chain, we did not observe this activity with our *sa*MenA overexpression strain. We also note that prenyl cleavage catalyzed the human MenA occurred more than a 1000 fold more slowly than the prenylation reaction, suggesting the existence of an additional enzyme in both human and bacterial cells that is required for utilization of exogenous quinones. The results suggest that both the *de novo* and salvage pathways must be inhibited to prevent growth of *S. aureus* in the presence of an external qunione source, and thus that MenA is an excellent target for drug discovery. It remains to be determined whether this salvage activity is sufficient to allow *S. aureus* to grow *in vivo* in the presence of compounds that inhibit menaquinone biosynthesis upstream from MenA.

## Experimental Procedures

*Materials and bacterial strains*

Chemicals: All general chemicals used in this study were purchased from Sigma-Aldrich. MK-4, Phylloquinone, ubiquinone-10, menadione and 1,4- naphthoquinone were also purchased from Sigma-Aldrich. MK-7 was purchased from Wako chemicals USA. GGPPi was purchased from Sigma-Aldrich. Bacterial culture media were purchased from BD. Bacteria: *S. aureus* RN4220 was provided by Dr. Stephen. Walker. The *menD*$^-$ *S. aureus* strain was a gift from Dr. Karsten Becker (Institute of Medical Microbiology, University of Münster, Germany).

*Cell growth recovering experiments*

Wild type. *S. aureus* RN4220 was grown on TSB agar containing 5% sheep blood. A single colony was used to inoculate 10 mL TSB media in a 50 mL falcon tube, which was subsequently incubated at 37 °C. After the culture had reached mid log phase ($OD_{600}$ value = 0.5-0.6), 100 μL bacterial culture was used to inoculate 50 mL sterile TSB, HM or CDM in a 200 mL flask, respectively. The flasks were shaken (200 rpm) at 37 °C for 36 h. The $OD_{600}$ value was monitored at different time point, and the bacterial growth curves were then depicted.

Mutant. The *menD*$^-$ *S. aureus* was grown on TSB agar containing 5% sheep blood. Colonies were used to inoculate 10 mL TSB media in a 50 mL falcon tube, which was subsequently incubated at 37 °C. After the culture had reached mid log phase ($OD_{600}$ value = 0.5-0.6), 100 μL bacterial culture was used to inoculate 50 mL sterile TSB, HM or CDM in a 200 mL flask, respectively. The flasks were shaken (200 rpm) at 37 °C for 36 h. The

$OD_{600}$ value was monitored at different time point, and the bacterial growth curves were then depicted.

Rescue. The *menD*$^-$ *S. aureus* was grown on TSB agar containing 5% sheep blood. Colonies were used to inoculate 10 mL TSB media in a 50 mL falcon tube, which was subsequently incubated at 37 °C. After the culture had reached mid log phase ($OD_{600}$ value = 0.5-0.6), 100 µL of the bacterial culture was used to inoculate 50 mL sterile CDM in a 200 mL flask. Quinones were dissolved in DMSO and were then added into bacterial cultures with a final concentration of 50 µg/mL. In a separate group, the *menD*$^-$ cells were incubated in CDM spiked with DMSO alone as a control. The flasks were shaken (200 rpm) at 37 °C for 36 h. The $OD_{600}$ value was monitored at different time point and the bacterial growth curves were then depicted.

*Menaquinone extraction from rescued menD*$^-$ *bacteria and menaquinone identification using MS/MS*

The *menD*$^-$ *S. aureus* was grown on TSB agar containing 5% sheep blood. Colonies were used to inoculate 10 mL TSB media in a 50 mL falcon tube, which was subsequently incubated at 37 °C. After the culture had reached mid log phase ($OD_{600}$ value = 0.5-0.6), 100 µL of the bacterial culture was used to inoculate 100 mL sterile CDM in a 200 mL flask. Quinones were dissolved in DMSO and were then added into bacterial cultures with a final concentration of 50 µg/mL. The final concentration of complements was 50 µg/ml. The flasks were shaken (200 rpm) at 37 °C until the cells have reached mid log phase ($OD_{600}$ value = 0.6). Cell pellets were collected by centrifugation (5000 rpm, 30min) and were washed with phosphate buffer (50 mM $KH_2PO_3$, pH 7.0). The cell pellets were then

suspended in 30 mL phosphate buffer. Lipid extraction was performed following the same protocol which has been discussed in Chapter II. The final MS/MS samples were prepared in 500 µl of methanol/chloroform (1/2, v/v). Identification of menaquinone in cell extracts was performed using APCI-MS/MS by monitoring the specific MRM ion transitions (Chapter II).

*Synthesis of deuterium label quinone isotopologues, and the utility of using these molecules to recover menaquinone biosynthesis in the menD⁻ strain*

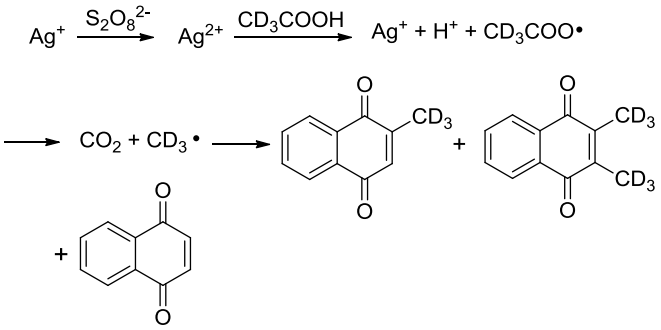


**Figure 3.19.** Mechanism of the radical reaction used for MD-$d_3$ and diMe-$d_3$ synthesis.

Deuterium-labeled menadione and 2,3-dimethyl-1,4-naphthoquinone were synthesized by methylation of 1,4-naphthoquinone. This reaction is a radial reaction and the mechanism is shown in **Figure 3.19**. In brief, 1 mmol 1,4-naphthoquinone, 2 mmol $AgNO_3$ and 2.5 mmol $Na_2S_2O_8$ were weighed out and were added to a 50 ml round bottom flask (RBF). 10 ml acetonitrile and 5 ml $D_2O$ were then added to the RBF and the mixture was subsequently heated to 65 °C using an oil bath. The reaction was initiated by adding 5 drops of $CD_3COOD$ and was stirred for 3 hr under inert conditions at 65 °C. The reaction was quench by adding 10 mL brine to the RBF and the products were extracted with ethyl

acetate twice. Separation of the products was conducted by running a silica column using ethyl acetate / hexane gradient (from 1/30 to 1/20 to 1/10).

The *menD*$^-$ cells were co-incubated with each compound in CDM. Cell lipid was subsequently extracted from harvested bacterial pellets as discussed in chapter II. APCI-MS/MS was used to identify the presence of menaquinone in cell extracts. MRM transition of normal and deuterium-labeled menaquinone species were both monitored simultaneously. Notably, both the parent ions and the daughter ions of MK-n-$d_3$ have a +3 Da shift due to the presence of the $CD_3$ group (**Table 3.2**).

**Table 3.2.** Primary and secondary ionization of MK-n-*$d_3$*.

| Compound | Parent ion (M+1) | Daughter ion |
|---|---|---|
| MK-4-$d_3$ | 448 | 190 |
| MK-5-$d_3$ | 516 | 190 |
| MK-6-$d_3$ | 584 | 190 |
| MK-7-$d_3$ | 652 | 190 |
| MK-8-$d_3$ | 720 | 190 |
| MK-9-$d_3$ | 788 | 190 |

*Antibacterial activity of CSU-20*

MIC values were determined with the microbroth dilution assay according to the Clinical and Laboratory Standards Institutes methods for antimicrobial susceptibility testes for aerobically growing bacteria (41). Procedures to determine MIC values have been discussed in chapter II. In this study, MICs were tested against *S. aureus* with or without addition of exogenous quinone molecules. Complements were dissolved in DMSO and were spiked into media to give a final concentration of 50 µg/ml. All antibacterial assays

were conducted at Stony Brook University (SBU), Department of Oral Biology and Pathology under Biosafety level-2 (BSL-2) conditions.

*Cloning, overexpression and separation of saMenA*

*S. aureus* RN4220 was cultured in MH broth at 37 °C to log phase ($OD_{600}$ value = 0.8). Cell pellets were collected by centrifugation (5,000 rpm, 30 min). Genomic DNA from RN4220 was extracted and purified using a commercial genomic DNA purification kit (Wizard®). The *samenA* gene was amplified using the polymerase chain reaction (PCR) with the following primers: 5'- GTTTAATTAATAAATGCCTGCAAATAATGC – 3' (forward) and 5'- AGCTCACTAGTATGAGTAATCAATATCAGC – 3' (reverse). The PCR product, confirmed by DNA gel, was digested with PacI and BclI (New England Biolab), and then inserted into pET15b plasmid (Novagen) (**Figure 3.20**). Successful insertion of the *samenA* gene was confirmed by DNA sequencing (the DNA Sequencing Facility, Health Science Center, SBU).

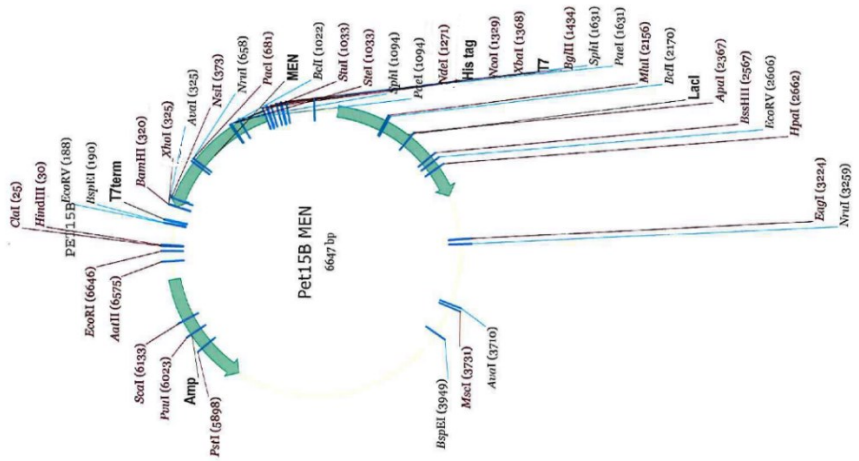


**Figure 3.20.** Cloning of *sa*menA into plasmid pET15b.

The *samenA* plasmid was transformed into the *E. coli* strain BL21 (DE3) cells which were then incubated on Luria Broth (LB) agar containing ampicillin (0.2 mg/ml). A single colony was used to inoculate 10 mL of LB media containing 0.2 mg/ml ampicillin. The culture was incubated overnight at 37 °C and then used to inoculate 1 L of LB media containing 0.2 mg/ml ampicillin. The culture was incubated at 37 °C until the optical density ($OD_{600}$) increased to 0.8 - 0.9. Protein expression was induced at 25 °C by adding isopropyl-1-thio-β-D-galactopyranoside (IPTG, 1mM) with a final concentration of 1 mM. The cell culture was then shaken at 25 °C for 16 hours. Bacterial cells were harvested by centrifugation (5,000 rpm, 30 min at 4 °C) and the resulting cell pellets were washed with and then resuspended in homogenization buffer containing 50 mM MOPS (pH 7.8), 0.25 M sucrose, 10 mM $MgCl_2$ and 5 mM 2-mercaptoethanol. Cells were disrupted by sonication on ice with 20 cycles of 30 sec on and 45 sec off. The resulting suspension was centrifuged at 8,000 rpm (27,000 × g) for 20 min. The pellets were discarded and the supernatant was centrifuged at 33,000 rpm (100,000 × g) for 60 min using a Beckman ultracentrifuge. After ultracentrifugation, the supernatant was carefully discarded and the pellet was resuspended in homogenization buffer, divided into aliquots and frozen at -80 ºC. The correct molecular weight of *sa*MenA was confirmed on a SDS protein gel.

*In vitro MenA reaction*

The *in vitro* MenA reaction was performed as described previously (42). 500 μM of quinone substrate (DHNA, MD, or PQ) and 10 μM of GGPPi were added to 2 mL reaction buffer containing 5 mM $MgCl_2$, 0.1% CHAPS and 100 mM MOPS (pH = 8). Reactions were performed at 30 °C after the addition of 10 μg *sa*MenA. The reaction was quenched

by adding 1 ml 0.1 M AcOH in MeOH. The product was extracted twice with 3 mL of hexanes and the combined extracts were dried under $N_2$. The residue was subsequently dissolved in 300 μL MeOH/$CHCl_3$ (1/2) for MS/MS analysis.

**References**


1. Proctor RA*, et al.* (2006) Small colony variants: a pathogenic form of bacteria that facilitates persistent and recurrent infections. *Nat Rev Microbiol* 4(4):295-305.
2. von Eiff C (2008) Staphylococcus aureus small colony variants: a challenge to microbiologists and clinicians. *Int J Antimicrob Agents* 31(6):507-510.
3. Colwell CA (1946) Small Colony Variants of Escherichia coli. *J Bacteriol* 52(4):417-422.
4. Bryan LE & Kwan S (1981) Aminoglycoside-resistant mutants of Pseudomonas aeruginosa deficient in cytochrome d, nitrite reductase, and aerobic transport. *Antimicrob Agents Chemother* 19(6):958-964.
5. HALL WH & SPINK WW (1947) In vitro sensitivity of Brucella to streptomycin; development of resistance during streptomycin treatment. *Proc Soc Exp Biol Med* 64(4):403-406.
6. Proctor RA & Peters G (1998) Small colony variants in staphylococcal infections: diagnostic and therapeutic implications. *Clin Infect Dis* 27(3):419-422.
7. Lannergård J*, et al.* (2008) Identification of the genetic basis for clinical menadione-auxotrophic small-colony variant isolates of Staphylococcus aureus. *Antimicrob Agents Chemother* 52(11):4017-4022.
8. Garcia LG*, et al.* (2012) Pharmacodynamic evaluation of the activity of antibiotics against hemin- and menadione-dependent small-colony variants of Staphylococcus aureus in models of extracellular (broth) and intracellular (THP-1 monocytes) infections. *Antimicrob Agents Chemother* 56(7):3700-3711.

9. Vaudaux P, Kelley WL, & Lew DP (2006) Staphylococcus aureus small colony variants: difficult to diagnose and difficult to treat. *Clin Infect Dis* 43(8):968-970.

10. Maduka-Ezeh A*, et al.* (2012) Thymidine auxotrophic Staphylococcus aureus small-colony variant endocarditis and left ventricular assist device infection. *J Clin Microbiol* 50(3):1102-1105.

11. von Eiff C, Proctor RA, & Peters G (2000) Staphylococcus aureus small colony variants: formation and clinical impact. *Int J Clin Pract Suppl* (115):44-49.

12. Tuchscherr L*, et al.* (2010) Staphylococcus aureus small-colony variants are adapted phenotypes for intracellular persistence. *J Infect Dis* 202(7):1031-1040.

13. Kahl BC*, et al.* (2003) Population dynamics of persistent Staphylococcus aureus isolated from the airways of cystic fibrosis patients during a 6-year prospective study. *J Clin Microbiol* 41(9):4424-4427.

14. von Eiff C, Proctor RA, & Peters G (2000) Small colony variants of Staphylococci: a link to persistent infections. *Berl Munch Tierarztl Wochenschr* 113(9):321-325.

15. Seaman PF, Ochs D, & Day MJ (2007) Small-colony variants: a novel mechanism for triclosan resistance in methicillin-resistant Staphylococcus aureus. *J Antimicrob Chemother* 59(1):43-50.

16. Proctor RA, van Langevelde P, Kristjansson M, Maslow JN, & Arbeit RD (1995) Persistent and relapsing infections associated with small-colony variants of Staphylococcus aureus. *Clin Infect Dis* 20(1):95-102.

17. Gómez-González C*, et al.* (2010) Clinical and molecular characteristics of infections with CO2-dependent small-colony variants of Staphylococcus aureus. *J Clin Microbiol* 48(8):2878-2884.

18. Slifkin M, Merkow LP, Kreuzberger SA, Engwall C, & Pardo M (1971) Characterization of CO 2 dependent microcolony variants of Staphylococcus aureus. *Am J Clin Pathol* 56(5):584-592.

19. McNamara PJ & Proctor RA (2000) Staphylococcus aureus small colony variants, electron transport and persistent infections. *Int J Antimicrob Agents* 14(2):117-122.

20. Koo SP, Bayer AS, Sahl HG, Proctor RA, & Yeaman MR (1996) Staphylocidal action of thrombin-induced platelet microbicidal protein is not solely dependent on transmembrane potential. *Infect Immun* 64(3):1070-1074.

21. Balwit JM, van Langevelde P, Vann JM, & Proctor RA (1994) Gentamicin-resistant menadione and hemin auxotrophic Staphylococcus aureus persist within cultured endothelial cells. *J Infect Dis* 170(4):1033-1037.

22. von Eiff C*, et al.* (2006) Phenotype microarray profiling of Staphylococcus aureus menD and hemB mutants with the small-colony-variant phenotype. *J Bacteriol* 188(2):687-693.

23. Bates DM*, et al.* (2003) Staphylococcus aureus menD and hemB mutants are as infective as the parent strains, but the menadione biosynthetic mutant persists within the kidney. *J Infect Dis* 187(10):1654-1661.

24. von Eiff C*, et al.* (1997) A site-directed Staphylococcus aureus hemB mutant is a small-colony variant which persists intracellularly. *J Bacteriol* 179(15):4706-4712.

25. Baumert N*, et al.* (2002) Physiology and antibiotic susceptibility of Staphylococcus aureus small colony variants. *Microb Drug Resist* 8(4):253-260.

26. Jamison JM, Gilloteaux J, Taper HS, & Summers JL (2001) Evaluation of the in vitro and in vivo antitumor activities of vitamin C and K-3 combinations against human prostate cancer. *J Nutr* 131(1):158S-160S.

27. Bolton-Smith C, Price RJ, Fenton ST, Harrington DJ, & Shearer MJ (2000) Compilation of a provisional UK database for the phylloquinone (vitamin K1) content of foods. *Br J Nutr* 83(4):389-399.

28. Beulens JW*, et al.* (2010) Dietary phylloquinone and menaquinones intakes and risk of type 2 diabetes. *Diabetes Care* 33(8):1699-1705.

29. Cox GB, Newton NA, Gibson F, Snoswell AM, & Hamilton JA (1970) The function of ubiquinone in Escherichia coli. *Biochem J* 117(3):551-562.

30. Søballe B & Poole RK (1999) Microbial ubiquinones: multiple roles in respiration, gene regulation and oxidative stress management. *Microbiology* 145 ( Pt 8):1817-1830.

31. Papa S*, et al.* (2002) The NADH: ubiquinone oxidoreductase (complex I) of the mammalian respiratory chain and the cAMP cascade. *J Bioenerg Biomembr* 34(1):1-10.

32. Hirota Y, *et al.* (2013) Menadione (vitamin K3) is a catabolic product of oral phylloquinone (vitamin K1) in the intestine and a circulating precursor of tissue menaquinone-4 (vitamin K2) in rats. *J Biol Chem* 288(46):33071-33080.

33. Okano T, *et al.* (2008) Conversion of phylloquinone (Vitamin K1) into menaquinone-4 (Vitamin K2) in mice: two possible routes for menaquinone-4 accumulation in cerebra of mice. *J Biol Chem* 283(17):11270-11279.

34. Nakagawa K, *et al.* (2010) Identification of UBIAD1 as a novel human menaquinone-4 biosynthetic enzyme. *Nature* 468(7320):117-121.

35. Kurosu M & Crick DC (2009) MenA is a promising drug target for developing novel lead molecules to combat Mycobacterium tuberculosis. *Med Chem* 5(2):197-207.

36. Dhiman RK, *et al.* (2009) Menaquinone synthesis is critical for maintaining mycobacterial viability during exponential growth and recovery from non-replicating persistence. *Mol Microbiol* 72(1):85-97.

37. Suhara Y, Wada A, & Okano T (2009) Elucidation of the mechanism producing menaquinone-4 in osteoblastic cells. *Bioorg Med Chem Lett* 19(4):1054-1057.

38. Davidson RT, Foley AL, Engelke JA, & Suttie JW (1998) Conversion of dietary phylloquinone to tissue menaquinone-4 in rats is not dependent on gut bacteria. *J Nutr* 128(2):220-223.

39. Kurosu M, Narayanasamy P, Biswas K, Dhiman R, & Crick DC (2007) Discovery of 1,4-dihydroxy-2-naphthoate [corrected] prenyltransferase inhibitors: new drug leads for multidrug-resistant gram-positive pathogens. *J Med Chem* 50(17):3973-3975.

40. Crick DC*, et al.* (2000) Polyprenyl phosphate biosynthesis in Mycobacterium tuberculosis and Mycobacterium smegmatis. *J Bacteriol* 182(20):5771-5778.

41. Institutes CaLS (2012) methods for antimicrobial susceptibility testes for aerobically growing bacteria.

42. Shineberg B & Young IG (1976) Biosynthesis of bacterial menaquinones: the membrane-associated 1,4-dihydroxy-2-naphthoate octaprenyltransferase of Escherichia coli. *Biochemistry* 15(13):2754-2758.

## Chapter IV. *In vivo* Antibacterial Activity of Enoyl-ACP Reductase (FabI) Inhibitors and the Impact of Drug-Target Kinetics on Therapeutic Efficacy

### Introduction

In traditional antibiotic development, evaluation of novel lead compounds depends heavily on *in vitro* thermodynamic parameters such as $IC_{50}$, $K_i$ and MIC values. Tight binding between drug molecules and their targets is commonly pursued in drug design and further modifications to enhance activity. Notably, these parameters are determined in a closed system while drug concentrations remain invariant. In contrast, the *in vivo* environment consists of an open system where the drug concentrations and target exposure fluctuate over time. As a consequence, *in vivo* results are often not accurately predicted by *in vitro* measurements (1). Indeed, thermodynamic parameters can only accurately predict therapeutic efficacy if *in vivo* drug levels are sufficiently constant that they approximate the equilibrium conditions.

In an open system, the kinetics of drug-target interactions becomes more important when predicting *in vivo* efficacy (2-6). The duration of drug binding is controlled by the dissociation rate constant ($k_{off}$), or residence time ($t_R$, $1/k_{off}$), and drugs with long residence time are proposed to have better efficacy (5, 7). The first work using residence time as a parameter for drug discovery was reported by Laysen *et al*. in 1986 (8). This concept gained more interest as Zhang *et al.* reported that 50 marketed drugs with long residence time demonstrated improved therapeutic efficacy (1). Recent evidence to support this hypothesis have been reported for Hsp90 inhibitors (9), renin inhibitors (10), purine nucleoside phosphorylase inhibitors (11), angiotensin II antagonists (12) and

antimuscarinics (13). In addition, further evidence for the importance of drug-target residence time has been obtained through studies in our lab, in which the *in vivo* efficacy of a series of diphenyl ether-based *Francisella tularensis* enoyl reductase (FabI) inhibitors correlated with residence time rather than with $K_i$ or MIC values (**Figure 4.1**) (14).

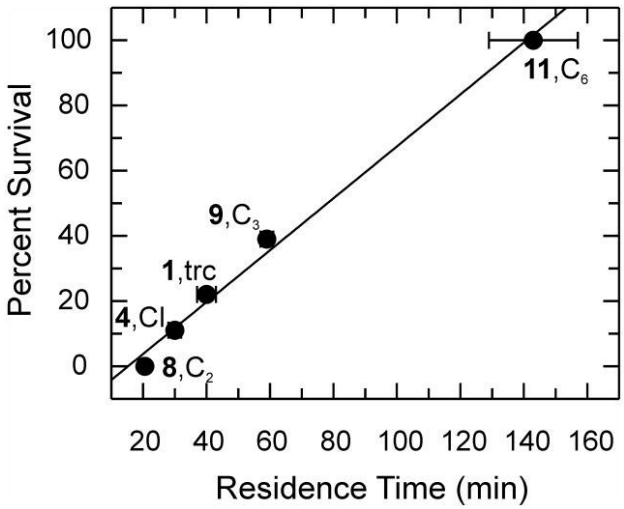


**Figure 4.1.** Correlation between residence time for a series of FabI inhibitors and their *in vivo* efficacy in a tularemia animal model of infection (14).

Until recently, relatively little has been known about the correlation between the kinetics of drug-target binding and *in vivo* efficacy. Further experimental evidence is needed to substantiate the concept that prolonged duration of *in vivo* activity results from longer residence time. In this project, the antibacterial activity of selected FabI inhibitors, with a range of $t_R$ values, was determined in a mouse model of MRSA infection. We then analyzed the correlation between residence time and the *in vivo* efficacy. Additionally, the *in vivo* post-antibiotic effect (PAE) of different drugs was measured and the potential correlation with residence time was explored. In addition, the *in vivo* activity of a series TLM derivatives was evaluated in a mouse model of MRSA.

## Result and Discussion

*MIC of FabI inhibitors against MRSA*

In this project, a series of diphenyl ether-based *S. aureus* FabI inhibitors were selected from our compound library for the evaluation of *in vivo* efficacy in a mouse model of MRSA (BAA 1762). The selection was based on a criterion that the compounds have similar chemical structures but have distinctive residence time ranging from 6 minutes to over 10 hours. The *in vitro* antibacterial activity of these *sa*FabI inhibitors was first determined. As shown in **Table 4.1**, the MIC values of these compounds were within a range of 0.5-8 μg/mL, indicating that these FabI inhibitors were active against MRSA.

**Table 4.1**. MIC values of diphenyl ether FabI inhibitors against MRSA (BAA1762).

| Compound | Structure | MIC (μg/mL)[a] | MIC (μM) | $t_R$ (min)[b] |
|---|---|---|---|---|
| PT-01 | 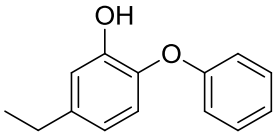 | 2 | 9.35 | 83.8 |
| PT-04 | 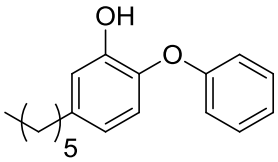 | 4 | 14.81 | 461.5[c] |
| PT-52 | 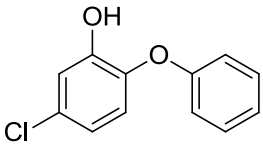 | 1 | 4.54 | 35.3 |
| PT-55 | 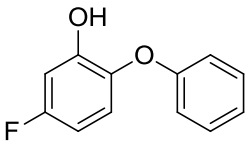 | 8 | 37.38 | 6.2 |

| | | | | |
|---|---|---|---|---|
| PT-119 | 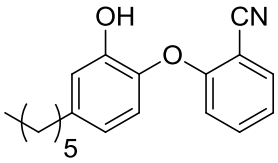 | 1 | 1.69 | 750[c] |
| PT-443 | 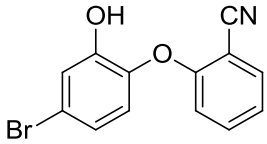 | 1 | 3.46 | 210.9 |

[a] MIC values were determined in duplicates and are shown in average.
[b] Determined by Dr. Andrew Chang.
[c] Determined by Weixuan Yu using a $^{32}$P-NAD-based method.

*In vivo activity of FabI inhibitors against MRSA infections*

We evaluated the *in vivo* activity of FabI inhibitors in two mouse infection models of MRSA, the systemic infection model and the thigh infection model. By using these two models, we explored the impact of drug residence time on systemic protection against lethal infection, which could be compared with our previous study; we also investigated how bacterial growth in a specific tissue was affected by drug with different residence time. In the systemic infection model, mice were inoculated with a lethal dose of bacterial inoculum and received doses of either vehicle or one of the FabI inhibitors. Survival of the infected mice is depicted in **Figure 4.2**. The overall survival percentage and average survival time in each group are summarized in **Table 4.2**. Our data showed that all animals treated with empty vehicle died within 2 days post infection, given an average survival time of 1.4 days. In contrast, the FabI inhibitors, except for PT-55, exhibited *in vivo* activity against MRSA, resulting in prolonged survival time and increased survival rate. Significantly, PT-119 rescued 50% of the infected mice (n=10) from mortality with an average survival time of 4.6 days.

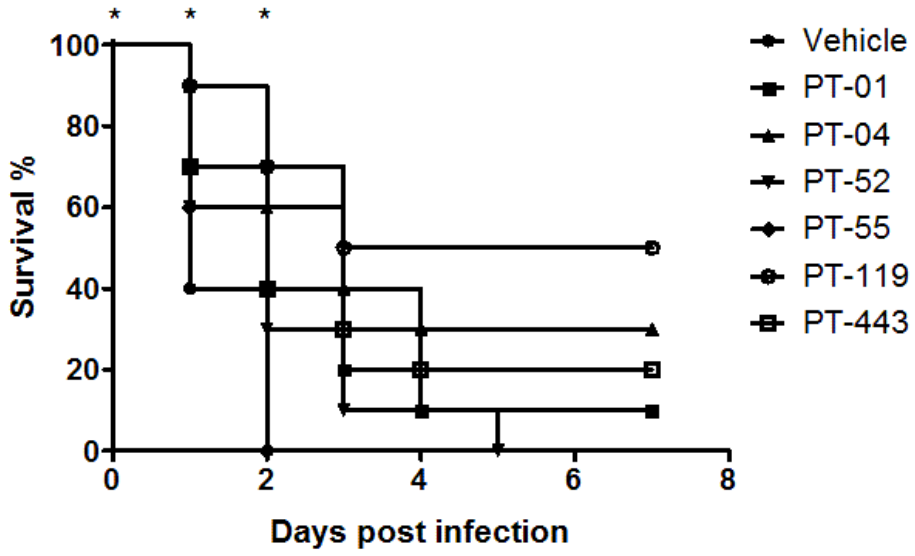


**Figure 4.2**. Survival of systemically infected mice treated with FabI inhibitors.
* time points when treatments were given.

**Table 4.2.** Percentage of survival and average survival time of infected animals treated with different agents.

| Treatment | Survival percentage (%) | Average survival time ± SEM (days) |
|---|---|---|
| Vehicle | 0 | 1.4 ± 0.22 |
| PT-01 | 10 | 2.6 ± 0.55 |
| PT-04 | 30 | 4.1 ± 0.77 |
| PT-52 | 0 | 2.1 ± 0.39 |
| PT-55 | 0 | 1.6 ± 0.22 |
| PT-119 | 50 | 4.6 ± 0.78 |
| PT-443 | 20 | 3.3 ± 0.89 |

We subsequently evaluated these FabI inhibitors in the thigh infection model of MRSA. As previously discussed, the infection was induced in CPA-rendered neutropenic mice by injecting bacterial inoculum into the left thigh muscle. The infected mice received

a single dose of either vehicle or one of the FabI inhibitors immediately following infection. A single dose treatment was used to better demonstrate the impact of residence time on *in vivo* efficacy, which would eliminate other potential effects such as drug accumulation. Bacterial load at infection site was determined 24 hours after inoculation. As shown in **Figure 4.3**, bacterial counts in thigh muscle was reduced in all drug treated groups in comparison to that observed in the vehicle control. Both PT-04 and PT-443 significanlty reduced bacterial burden by 1.71 and 1.64 log CFU/thigh, P value =0.05. Consistent with our data from the systemic infection model, PT-119 exhibited the best *in vivo* anti-MRSA activity, resulting in the greatest decrease of bacterial burden of 3.06 log CFU/thigh (P value =0.001) (**Figure 4.4**).

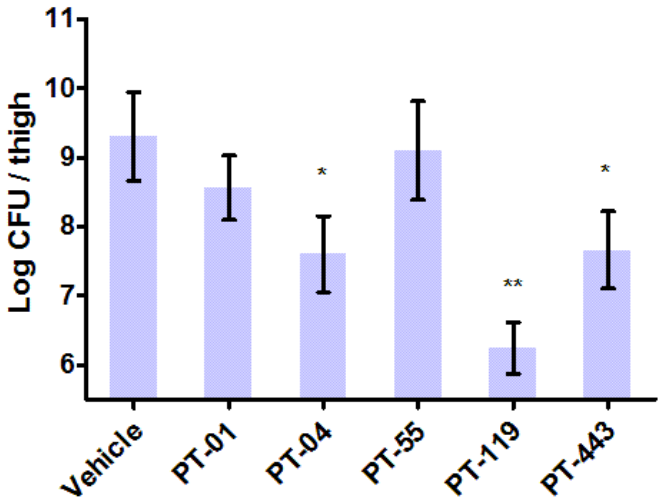


**Figure 4.3.** Thigh muscle bacterial load in mice treated with FabI inhibitors. Error bars represent SEM. * P value = 0.05. ** P value = 0.001.

*Correlation between in vivo antibacterial activity and residence time*

As discussed above, the lifetime of a drug-target complex ($t_R$) is thought to be an important component of *in vivo* drug efficacy given that drug concentration fluctuates in

the human body. We thus assessed the impact of drug-target residence time on the activity of the FabI inhibitors. The $K_i$, MIC and $t_R$ values of the FabI inhibitors together with their *in vivo* activity are given in **Table 4.3**.

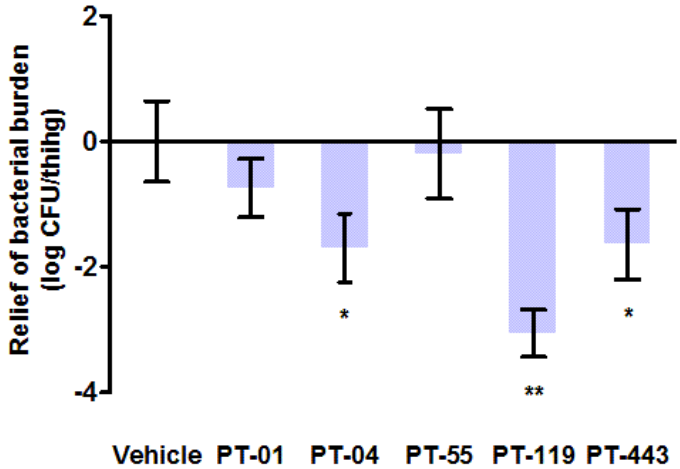


**Figure 4.4.** Reduction of bacterial burden in thigh infection model. Error bars represent SEM. * P value = 0.05. ** P value = 0.001.

**Table 4.3**. *In vitro* and *in vivo* data of tested FabI inhibitors.

| Compound | $K_i$ (nM)[a] | MIC[b] (μM) | $t_R$ (min)[a] | Survival rate (%) | Relief of bacterial burden (Log CFU/thigh) |
|---|---|---|---|---|---|
| PT-01 | 0.09 ± 0.01 | 9.35 | 83.8 | 10 | 0.74 ± 0.32 |
| PT-04 | 0.01 | 14.81 | 461.5[c] | 30 | 1.70 ± 0.49 |
| PT-52 | 0.12 ± 0.02 | 4.54 | 35.3 | 0 | 0.16 ± 0.33 |
| PT-55 | 1.42 ± 0.10 | 37.38 | 6.2 | 0 | 0.18 ± 0.45 |
| PT-119 | 0.01 | 1.69 | 750[c] | 50 | 3.06 ± 0.33 |
| PT443 | 0.05 ± 0.01 | 3.46 | 210.9 | 20 | 1.64 ± 0.45 |

[a] Determined by Dr. Andrew Chang.
[b] Determined against MRSA strain BAA 1762
[c] Determined by Weixuan Yu using a $^{32}$P-NAD-based method

The *in vivo* efficacy of the FabI inhibitors was first plotted with respect to their MIC values (**Figure 4.5**). We observed that both animal survival rate (left) and relief of bacterial burden (right) did not correlate well with MIC ($R^2$ = 0.224 and 0.577, respectively). For example, PT-119, PT-443 and PT-52 showed very similar MIC values but exhibited significantly different *in vivo* activity. Although MIC describes by definition the minimum concentration required to inhibit bacterial growth, it can only describe antibacterial activity of an agent when drug concentration is constant. Our data further support the hypothesis that *in vivo* efficacy cannot be precisely predicted from MIC values.

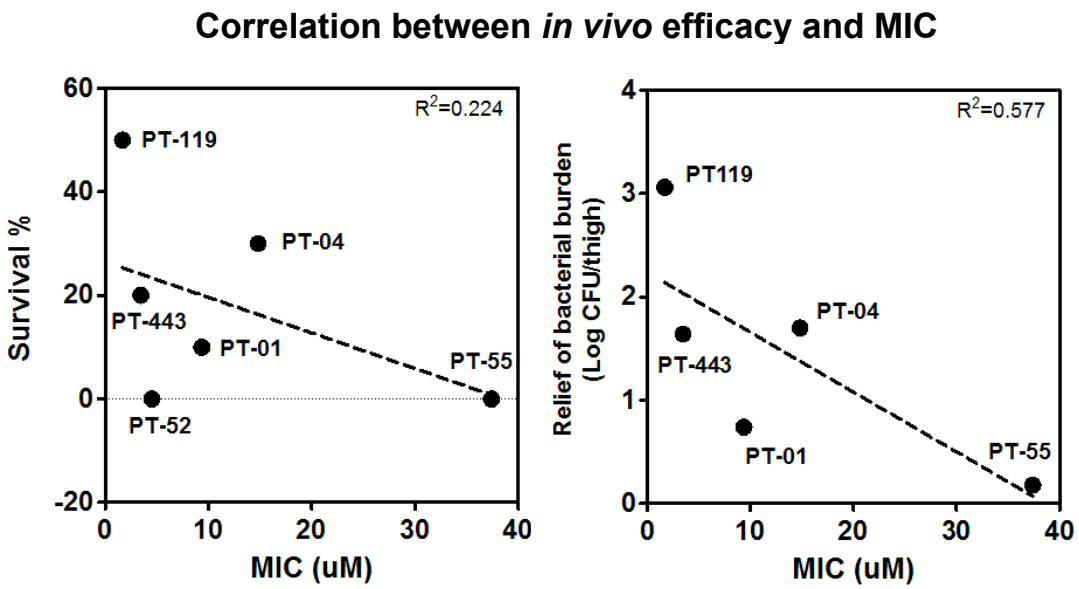


**Figure 4.5.** Correlation between *in vivo* activities for FabI inhibitors against systemic (left) and thigh (right) infection of MRSA and their corresponding MIC values. Dash lines represent linear regression.

The *in vivo* efficacy of FabI inhibitors was then correlated with their $K_i$ values, which describe the binding affinity between drug molecules and the target enzyme. As shown in **Figure 4.6**, FabI inhibitors including PT-01, PT-04, PT-52, PT119 and PT443

increased the survival rate in systemic infection mice, and the *in vivo* activity exhibited a linear correlation with their $K_i$ values ($R^2 = 0.842$). However, this correlation excluded data collected from PT-55 treated mice (no survival) because PT-55 has a $K_i$ value that is 100 fold greater PT-04 and PT-119. When PT-55 was incorporated (figure not shown), no correlation was observed ($R^2 < 0.250$). Additionally, PT-04 and PT-119, which gave identical $K_i$ values, resulted in significantly different *in vivo* outcomes in both infection models. Our observations suggest the inaccuracy of predicting *in vivo* therapeutic activity based on equilibrium-based parameters.

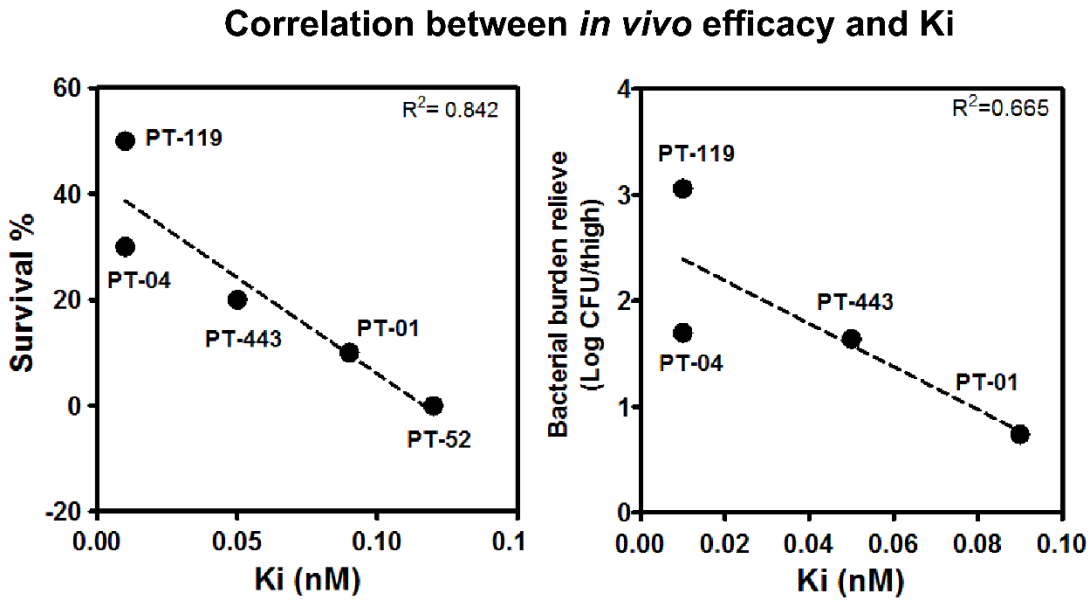


**Figure 4.6.** Correlation between *in vivo* activities for FabI inhibitors against systemic (left) and thigh (right) infection of MRSA and their corresponding $K_i$ values. Dash lines represent linear regression.

Finally, the *in vivo* efficacy of FabI inhibitors was correlated with their residence times. As shown in **Figure 4.7**, linear correlations were observed in both infection models ($R^2 = 0.947$ and 0.903), suggesting that longer residence time had significant impact on

improving *in vivo* antibacterial activity. For example, treatment of PT-119, which has the longest $t_R$, resulted in the highest survival rate and the greatest reduction of bacterial burden. In contrast, PT-55, which is a rapid reversible FabI inhibitor, barely exhibited any activity against MRSA *in vivo*. Unlike $K_i$ and MIC that are determined under equilibrium conditions, residence time and the more fundamental parameter $k_{off}$ represent the dissociation rate that is resistant to changes of environmental drug levels.

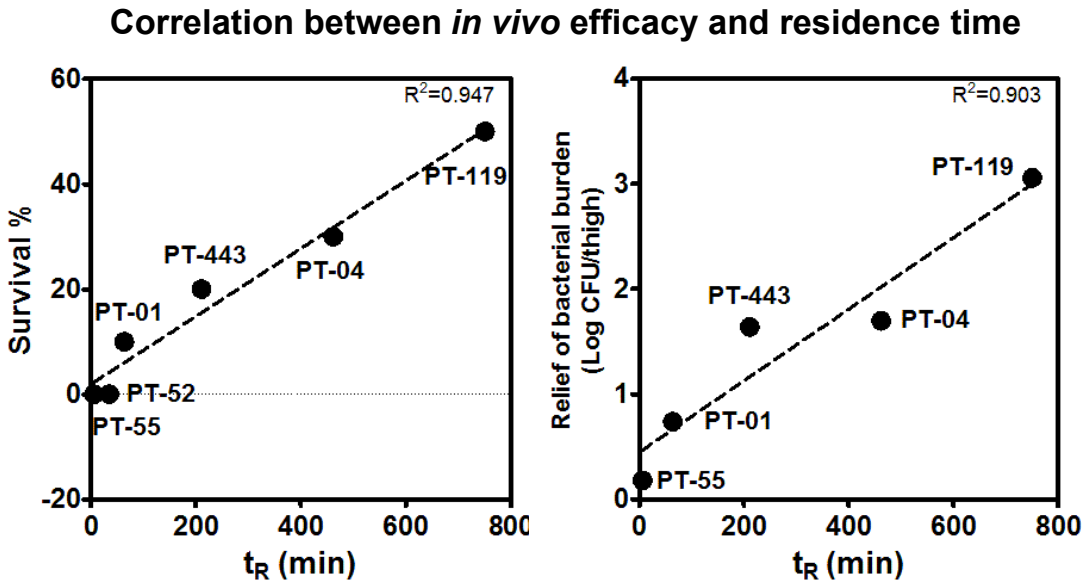


**Figure 4.7.** Correlation between *in vivo* activities of FabI inhibitors against systemic (left) and thigh (right) infection and their corresponding $t_R$ values. Dash lines represent linear regression.

Indeed, we are aware that *in vivo* activity of even structurally related molecules is affected by many other factors, such as drug distribution and metabolism. It is also unlikely that residence time can be utilized as a sole determinant to predict *in vivo* efficacy of a drug in such a complex system. Additionally, residence times of drugs that belong to different classes are difficult to compare with each other. Nevertheless, our data highlight the

limitations of correlating the equilibrium-based thermodynamic parameters with outcomes of *in vivo* studies. The results further emphasize the importance of residence time, which provides a relevant approach to translate *in vitro* data into therapeutic efficacy. In summary, our study substantiates the concept that the kinetics of drug-target interaction should be utilized, together with thermodynamic data, in advancing compounds along the drug discovery pipeline.

*Pharmacokinetic measurements on FabI inhibitors*

Pharmacokinetics (PK) is the study of the time course of drug concentration in different body compartments such as blood, urine and tissues. To understand the combined effect from residence time and PK on *in vivo* efficacy, we performed PK measurements on selected FabI inhibitors (PT-01, PT-04, PT-52 and PT-119) with a range of $t_R$ values. A representative drug concentration-time curve (from PT-52) is depicted in **Figure 4.8**, and the core PK parameters are summarized in **Table 4.4**. We observed that the PK profiles of FabI inhibitors were relatively similar. These results were expected given that these compounds share the same diphenyl ether backbone. Notably, all of these FabI inhibitors showed fast elimination from plasma, which was a consequence of tissue distribution due to their lipophilic property. The results also demonstrate that the *in vivo* antibacterial efficacy was not solely determined by PK profile. For example, PT-01 and PT-04 had greater peak plasma concentrations ($C_{max}$) and area under the curve values ($AUC_{0\text{-}24h}$) than PT-119, but were not as effective in terms of treating MRSA infections *in vivo*. Our data further support the hypothesis that residence time has significant impact on *in vivo* efficacy of the FabI inhibitors.

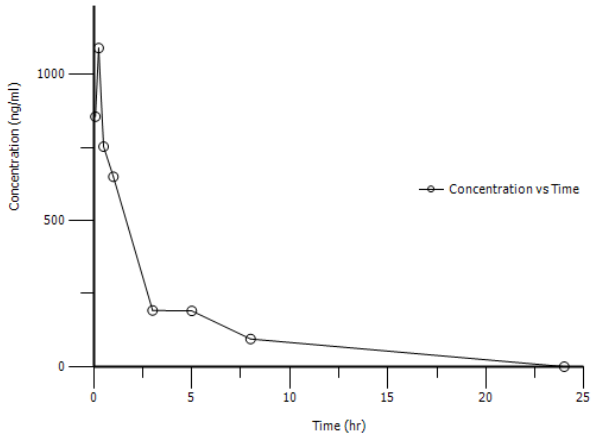


**Figure 4.8.** Representative drug concentration-time curve in PT52 treated mice.

**Table 4.4.** Core PK parameters of FabI inhibitors.

| | PT-01[a] | PT-04[a] | PT-52 | PT-119 |
|---|---|---|---|---|
| Dose (mg/kg) | 100 | 200 | 100 | 100 |
| $\lambda_z$ ($hr^{-1}$) | 0.2210 | 0.1556 | 0.2619 | 0.1418 |
| $T_{max}$ (hr) | 0.5 | 1.0 | 0.25 | 1 |
| $C_{max}$ (ng/mL) | 3229.3 | 3706.2 | 1240.4 | 1256.8 |
| $AUC_{0-24}$ (hr×ng/mL) | 6953.8 | 11798.4 | 3839.2 | 4264.9 |
| $T_{1/2}$ (hr) | 3.13 | 4.5 | 2.2 | 4.88 |

[a] Determined by Dr. Li Liu.

*Determination of in vivo post-antibiotic effect (PAE)*

To investigate whether antibiotics with long residence time have prolonged duration of action *in vivo*, we then determined the post-antibiotic effect (PAE) of several FabI inhibitors in the thigh infection model of MRSA. PAE is a widely used measurement that describes the persistent antimicrobial effect following drug removal (15, 16). Though various mechanisms may contribute simultaneously to such phenomena (17, 18), residence

time is known to be a factor that can contribute to extended duration of drug action. To determine whether our FabI inhibitors produced a PAE *in vivo*, we identified the bacterial burden in a thigh infection model at different time points after drug treatment. Three FabI inhibitors with distinctive $t_R$ values (PT-52, PT-04 and PT-119) were evaluated. The initial phase of *in vivo* MRSA growth is depicted in **Figure 4.9**. A bacterial growth curve almost identical to the control was observed in PT-52 treated mice, except for a minimal delay in the first hour. The PK data suggest that the *in vivo* PT-52 concentration decreases to a sub-MIC level within 15 minutes. Previous kinetic studies suggest that PT-52 has a short residence time ($t_R$ = 35 minutes). Therefore, it is understandable that we observed recovery of bacterial growth in PT-52 treated mice resembling the control group. In contrast, significantly delayed bacterial growth was observed in PT-119 treated groups, in which no increase of bacterial load was detected until 6 hours post inoculation. We noted that the plasma drug concentration of PT-119 dropped to a sub-MIC level within 1 hour after administration. This result suggests that drugs with longer residence time had persistent *in vivo* efficacy. Additionally, bacteria exhibited slower growth rate in PT-119 treated mice in comparison to the control and the PT-52 treated group. We hypothesize that the slow dissociation of this long residence time extended the duration of drug action.

Notably, the drug removal step, which is simple in an *in vitro* PAE experiment, is impossible to perform in an animal model. This makes it difficult to select the starting "zero" time point. Therefore, we have to use PK measurements when correlating persistent *in vivo* efficacy with residence time. Nevertheless, our data demonstrate that residence time has significant impact on duration of drug action *in vivo*. This is important because prolonged therapeutic activity is a critical benefit when pursuing drug development. Our

work also provides valuable information for further *in vitro* and *in vivo* studies on drug-target binding kinetics. More importantly, our study can be integrated with pharmacokinetic and pharmacodynamics (PK/PD) modeling in future to generate a more comprehensive, more predictive model to facilitate drug discovery.

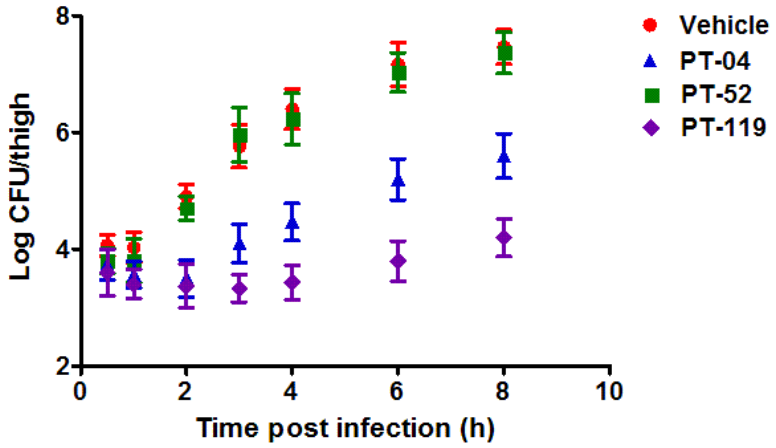


**Figure 4.9.** Bacterial burdens at the early phase of thigh infection in mice treated with vehicle (●, n=5), PT-04 (▲, n=5), PT-52 (■, n=5), and PT-119 (♦, n=5). The error bars represent SEM. PT-52 and PT-119 demonstrate prolonged *in vivo* efficacy in terms of inhibiting the growth of bacterial burden in thigh muscle.

*In vivo efficacy and target specificity of a 4-pyridone-based FabI inhibitor, PT-166*

Diphenyl ether derivatives have recently been reported in the antibacterial pipeline of different drug companies (19-21). For example, Mutabilis has identified a traiclosan-based candidate, MUT056399 (22, 23). This compound is reported active against *S. aureus* with MIC values ranging between 0.05-0.1 μg/mL, and has activity in mouse infection models (24). Despite these promising initial results, MUT056399 exhibited a limitation in terms of its pharmacokinetic feature: the hydroxyl group is unstable that resulted in rapid phase II metabolism (25). To overcome this problem, a modified scaffold in which the phenyl ring is replaced by a pyridone was developed, and the new candidate showed similar

activity with enhanced PK properties (25). In addition, the phenol ring was replaced by a pyridone in another case of CG400549 developed by CrystalGenomics. CG400549 has been reported active against both methicillin-sensitive and methicillin-resistant strains of *S. aureus,* and has passed the Phase 2a study by showing human efficacy without serious adverse events. In our efforts to develop FabI inhibitors, we have also explored replacing the diphenyl ether with a pyridone-based scaffold. A series of pyridone-based compounds have been demonstrated active *in vitro* (**Table 4.5**). In this initial study, the PK profile and the *in vivo* anti-MRSA efficacy of a representative pyridone FabI inhibitor, PT-166 were determined. In addition, the cellular target of this compound in *S. aureus* was elucidated.

**Table 4.5.** *In vitro* activity of reprehensive pyridone-based FabI inhibitors against *S. aureus*.

| Inhibitor | Structure | $K_i$ (nM)[a] | MIC (μg/mL)[b] |
|---|---|---|---|
| CG-400549 | 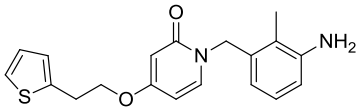 | 1.27 ± 0.13 | 4 |
| PT-173 | 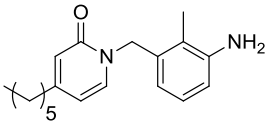 | 1.97 ± 0.42 | 8 |
| PT-172 | 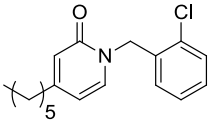 | 10.98 ± 0.35 | 16 |
| PT-166 | 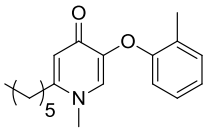 | 2.71 ± 0.57 | 0.5 |
| PT-159 | 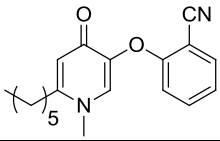 | 11.04 ± 0.92 | 16 |

[a] Determined by Dr. Andrew Chang

[b] MIC values were measured against MRSA strain, BAA 1762

We first demonstrated that PT-166 was active against the MRSA strain *in vitro*, having an identical MIC of 0.5 µg/mL as against MSSA (**Table 4.5**). We then evaluated the *in vivo* efficacy of this compound in a MRSA thigh infection model in neutropenic mice. As shown in **Figure 4.10**, PT-166 (100 mg/kg) significantly reduced bacterial burden at the infection site by 2.9 log CFU / thigh. Moreover, PT-166 was more active than its diphenyl-ether analogue PT-04 and the control drug (oxacillin). In addition, PT-166 possessed a better PK profile than PT-04 (**Table 4.6**), resulting in 9-fold and 5-fold increases in $C_{max}$ and $AUC_{0\text{-}24h}$, respectively. Our results suggest that the pyridone-based FabI inhibitors are promising candidates for future development.

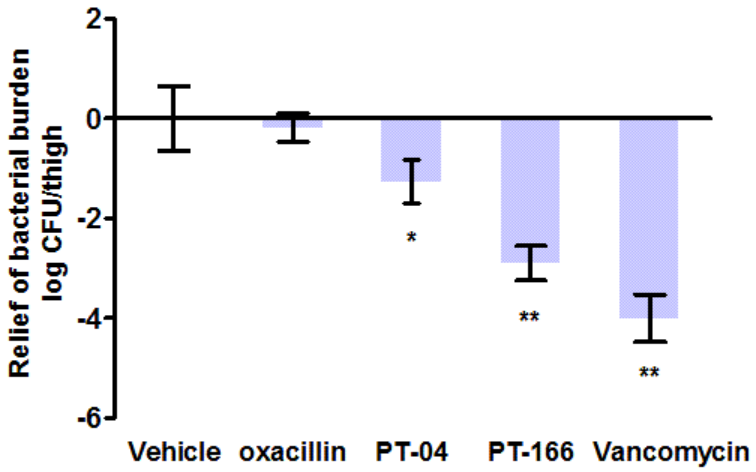


**Figure 4.10.** Reduction of thigh bacterial burden in PT-166 treated mice (100 mg/kg, n=5) comparing to vehicle control. * P=0.05. ** P≤0.002

**Table 4.6.** Core PK parameters of PT-166 and PT-04

| | PT-166 | PT-04[a] |
|---|---|---|
| Dose (mg/kg) | 100 | 200 |
| $T_{max}$ (hr) | 0.25 | 1.0 |
| $C_{max}$ (ng/mL) | 45880.3 | 5106.2 |
| $AUC_{0-24}$ (hr×ng/mL) | 55031.8 | 11798.4 |
| $T_{1/2}$ (hr) | 2.7 | 4.5 |

[a] Determined by Dr. Li Liu

In order to confirm that *sa*FabI is the main cellular target of PT166, we performed selection experiments by investigating mutations in the *fabI* gene from *S. aureus* strains resistant to PT-166. Notably, spontaneous resistance was induced at a relatively low frequency between $1.4 \times 10^{-8}$ and $5.6 \times 10^{-8}$ when exposed to this molecule at 5 × MIC level. By examining the *fabI* sequence in resistant bacteria, we observed point mutations including the previously characterized A95V (**Table 4.7**) that was conserved in all isolated strains (26, 27). X-ray crystal structures of *sa*FabI in complex with inhibitors have previously demonstrated that Ala97 plays a critical role in drug binding (27). Therefore, our data suggest that FabI is the cellular target of PT-166 in *S. aureus*.

**Table4.7**. Point mutations observed in PT166 resistant *S. aureus* strains

| Strain | Nucleotide change | Amino acid change | MIC (μM) |
|---|---|---|---|
| RN4220 | - | - | 0.8 |
| 166R.1 | GCA → GTA | A95V | 8.8 |
| 166R.2 | GCA → GTA | A95V | 8.8 |
| 166R.3 | GCA → GTA<br>TTC → TTG | A95V<br>F252L | 8.8 |
| 166R.4 | GCA → GTA<br>GAA → GAT | A95V<br>E71D | 8.8 |
| 166R.5 | No change | No change | 17.6 |

*Antibacterial activity of thiolactomycin (TLM) derivatives against MRSA*

The elongation step in FAS-II is catalyzed by β-ketoacyl-ACP synthases (KAS) *via* decarboxylative Claisen condensation (28, 29). KAS has been previously demonstrated as another potential antibacterial target in various pathogens (30-32). Thiolactomycin (TLM) was first isolated by Okazaki *et al.* (33-35) and was characterized as a reversible inhibitor for KAS enzymes. Despite moderate MIC values, TLM showed broad spectrum *in vivo* antibacterial activity against various Gram-positive, Gram-negative and *Mycobacteria* (35, 36). In a parallel project, we determined the *in vitro* and *in vivo* activity of a series of TLM derivatives against MRSA. As summarized in **Table 4.8**, several TLM derivatives, which have different substitutions on C3 position, gave MIC values significantly lower than that of TLM. The SAR analysis suggested that an acetyl-based C3 side chain resulted in improved activity. As an initial study, we then evaluated several active derivatives including TLM-5, TLM-6, TLM-9 and TLM-11, in addition to the parent drug TLM, in a

systemic MRSA infection model in mice. As shown in **Figure 4.11**, TLM-6 was the only TLM analogue that exhibited *in vivo* efficacy, which significantly prolonged the average survival time of the infected mice from 1.4 ± 0.22 days to 4.2 ± 1.04 days. This was important because TLM derivatives have not been used as antibacterial agents against *S. aureus*. We then conducted a dose escalating study on TLM-6 and demonstrated that the *in vivo* efficacy of this compound was dose dependent (**Figure 4.12**). Despite the similar chemical structure and the similar in MIC value, TLM-6, which has a C3-trifluoro-methyl acetyl substituent, exhibited distinctively different *in vivo* efficacy from TLM-5, which constitutes a C3-methyl acetyl group. These data were understandable given that trifluoro-methyl group has been previously reported to facilitate PK parameters, and to ultimately improve the *in vivo* efficacy of drugs (37, 38). In future work, detail PK evaluations on TLM-based compounds will be performed to elucidate mechanism of the enhanced *in vivo* efficacy of TLM-6. Nevertheless, our data demonstrate that a series of TLM derivatives were active against MRSA both *in vitro* and *in vivo*, and have the potential to be developed as novel candidates for this prominent resistant pathogen.

**Table 4.8.** *In vitro* antibacterial activity of TLM derivatives against *S. aureus*

| Compound | Structure | | MIC (µg/mL) | |
|---|---|---|---|---|
| | R | R’ | MSSA (RN4220) | MRSA (BAA1762) |
| TLM | -OH | $-CH_3$ | 96 | 96 |
| TLM-2 | -OH | -H | >128 | >128 |
| TLM-3 | -OH | $-CH_2CH_3$ | >128 | >128 |
| TLM-4 | -OH | $-(CH_2)_2CH_3$ | >128 | >128 |
| TLM-5 | -OH | | 64 | 32 |
| TLM-6 | -OH | | 128 | 64 |
| TLM-7 | -OH | | 16 | 32 |
| TLM-8 | -OH | | >128 | >128 |
| TLM-9 | -OH | | 0.5 | 1 |
| TLM-10 | -OH | | 32 | 32 |

| | | | | |
|---|---|---|---|---|
| TLM-11 | -OH | 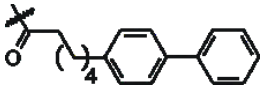 | 0.5 | 2 |
| TLM-12 | -OH | 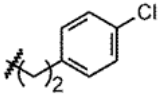 | 64 | 96 |
| TLM-13 | -OH | 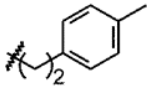 | >128 | >128 |
| TLM-14 | -OH | 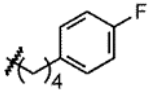 | 64 | 96 |
| TLM-15 | -OH | 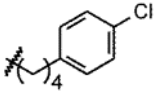 | 32 | 48 |
| TLM-16 | -OH | 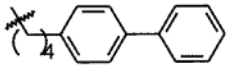 | 16 | 32 |
| TLM-17 | -OH | 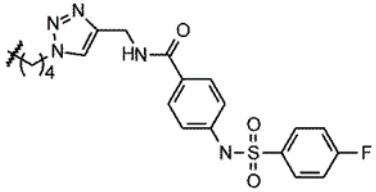 | >128 | >128 |
| TLM-18 | -OH | 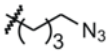 | >128 | >128 |
| TLM-19 | -OH | 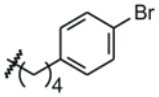 | 32 | 48 |
| TLM-20 | -OH | 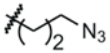 | >128 | >128 |
| TLM-21 | -OH | 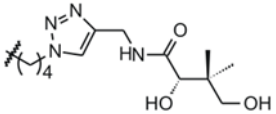 | >128 | >128 |

| | | | | |
|---|---|---|---|---|
| TLM-22 | 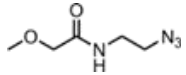 | -H | >128 | >128 |
| TLM-23 | 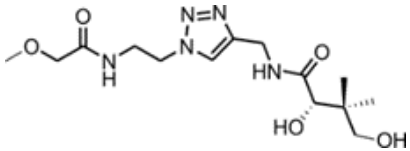 | -H | >128 | >128 |
| TLM-24 | 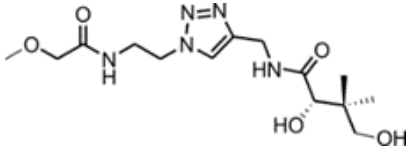 | -H | >128 | >128 |
| TLM-25 | 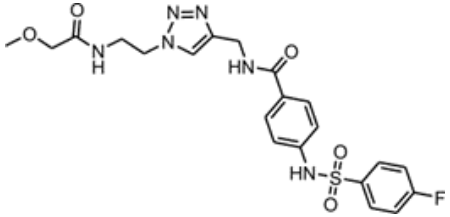 | H | >128 | >128 |
| TLM-26 | -OH | 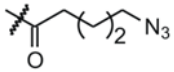 | 16 | 16 |

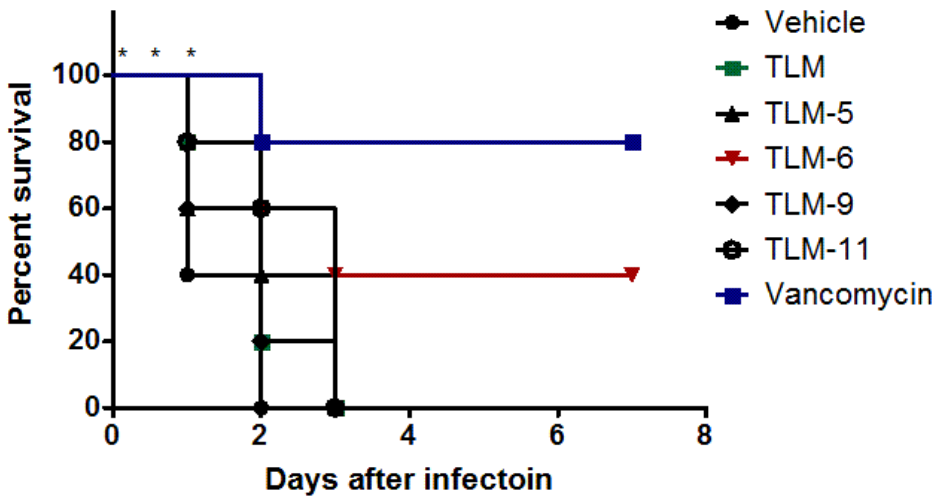


**Figure 4.11.** Survival of systemically infected mice treated with TLM derivatives (n=5) or vancomycin (n=5). * represents drug administrations**.**

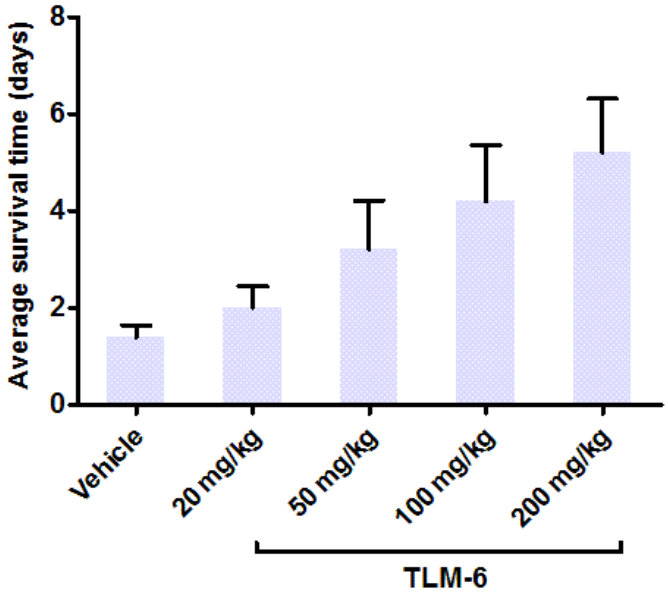


**Figure 4.12.** Average survival times of the infected mice treated with escalating doses of TLM-6 (n=5).

**Summary**

There is growing evidence that thermodynamic parameters such as $IC_{50}$, $K_i$ and MIC values should be supplemented with data on drug-target binding kinetics given that drug concentration fluctuates in the human body so that drug and target are not at equilibrium. To further explore the correlation between residence time and *in vivo* antibacterial efficacy of our inhibitors that target the enoyl-ACP reductase (FabI) from *S. aureus*, we evaluated a series of FabI inhibitors in a mouse model of MRSA infection. We demonstrate that the *in vivo* activity of the tested compounds, represented by prolonged survival time and reduction of bacterial burden at infection site, correlates more directly with residence time than with $K_i$ or MIC values. We also show, by determining the post-antibiotic effect (PAE) of FabI inhibitors in animal models, that longer residence time contribute to persistent *in vivo* antibacterial efficacy. Taken together, our experiments support the concept that the kinetics of drug-target interaction, in addition to the thermodynamic factors of drugs, should be considered in development of novel antibiotics.

## Experimental Procedures

Determination *of* MIC values

MIC values were determined with the microbroth dilution assay according to the Clinical and Laboratory Standards Institutes methods for antimicrobial susceptibility tests for aerobically growing bacteria (39). Procedures to determine MIC values have been discussed in Chapter II. All MIC values were tested in duplicate and the means were calculated.

*Identification of in vivo efficacy, in vivo PAE and PK profile*

The present animal studies were approved by the Institutional Animal Care and Use Committee (IACUC) at Stony Brook University. All animals were maintained in accordance with the American Association for Accreditation of Laboratory Animal Care criteria. Experiments were conducted under BSL-2 conditions in the Division of Laboratory Animal Resource (DLAR) at Stony Brook University. Six-week old, specific-pathogen free, male Swiss Webster mice weighing 27g to 32g (Taconic) were used in this study. Mice were provided *ad libitum* access to food and water through the entire experimental course.

Establishment of the systemic infection model and the thigh infection model in mice was discussed in Chapter II. Briefly, in the systemic infection model, infected animals were given daily treatments of vehicle (40% saline, 40% ethanol, 20% PEG-400) or one of the tested compounds, with dosage of 100 mg/kg, in the first three days post infection. Mortality of infected mice were checked every 12 hours for 7 days. Dead mice were immediately removed from the study. Surviving animals at the end of the experiment were

euthanized by $CO_2$ inhalation as recommended by the American Veterinary Medical Association (AVMA) Guidelines on Euthanasia. Overall survival rate and average survival time were calculated for each drug treatment group. In the thigh infection model, infected neutropenic mice were given a single dose of vehicle or one of the antibacterial agents, with a dosage of 100 mg/kg, 1 hour post infection. Mice were euthanized by $CO_2$ inhalation at 24 hours (efficacy), or at different time point post infection (*in vivo* PAE). Muscle tissue from the infected thighs was collected, weighed and homogenized in 2 mL of saline. Serial dilutions of each homogenized sample were plated on Mueller Hinton II agar containing 5% sheep blood. The number of viable bacteria were then counted following overnight incubation of plates at 37 °C. Bacterial burdens were subsequently calculated.

Pharmacokinetic (PK) studies were conducted in CD-1 mice via intraperitoneal administration of the tested agents in a vehicle of 40% $H_2O$ / 40% EtOH / 20% PEG-400. Plasma samples were collected from animals at eight distinct time points (5 min, 15 min, 30 min, 1 hour, 2 hours, 4 hours, 8 hours and 24 hours post-injection). Three mice were sampled per time point. Plasma concentrations for each sample were measured by LC/MS/MS with a pre-generated calibration curve, and PK parameters were calculated with WinNonlin (Pharsight Corporation, Mountain View, CA, USA).

*Selection for S. aureus RN4220 resistance to PT166*

RN4220 was cultured in Mueller Hinton II broth (MH-II) broth at 37 °C to log phase ($OD_{600}$ = 1.0, $10^9$ cells/mL). 250µl cell culture was incubated on a MH-agar plate consisting PT166 (2 µg/mL, 5 times MIC) at 37 °C for 48 hours. Numbers of viable colonies were counted. The "resistant" colonies were randomly picked from agar plates

and re-streaked on MH-II agar plates containing PT-166 (2 μg/mL) to confirm the induced resistance. Genomic DNA (gDNA) was extracted from resistant *S. aureus* strains and was purified using a Quick g-DNA Mini Prep kit (ZYMO research). The target fabI gene from each colony was amplified by PCR using the following primers: 5'-CTAATTAGGCATATGTTAAATCTTGAAAACAAAACG-3' (foward) and 5'-GTAAGTGCTCGAGTTATTTAATTGCGTGGAATCC-3' (reverse). Sequence of the PCR products were identified by the DNA Sequencing Facility at Stony Brook University.

**References:**


1. Swinney DC (2004) Biochemical mechanisms of drug action: what does it take for success? *Nat Rev Drug Discov* 3(9):801-808.
2. Swinney DC (2009) The role of binding kinetics in therapeutically useful drug action. *Curr Opin Drug Discov Devel* 12(1):31-39.
3. Copeland RA, Pompliano DL, & Meek TD (2006) Drug-target residence time and its implications for lead optimization. *Nat Rev Drug Discov* 5(9):730-739.
4. Tummino PJ & Copeland RA (2008) Residence time of receptor-ligand complexes and its effect on biological function. *Biochemistry* 47(20):5481-5492.
5. Lu H & Tonge PJ (2010) Drug-target residence time: critical information for lead optimization. *Curr Opin Chem Biol* 14(4):467-474.
6. Zhang R & Monsma F (2009) The importance of drug-target residence time. *Curr Opin Drug Discov Devel* 12(4):488-496.
7. Kumar P*, et al.* (2009) Update of KDBI: Kinetic Data of Bio-molecular Interaction database. *Nucleic Acids Res* 37(Database issue):D636-641.
8. Leysen J, and Gommeren, W. (1986) Drug-receptor dissociation time, new tool for drug research: receptor binding affinity and drug-receptor dissociation profiles of Serontonin-S2, dopamine-D2, Histamine-H1 antagonists, and opiates. (Drug Develop. Res.), pp 119-131.
9. Tillotson B*, et al.* (2010) Hsp90 (heat shock protein 90) inhibitor occupancy is a direct determinant of client protein degradation and tumor growth arrest in vivo. *J Biol Chem* 285(51):39835-39843.

10. Gossas T, *et al.* (2012) Aliskiren displays long-lasting interactions with human renin. *Naunyn Schmiedebergs Arch Pharmacol* 385(2):219-224.

11. Lewandowicz A, Tyler PC, Evans GB, Furneaux RH, & Schramm VL (2003) Achieving the ultimate physiological goal in transition state analogue inhibitors for purine nucleoside phosphorylase. *J Biol Chem* 278(34):31465-31468.

12. Fuchs B, *et al.* (2000) Comparative pharmacodynamics and pharmacokinetics of candesartan and losartan in man. *J Pharm Pharmacol* 52(9):1075-1083.

13. Disse B, Speck GA, Rominger KL, Witek TJ, & Hammer R (1999) Tiotropium (Spiriva): mechanistical considerations and clinical profile in obstructive lung disease. *Life Sci* 64(6-7):457-464.

14. Lu H, *et al.* (2009) Slow-onset inhibition of the FabI enoyl reductase from francisella tularensis: residence time and in vivo activity. *ACS Chem Biol* 4(3):221-231.

15. MacKenzie FM & Gould IM (1993) The post-antibiotic effect. *J Antimicrob Chemother* 32(4):519-537.

16. Stubbings W, Bostock J, Ingham E, & Chopra I (2006) Mechanisms of the post-antibiotic effects induced by rifampicin and gentamicin in Escherichia coli. *J Antimicrob Chemother* 58(2):444-448.

17. Yan S, Bohach GA, & Stevens DL (1994) Persistent acylation of high-molecular-weight penicillin-binding proteins by penicillin induces the postantibiotic effect in Streptococcus pyogenes. *J Infect Dis* 170(3):609-614.

18. Nikravesh A, *et al.* (2007) Antisense PNA accumulates in Escherichia coli and mediates a long post-antibiotic effect. *Mol Ther* 15(8):1537-1542.

19. Seefeld MA*, et al.* (2003) Indole naphthyridinones as inhibitors of bacterial enoyl-ACP reductases FabI and FabK. *J Med Chem* 46(9):1627-1635.

20. Payne DJ, Gwynn MN, Holmes DJ, & Pompliano DL (2007) Drugs for bad bugs: confronting the challenges of antibacterial discovery. *Nat Rev Drug Discov* 6(1):29-40.

21. Kaplan N*, et al.* (2012) Mode of action, in vitro activity, and in vivo efficacy of AFN-1252, a selective antistaphylococcal FabI inhibitor. *Antimicrob Agents Chemother* 56(11):5865-5874.

22. Gerusz V*, et al.* (2012) From triclosan toward the clinic: discovery of nonbiocidal, potent FabI inhibitors for the treatment of resistant bacteria. *J Med Chem* 55(22):9914-9928.

23. Escaich S*, et al.* (2011) The MUT056399 inhibitor of FabI is a new antistaphylococcal compound. *Antimicrob Agents Chemother* 55(10):4692-4697.

24. Park HS*, et al.* (2007) Antistaphylococcal activities of CG400549, a new bacterial enoyl-acyl carrier protein reductase (FabI) inhibitor. *J Antimicrob Chemother* 60(3):568-574.

25. Yum JH*, et al.* (2007) In vitro activities of CG400549, a novel FabI inhibitor, against recently isolated clinical staphylococcal strains in Korea. *Antimicrob Agents Chemother* 51(7):2591-2593.

26. Xu H*, et al.* (2008) Mechanism and inhibition of saFabI, the enoyl reductase from Staphylococcus aureus. *Biochemistry* 47(14):4228-4236.

27. Schiebel J, *et al.* (2014) Rational Design of Broad Spectrum Antibacterial Activity Based on a Clinically Relevant Enoyl-Acyl Carrier Protein (ACP) Reductase Inhibitor. *J Biol Chem* 289(23):15987-16005.

28. Campbell JW & Cronan JE (2001) Bacterial fatty acid biosynthesis: targets for antibacterial drug discovery. *Annu Rev Microbiol* 55:305-332.

29. Borgaro JG, Chang A, Machutta CA, Zhang X, & Tonge PJ (2011) Substrate recognition by β-ketoacyl-ACP synthases. *Biochemistry* 50(49):10678-10686.

30. Machutta CA, *et al.* (2010) Slow onset inhibition of bacterial beta-ketoacyl-acyl carrier protein synthases by thiolactomycin. *J Biol Chem* 285(9):6161-6169.

31. Schiebel J, *et al.* (2013) Structural basis for the recognition of mycolic acid precursors by KasA, a condensing enzyme and drug target from Mycobacterium tuberculosis. *J Biol Chem* 288(47):34190-34204.

32. Kapilashrami K, *et al.* (2013) Thiolactomycin-based β-ketoacyl-AcpM synthase A (KasA) inhibitors: fragment-based inhibitor discovery using transient one-dimensional nuclear overhauser effect NMR spectroscopy. *J Biol Chem* 288(9):6045-6052.

33. Oishi H, *et al.* (1982) Thiolactomycin, a new antibiotic. I. Taxonomy of the producing organism, fermentation and biological properties. *J Antibiot (Tokyo)* 35(4):391-395.

34. Sasaki H, *et al.* (1982) Thiolactomycin, a new antibiotic. II. Structure elucidation. *J Antibiot (Tokyo)* 35(4):396-400.

35. Noto T, Miyakawa S, Oishi H, Endo H, & Okazaki H (1982) Thiolactomycin, a new antibiotic. III. In vitro antibacterial activity. *J Antibiot (Tokyo)* 35(4):401-410.

36. Hamada S*, et al.* (1990) Antimicrobial activities of thiolactomycin against gram-negative anaerobes associated with periodontal disease. f1. *Oral Microbiol Immunol* 5(6):340-345.

37. Axten JM*, et al.* (2012) Discovery of 7-methyl-5-(1-{[3-(trifluoromethyl)phenyl]acetyl}-2,3-dihydro-1H-indol-5-yl)-7H-pyrrolo[2,3-d]pyrimidin-4-amine (GSK2606414), a potent and selective first-in-class inhibitor of protein kinase R (PKR)-like endoplasmic reticulum kinase (PERK). *J Med Chem* 55(16):7193-7207.

38. Foley TL*, et al.* (2014) 4-(3-Chloro-5-(trifluoromethyl)pyridin-2-yl)-N-(4-methoxypyridin-2-yl)piperazine-1-carbothioamide (ML267), a potent inhibitor of bacterial phosphopantetheinyl transferase that attenuates secondary metabolism and thwarts bacterial growth. *J Med Chem* 57(3):1063-1078.

39. Institutes CaLS (2012) methods for antimicrobial susceptibility testes for aerobically growing bacteria.

## Chapter V: Biological Evaluation of Enoyl-ACP Reductase Inhibitors using Positron Emission Tomography (PET)

### Introduction

Imaging techniques are becoming increasingly popular in medical practice and medical research. The most prominent advantage of medical imaging is that it provides a non-invasive approach for diagnosis and for monitoring disease progression. Positron Emission Tomography (PET) is one of the most advanced imaging techniques, which images drugs and other molecules labeled with positron-emitting isotopes such as carbon-11 ($^{11}C$), nitrogen-13 ($^{13}N$), and fluorine-18 ($^{18}F$) (**Table 5.1**) (1). In this method, a radionuclide on a labeled molecule (radiotracer) decays by positron emission ($\beta^+$ decay). Two 511 keV $\gamma$-rays are generated and emitted in opposite directions after annihilation between a positron and an electron (**Figure 5.1**), and have sufficient energy to penetrate tissue. During a PET scan, the instrument counts when each detector pair is hit in coincidence (2, 3). In subsequent two-dimensional (2D) or three-dimensional (3D) reconstruction algorithms, raw data from a PET scan that are simply a list of counts obtained along each line of response are converted into high-quality images for further analysis.

**Table 5.1.** Commonly used positron-emitting isotopes.

| Radionuclide | Half-life (min) | Nuclear reaction | Product | Decay product |
|---|---|---|---|---|
| $^{11}C$ | 20.4 | $^{14}N(p,\alpha)^{11}C$ | $[^{11}C]CO_2$<br>$[^{11}C]CH_4$ | $^{11}B$ |
| $^{13}N$ | 9.97 | $^{16}O(p,\alpha)$ | $[^{13}N]NO_x$<br>$[^{13}N]NH_3$ | $^{13}C$ |
| $^{15}O$ | 2.04 | $^{15}N(d,n)^{15}O$ | $[^{15}O]O_2$ | $^{15}N$ |
| $^{18}F$ | 110 | $^{18}O(p,n)^{18}F$ | $[^{18}F]F_2$ | $^{18}O$ |

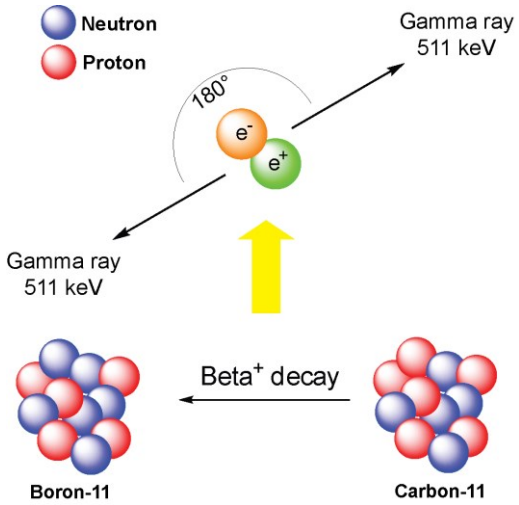


**Figure 5.1**. Mechanism of positron emission.

Since the invention of the first single-plane PET scanner in 1961 (4-6), advancement of PET imaging technique has come a long way, and PET has become an important medical probe to investigate location of diseases and the dynamics of drug absorption, distribution, metabolism, and elimination *in vivo*. Compared to other imaging techniques such as fluorescence imaging, PET does not require excitation of imaging agents from an external light source (7). Additionally, in design and preparation of PET

radiotracers, molecules of interest are labeled with isotopic elements instead of fluorophores which may affect the biological properties. Moreover, PET can map three-dimensional tissue distribution of a labeled molecule over time. Although it lacks spatial resolution in comparison to techniques such as magnetic resonance imaging (MRI), PET provides another important advantage that it allows quantitative imaging. The reliability of PET was demonstrated as good as that directly measured from biopsy samples. Therefore, PET has been identified as a powerful tool to study cancer (8-10), CNS diseases (11-14), and cardiovascular disease (15, 16).

PET technique has also been used for imaging infectious diseases, but has been largely limited to 2-[$^{18}$F]-fluorodeoxy-D-glucose ([$^{18}$F]-FDG). [$^{18}$F]-FDG was developed by Fowler *et al*. as a biomarker to monitor *in vivo* tissue uptake of glucose. The utility of [$^{18}$F]-FDG to detect infections is based on the mechanism that leukocytes consume glucose as the energy source (17-19). However, the application of [$^{18}$F]-FDG has significantly limitations such as accumulation in surrounding tissues. In addition, not all infections induce inflammatory response especially at an early stage. The [$^{18}$F]-FDG probes, which fundamentally depends induction of inflammatory responses, cannot precisely identify infections. In contrast, development of probes directly targeting pathogenic agents is relatively underexploited. Recently, radiolabeled antibiotics and antibacterial peptides have been demonstrated as potential probes for imaging infections. For example, ciprofloxacin, lemofloxacin, ceftzoxime, isoniazid and fluconazole have been successfully radiolabeled (20-25), and [$^{99}$Tc]-ciprofloxacin has been extensively studied *in vivo*. Nevertheless, uptake of these radiotracers at the infection sites was not as significant as expected that the infections were not clearly distinguished from the background (21, 26).

A primary reason of this observation was that most radiotracers also accumulate in the background tissue. Therefore, development of radiotracers with bacteria-specific target is a potential approach. Moreover, a persistent binding between a tracer molecule and its target in bacterial cells is beneficial for imaging. This is because that prolonged tracer accumulation in bacterial cells, in couple with continuous tracer elimination from the background, can facilitate to improve imaging resolution. As discussed in Chapter IV, the lifetime of a molecule physically bound to its target is determined by the dissociation rate constant ($k_{off}$) or residence time ($t_R$, $1/k_{off}$). Thus, labeling antibacterial agents that have long residence time may lead to better radiotracers for imaging infections.

In this initial study, we will investigate the biological and pharmaceutical properties of radiolabeled FabI inhibitors, such as cell uptake and *in vivo* distribution in animal models. The ultimate goal is to develop promising radiotracers for infection diagnosis and localization.

## Results and Discussion

*In vitro uptake of radiolabeled compounds by S. aureus*

We first exposed *S. aureus* cells to two radiotracers, [$^{18}$F]-FDG and [$^{11}$C]-PT-119, and examined radioactivity in cell pellets at different time points. As shown in **Figure 5.2**, [$^{18}$F]-FDG showed a time dependent uptake by *S. aureus*, exhibiting a linear accumulation of radioactivity in treated bacteria. In contrast, [$^{11}$C]-PT-119 incorporated into bacterial cells very quickly that approximately 40% of the injected dose were detected at 15 minutes. Additionally, no further cellular accumulation of this radiotracer was observed. These results suggest that cell uptake of [$^{11}$C]-PT-119 was much faster than that of [$^{18}$F]-FDG, and membrane incorporation contributed significantly.

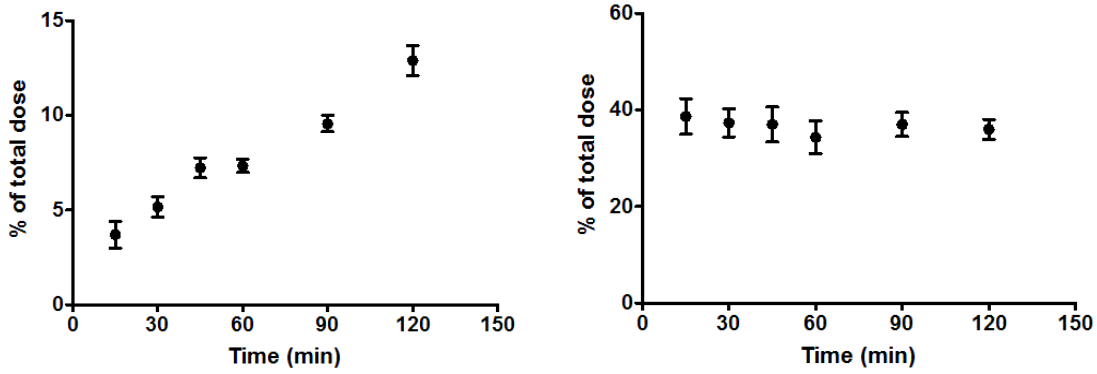


**Figure 5.2**. *In vitro* uptake of [$^{18}$F]-FDG (left) and [$^{11}$C]-PT-119 (right) by *S. aureus* cells. The error bars represent the standard error of the mean (SEM).

To understand the mechanism of FDG and PT-119 accumulation in bacterial cells, we subsequently executed cell exposure assays at a lower temperature. As shown in **Figure 5.3**, uptake of [$^{18}$F]-FDG by bacterial cells occurred more slowly at 4°C, which is a consequence of reduced bacterial activity and membrane fluidity. In contrast, correlation

between [$^{11}$C]-PT-119 accumulation and experimental temperature was less evident. This observation further suggests the contribution of membrane incorporation during PT-119 uptake. Additionally, we conducted an uptake competition study in which the bacterial cells were pre-exposed to corresponding "cold" glucose and PT-119 (**Figure 5.4**). We observed that addition of glucose resulted in a significant decrease in [$^{18}$F]-FDG uptake at 20 minute ($P < 0.005$). In contrast, pre-treatment with cold PT-119 did not significantly affect cellular incorporation of [$^{11}$C]-PT-119. Taken together, our data suggest that the uptake of [$^{18}$F]-FDG is a saturable process, which is consistent with our knowledge that cellular glucose uptake was facilitated by membrane-associated transporters (27, 28). Meanwhile, the incorporation of [$^{11}$C]-PT-119 depended on passive diffusion.

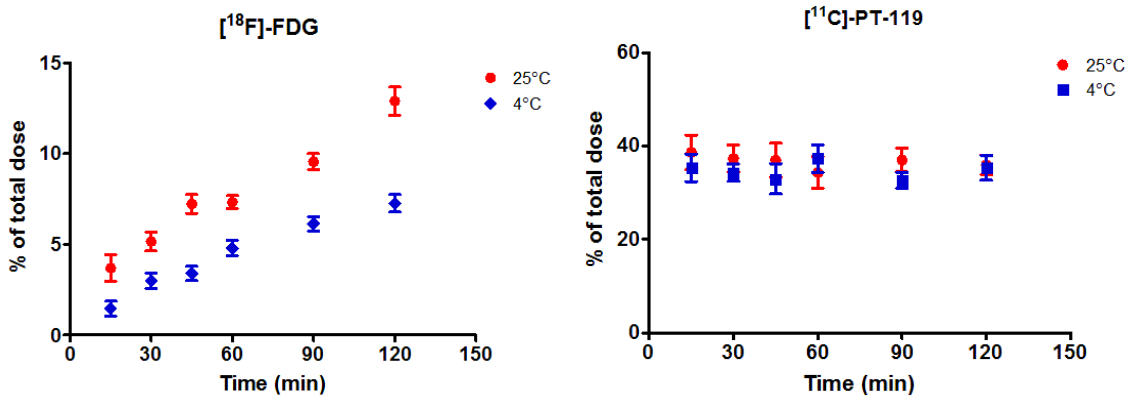


**Figure 5.3**. *In vitro* uptake of [$^{18}$F]-FDG (left) and [$^{11}$C]-PT-119 (right) by *S. aureus* cells at different temperatures. The error bars represent the standard error of the mean, SEM.

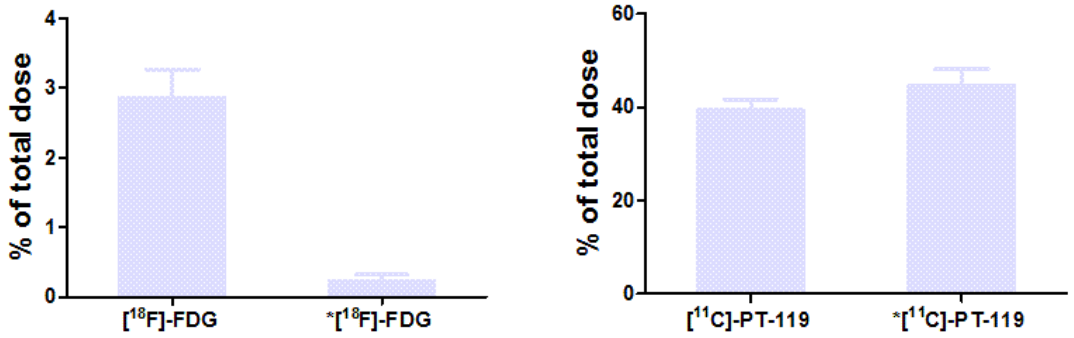


**Figure 5.4**. *In vitro* uptake of [$^{18}$F]-FDG (left) and [$^{11}$C]-PT-119 (right) at 20 minutes after co-incubation. Groups marked with * were pretreated with glucose or cold PT-119.

*Biodistribution of radiolabeled [$^{11}$C]-PT-119 in mice*

We subsequently investigated the biodistribution of PT-119 in a mouse model. Briefly, [$^{11}$C]-PT-119 was delivered into mice by intravenous (*iv*) injection. Radioactivity in peripheral organs including spleen, liver, kidneys, lungs and blood was measured at different time points following mice euthanasia and dissection. As shown in **Figure 5.5**, we detected radioactivity in all dissected organs. Significantly, accumulation of the radiotracer in all organs decreased over time. This is consistent with our observation from PK measurements that this compound eliminates rapidly. Our data showed that liver was the major target organ of [$^{11}$C]-PT-119 distribution. In addition, the radioactivity counting demonstrated that [$^{11}$C]-PT-119 also concentrated in lungs more extensively than in other high blood perfusion organs such as kidneys. The discovery of PT-119 being able to penetrate in to lungs was significant. It substantiates the potential of this compound as an anti-MRSA candidate since pneumonia is a typical MRSA related systemic infections. Furthermore, the exploration of drug distribution using PET technique was more time- and labor-efficient than traditional methods. However, this method has its limitations. For

examples, timeframes of radioactive studies are limited due to quick decay of the radionuclides. Therefore, tissue drug concentration at later time points cannot be determined using this method. To overcome, incorporation of positron emitting isotopes with a longer half-life is a potential strategy.

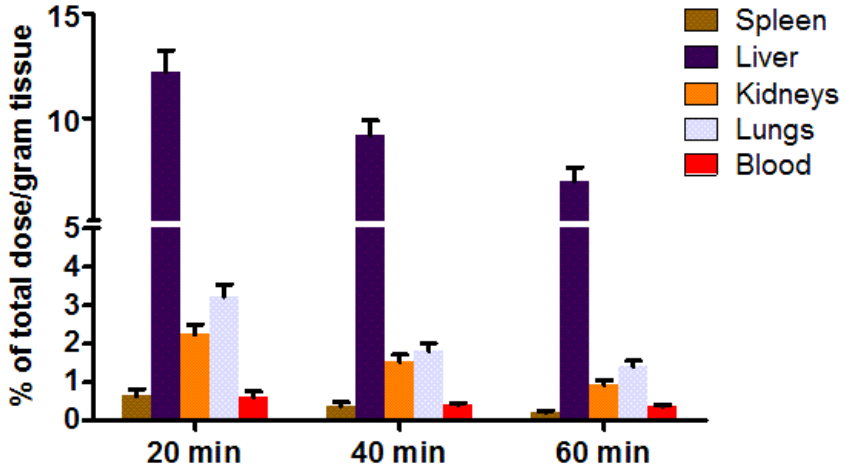


**Figure 5.5**. Distribution of [$^{11}$C]-PT-119 in peripheral organs / tissues in mice following intravenous administration.

*Distribution of [$^{18}$F]-FDG, [$^{11}$C]-PT-70 and [$^{11}$C]-PT-119 in a mouse model of MRSA*

We then conducted a series of experiments to determine biodistribution of radiotracers, including [$^{18}$F]-FDG, [$^{11}$C]-PT-70 and [$^{11}$C]-PT-119, in peripheral organs and tissues in a mouse of MRSA.

[$^{18}$F]-FDG. We first examined distribution of [$^{18}$F]-FDG in different organs in both healthy mice and mice with systemic MRSA infection. To get a better insight, we infected the animals with two doses of bacterial inoculums. Additionally, in order to eliminate the potential effect from inflammation rather than infection, mice were rendered neutropenic by treating with CPA prior to inoculation. As shown in **Figure 5.6**, a higher radioactivity

count was detected in spleen and liver in the infected mice than in healthy mice. In particular, the radioactive count in spleen was 2.7 and 1.8 fold higher in high-dose infected and low-dose infected mice than control, respectively. This result is consistent with our knowledge that spleen is the major target organ of MRSA after systemic infection (29). This study suggests that the PET-based method is a potential approach to detect systemic infection of MRSA.

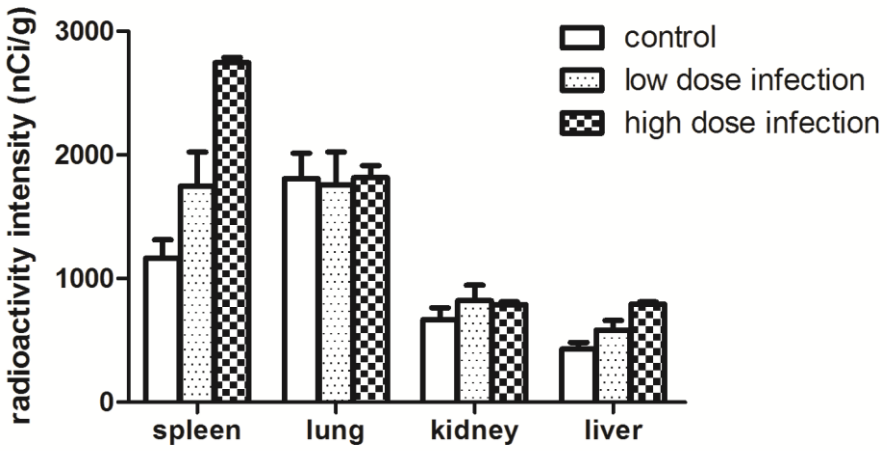


**Figure 5.6**. Radioactivity counts in different organs in healthy (control), low-dose infected and high-dose infected mice.

We then examined distribution of [$^{18}$F]-FDG in a thigh infection mouse model. As a control, ratio of radioactivity in the infected thigh (left thigh) over that in the uninfected thigh (right thigh) was determined. However, no tracer accumulation was observed at the site of infection. More surprisingly, radioactivity was continuously lower in the infected thigh (L/R ratio ranges 0.6-0.8). An explanation of this observation is that the infected mice developed significant necrosis in left thigh muscle, which could have prevented the radiotracer from reaching bacterial cells. Thus, we reduced inoculation dose but still did not observe significantly tracer accumulation.

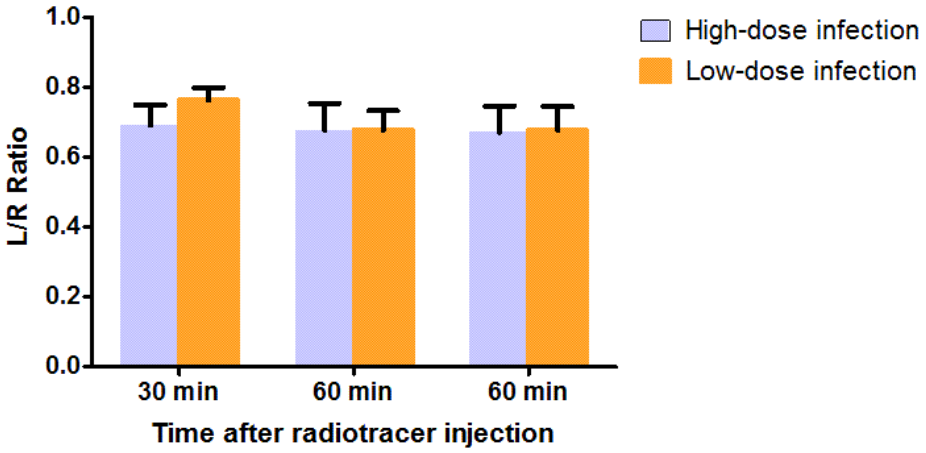


**Figure 5.7**. Ratio of radioactivity accumulated in infected thigh (T) over uninfected thigh (NT). Two inoculating sizes were applied.

[$^{11}$C]-PT-70 and [$^{11}$C]-PT-119. We also examined distribution of [$^{11}$C]-PT-70 and [$^{11}$C]-PT-119 in peripheral organs and tissue in systemic infection model and thigh infection model. As shown in **Figure 5.8**, [$^{11}$C]-PT-119 exhibited similar organ distribution in healthy and infected mice. We detected the highest tracer concentration at the first time point of 20 minutes, consistent with our previous data. Similar results were observed in thigh infection model. Furthermore, we did not see significantly increased accumulation of [$^{11}$C]-PT-70 and [$^{11}$C]-PT-119 in the infected thigh (**Figure 5.9**). This result failed to correlate with our *in vivo* efficacy study in which PT-119 was demonstrated as an active agent against MRSA in both systemic and thigh infection models. A possibility is that the dose of radiotracer in this study was significantly lower than that used in efficacy studies. Our data also emphasize another limitation of incorporating $^{11}$C in molecules of interest. Although this strategy allows possibility to label most organic compounds, the extremely short half-life of $^{11}$C limits the length of experiments. Application of other radionuclides will be tested in future studies.

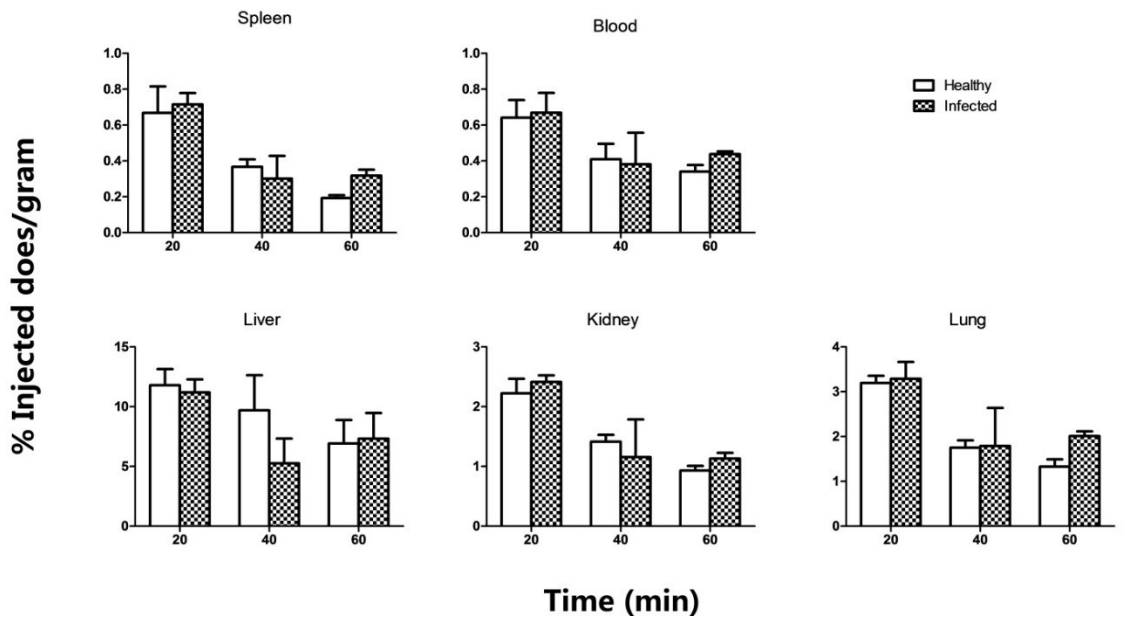


**Figure 5.8**. Biodistribution of [$^{11}$C]-PT-119 in MRSA systemic infection model.

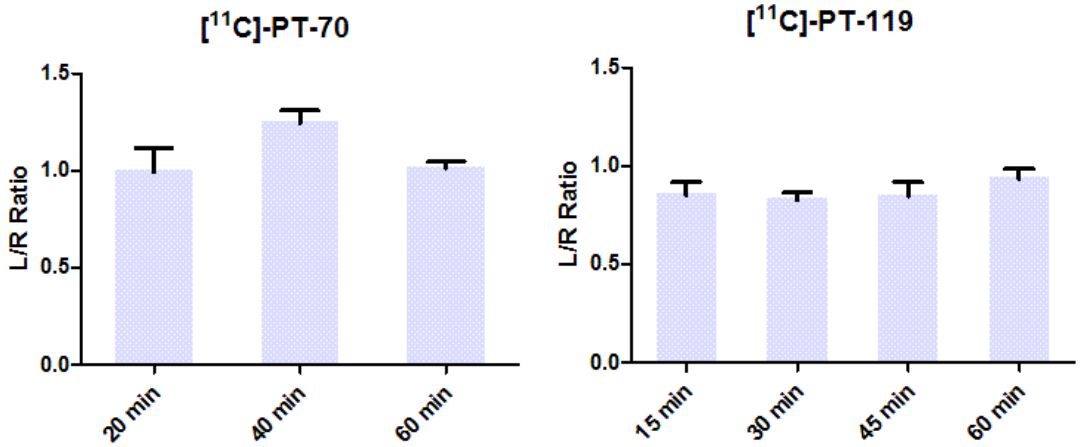


**Figure 5.9**. Biodistribution of [$^{11}$C]-PT-70 (top) and [$^{11}$C]-PT-119 (bottom) in MRSA thigh infection model. Ratio of radioactivity in infected thigh (L) over healthy thigh (R) was presented.

*In vivo imaging of [$^{18}$F]-FDG, [$^{11}$C]-PT-70 and [$^{11}$C]-PT-119 in mouse models*

The previous radioactive-based drug distribution studies depended on dissection and direct measurement of organ and tissue samples that were invasive. The ultimate goal of PET

technique is to provide a non-invasive approach *via* imaging to execute important *in vivo* examinations. Hence, we also conducted an initial PET imaging experiment to monitor distribution of radiotracers in living animals. As shown in **Figure 5.10**, radiotracers were visualized in 2-D PET images. Scan of mice dosed with [$^{18}$F]-FDG showed a similar organ distribution as observed in *ex vivo* radio-counting study. Similarly, higher accumulation of [$^{11}$C]-PT-70 and [$^{11}$C]-PT-119 in liver, kidney and lungs was observed in PET images, consistent with our previous data. Moreover, PET imaging allowed continuous data acquisition providing dynamic monitoring of *in vivo* drug distribution. **Figure 5.11** showed PET images taken from a single mouse dosed with and [$^{11}$C]-PT-119 at different time points. However, the imaging resolution was lower in mice treated with radiolabeled PT compounds than in [$^{18}$F]-FDG mice. We hypothesize that this phenomenon is caused by three factors. First, $^{11}$C has a much shorter half-life in comparison to $^{18}$F. Second, PT-119 eliminates from peripheral organs/tissue rapidly. Third, PT-119 distributes extensively in liver, which leads to low relative radioactivity in surrounding organs.

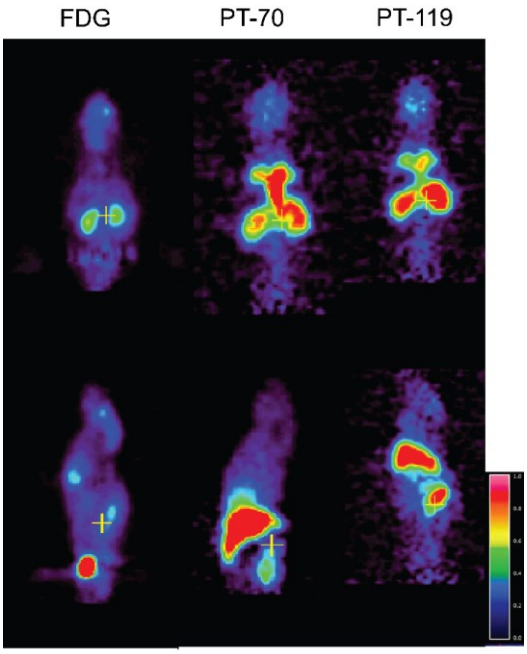


**Figure 5.10**. PET images acquired from healthy mice injected with [$^{18}$F]-FDG, [$^{11}$C]-PT-70 and [$^{11}$C]-PT-119. Images were acquired 30 min after administration.

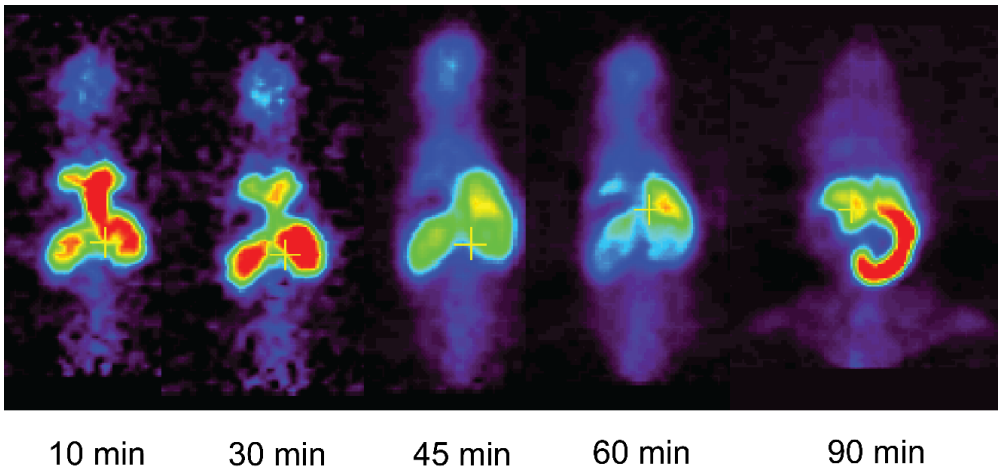


**Figure 5.11**. Dynamics of the *in vivo* distribution of [$^{11}$C]-PT-119. Images acquired from a single study animal at different time points.

We also imaged the distribution of [$^{18}$F]-FDG, [$^{11}$C]-PT-70 and [$^{11}$C]-PT-119 in infected mice. PET images taken from healthy, thigh infected and systemic infected mice are compared in **Figure 5.12**. We observed accumulation of radioactivity at target areas

such as left thigh in thigh infection model and spleen in systemic infection model. However, it was difficult to distinguish spleen from background due to high radioactivity accumulated in the liver. A primary limitation of these studies was that the microPET scanner was not coupled with a computerized tomography (CT), which can significantly improve anatomical co-registration. In future work, imaging will be performed using a new PET-CT scanner.

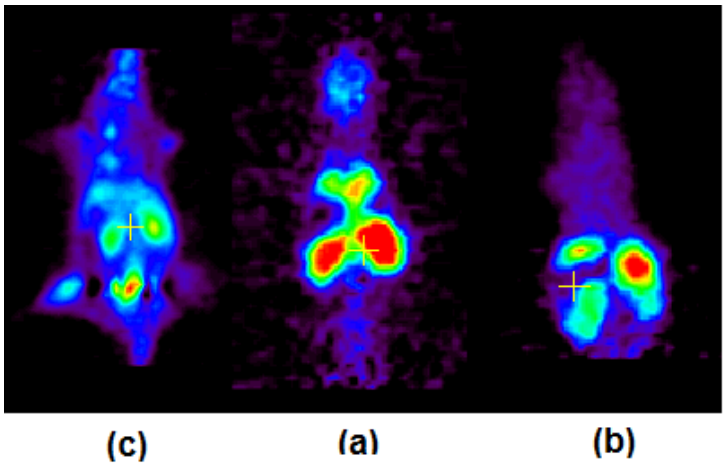


**Figure 5.12**. Images acquired from (a) healthy, (b) systemic infection, and (c) thigh infection mice after administration of [$^{11}$C]-PT-119.

**Summary**

In summary, we radiolabeled two FabI inhibitors with $^{11}C$ and determined the *in vitro* bacterial uptake as well as the *in vivo* distribution of these molecules. Our studies provide a more time- and labor-efficient approach to perform pharmacokinetic (PK) measurements than the traditional methods. The data also allowed us opportunities to review and modify the PET-based experiments, which will ultimately facilitate the determination of PK/PDs relationship.

## Experimental Procedures

*Chemistry*

[$^{18}$F]-FDG (5-10 mCi) was purchased from Cardinal Health (Plainview, NY) on each day of experiment. Synthesis of [$^{11}$C]-PT-70 and [$^{11}$C]-PT-119 were done by Dr. Li Liu and Hui Wang (Stony Brook University).

*In vitro assay for the uptake of radiolabeled compounds by bacteria*

*S. aureus* RN4220 strain was grown to mid-log phase (OD = 0.8) in Muller-Hilton II (MH-II) broth. 1 ml of culture was centrifuged at 10,000 rpm for 3 min and the cell pellet was resuspended in 1 ml of saline. Radiolabeled compound (~1mCi in 1-2 ml saline, specific activity = 50-200 mCi/μmol at the time of incubation) was subsequently added to the bacterial suspension (20 ml) while "cold" compound was added to the control group. The bacterial suspension was incubated at 37 °C and aliquots (1 ml) were removed at 5 min, 10 min, 20 min, 40 min, 1 hr, 2 hr, centrifuged and washed once with saline to reduce the background signal. An empty tube without bacteria was incorporated as a control for background correction. A well counter (Picker, Cleveland, OH) was used to measure radioactivity in each set of samples. The radioactive counts were decay corrected to the time of that the incubation was initiated.

*In vivo radioactive studies*

All of the animal experiments were approved by the Brookhaven Institutional Animal Care and Use Committee or Stony Brook University Institutional Animal Care and

Use Committee. Animals were purchased from Taconic or Charles River. The systemic infection model and the thigh infection model were established as discussed in chapter II.

The *in vivo* biodistribution of [$^{11}$C]-PT-119 was determined in healthy mice and in both systemic infection and thigh infection models. In brief, mice were anesthetized using isoflurane and stabilized in a mouse restrainer. Approximately 100 µCi of [$^{11}$C]-PT-119 in 50 – 200 µl ethanol/saline (1/3. v/v) was administered using the lateral tail vein. Treated mice were returned to their cages, allowed to recover from anesthesia and were free to move during the uptake period. Mice were euthanized by cervical dislocation at different time points. In the systemic infection group, infected mice as well as healthy control mice were sacrificed at 20 min, 40 min and 60 min. The carcasses were dissected immediately and organs of interest (spleen, lung, liver and kidney) were harvested. Blood samples were collected by cardiac puncture. Tissue or blood samples were transferred into glass vials, weighed and counted using a well counter (Picker, Cleveland, OH). In the thigh infection group, infected mice and healthy control mice were euthanized at 15 min, 30 min, 45 min and 60 min. Muscle tissue from both thighs, as well as blood, were collected, weighed and counted. Radioactivity values are given as the percentage of total injection dose/g (%ID/g) and are expressed as the mean ± standard deviation (SD, n=3).

*In vivo* imaging was conducted using a single study mouse under anesthesia. Anesthesia was initiated with 5% isoflurane and maintained with 1-4% isoflurane during the imaging process. Mice were placed on the mPET (MicroPET R4, Siemens) scanner prior to injection of radiolabeled compounds ([$^{18}$F]-FDG, [$^{11}$C]-PT-119, or [$^{11}$C]-PT-70). Data acquisition was started simultaneously with the injection of radiolabeled compound. During the scan, the mice were immobilized with surgical tape and kept warm at 30°C

during imaging using a heating lamp. Dynamic PET scans (60- 120 min) were performed in 3D mode, and the raw data were reconstructed by 3D filtered-back projection (FBP). Results were analyzed using AMIDE software.

**Reference**


1. Miller PW, Long NJ, Vilar R, & Gee AD (2008) Synthesis of 11C, 18F, 15O, and 13N radiolabels for positron emission tomography. *Angew Chem Int Ed Engl* 47(47):8998-9033.
2. Turkington TG (2001) Introduction to PET instrumentation. *J Nucl Med Technol* 29(1):4-11.
3. Gambhir SS (2002) Molecular imaging of cancer with positron emission tomography. *Nat Rev Cancer* 2(9):683-693.
4. Karp JS*, et al.* (1990) Continuous-slice PENN-PET: a positron tomograph with volume imaging capability. *J Nucl Med* 31(5):617-627.
5. Phelps ME, Hoffman EJ, Mullani NA, & Ter-Pogossian MM (1975) Application of annihilation coincidence detection to transaxial reconstruction tomography. *J Nucl Med* 16(3):210-224.
6. Anonymous (2010) A Vital legacy: Biological and Environmental Research in the Atomic Age. (U.S. Department of Energy, The Office of Biological and Environmental Research), pp 25-26.
7. Signore A, Mather SJ, Piaggio G, Malviya G, & Dierckx RA (2010) Molecular imaging of inflammation/infection: nuclear medicine and optical imaging agents and methods. *Chem Rev* 110(5):3112-3145.
8. Rajagopalan KN & DeBerardinis RJ (2011) Role of glutamine in cancer: therapeutic and imaging implications. *J Nucl Med* 52(7):1005-1008.
9. Qu W*, et al.* (2012) Preparation and characterization of L-[5-11C]-glutamine for metabolic imaging of tumors. *J Nucl Med* 53(1):98-105.

10. Herrmann K, *et al.* (2011) (18)F-FDG-PET/CT in evaluating response to therapy in solid tumors: where we are and where we can go. *Q J Nucl Med Mol Imaging* 55(6):620-632.

11. Fowler JS, *et al.* (2003) Low monoamine oxidase B in peripheral organs in smokers. *Proc Natl Acad Sci U S A* 100(20):11600-11605.

12. Fowler JS, *et al.* (2003) Monoamine oxidase A imaging in peripheral organs in healthy human subjects. *Synapse* 49(3):178-187.

13. Lister-James J, *et al.* (2011) Florbetapir f-18: a histopathologically validated Beta-amyloid positron emission tomography imaging agent. *Semin Nucl Med* 41(4):300-304.

14. Clark CM, *et al.* (2011) Use of florbetapir-PET for imaging beta-amyloid pathology. *JAMA* 305(3):275-283.

15. Botnar RM & Makowski MR (2012) Cardiovascular magnetic resonance imaging in small animals. *Prog Mol Biol Transl Sci* 105:227-261.

16. Schuster A, *et al.* (2012) Platelets in cardiovascular imaging. *Curr Vasc Pharmacol* 10(5):619-625.

17. Welling MM & Alberto R (2010) Performance of a 99mTc-labelled 1-thio-beta-D-glucose 2,3,4,6-tetra-acetate analogue in the detection of infections and tumours in mice: a comparison with [18F]FDG. *Nucl Med Commun* 31(3):239-248.

18. Kosterink JG (2011) Positron emission tomography in the diagnosis and treatment management of tuberculosis. *Curr Pharm Des* 17(27):2875-2880.

19. Kubota R*, et al.* (1992) Intratumoral distribution of fluorine-18-fluorodeoxyglucose in vivo: high accumulation in macrophages and granulation tissues studied by microautoradiography. *J Nucl Med* 33(11):1972-1980.

20. Solanki KK, Mather SJ, Janabi MA, & Britton KE (1988) A rapid method for the preparation of 99Tcm hexametazime-labelled leucocytes. *Nucl Med Commun* 9(10):753-761.

21. Fischman AJ*, et al.* (1997) Pharmacokinetics of 18F-labeled trovafloxacin in normal and Escherichia coli-infected rats and rabbits studied with positron emission tomography. *Clin Microbiol Infect* 3(3):379.

22. Fischman AJ*, et al.* (1992) Pharmacokinetics of 18F-labeled fleroxacin in rabbits with Escherichia coli infections, studied with positron emission tomography. *Antimicrob Agents Chemother* 36(10):2286-2292.

23. Langer O*, et al.* (2005) In vitro and in vivo evaluation of [18F]ciprofloxacin for the imaging of bacterial infections with PET. *Eur J Nucl Med Mol Imaging* 32(2):143-150.

24. Siaens RH, Rennen HJ, Boerman OC, Dierckx R, & Slegers G (2004) Synthesis and comparison of 99mTc-enrofloxacin and 99mTc-ciprofloxacin. *J Nucl Med* 45(12):2088-2094.

25. Singh N & Bhatnagar A (2010) Clinical Evaluation of Efficacy of (99m)TC - Ethambutol in Tubercular Lesion Imaging. *Tuberc Res Treat* 2010:618051.

26. Babich JW*, et al.* (1996) 18F-labeling and biodistribution of the novel fluoro-quinolone antimicrobial agent, trovafloxacin (CP 99,219). *Nucl Med Biol* 23(8):995-998.

27. Rohwer JM, Meadow ND, Roseman S, Westerhoff HV, & Postma PW (2000) Understanding glucose transport by the bacterial phosphoenolpyruvate:glycose phosphotransferase system on the basis of kinetic measurements in vitro. *J Biol Chem* 275(45):34909-34921.

28. Natarajan A & Srienc F (2000) Glucose uptake rates of single E. coli cells grown in glucose-limited chemostat cultures. *J Microbiol Methods* 42(1):87-96.

29. Bates DM*, et al.* (2003) Staphylococcus aureus menD and hemB mutants are as infective as the parent strains, but the menadione biosynthetic mutant persists within the kidney. *J Infect Dis* 187(10):1654-1661.

## Bibliography

### Chapter I


1. Dobson AP & Carper ER (1996) Infectious diseases and human population history - Throughout history the establishment of disease has been a side effect of the growth of civilization. *Bioscience* 46(2):115-126.
2. Wolfe ND, Dunavan CP, & Diamond J (2007) Origins of major human infectious diseases. *Nature* 447(7142):279-283.
3. Boyden SV & Australian Academy of Science. (1970) *The Impact of civilisation on the biology of man* (Australian National University Press, Canberra,) pp xx, 233 p.
4. Cockburn TA (1971) Infectious diseases in ancient populations. *Current anthropology* 12:45-62.
5. Haensch S*, et al.* (2010) Distinct clones of Yersinia pestis caused the black death. *PLoS pathogens* 6(10):e1001134.
6. Bryk R, Lima CD, Erdjument-Bromage H, Tempst P, & Nathan C (2002) Metabolic enzymes of mycobacteria linked to antioxidant defense by a thioredoxin-like protein. *Science* 295(5557):1073-1077.
7. Ahmad S (2011) Pathogenesis, immunology, and diagnosis of latent Mycobacterium tuberculosis infection. *Clinical & developmental immunology* 2011:814943.
8. WHO (2014) WHO Global Tuberculosis Report 2013
9. McNeill WH (1978) Disease in history. *Social science & medicine* 12(2B):79-84.
10. Lindblad WJ (2008) Considerations for determining if a natural product is an effective wound-healing agent. *The international journal of lower extremity wounds* 7(2):75-81.
11. Kingston W (2008) Irish contributions to the origins of antibiotics. *Ir J Med Sci* 177(2):87-92.
12. Landsberg E (1949) Cerebral palsy; a public health problem. *Journal of the American Medical Women's Association* 4(8):338-340.
13. Bosch F & Rosich L (2008) The contributions of Paul Ehrlich to pharmacology: a tribute on the occasion of the centenary of his Nobel Prize. *Pharmacology* 82(3):171-179.
14. Fleming A (1955) The story of penicillin. *Bulletin. Georgetown University. Medical Center* 8(4):128-132.

15. Sykes R (2001) Penicillin: from discovery to product. *Bulletin of the World Health Organization* 79(8):778-779.
16. Pelaez F (2006) The historical delivery of antibiotics from microbial natural products--can history repeat? *Biochemical pharmacology* 71(7):981-990.
17. Wright GD (2007) The antibiotic resistome: the nexus of chemical and genetic diversity. *Nature reviews. Microbiology* 5(3):175-186.
18. Lowy FD (2003) Antimicrobial resistance: the example of Staphylococcus aureus. *The Journal of clinical investigation* 111(9):1265-1273.
19. WHO (2004) Use of antimicrobials outside human medicine and resultant antimicrobial resistance in humans.
20. Fleming A (1945) Penicillin. (Nobel Lecture).
21. Cohen ML (1992) Epidemiology of drug resistance: implications for a post-antimicrobial era. *Science* 257(5073):1050-1055.
22. Levy SB & Marshall B (2004) Antibacterial resistance worldwide: causes, challenges and responses. *Nature medicine* 10(12 Suppl):S122-129.
23. Payne DJ, Gwynn MN, Holmes DJ, & Pompliano DL (2007) Drugs for bad bugs: confronting the challenges of antibacterial discovery. *Nature reviews. Drug discovery* 6(1):29-40.
24. Fleischmann RD*, et al.* (1995) Whole-genome random sequencing and assembly of Haemophilus influenzae Rd. *Science* 269(5223):496-512.
25. Walsh C (2000) Molecular mechanisms that confer antibacterial drug resistance. *Nature* 406(6797):775-781.
26. McDevitt D & Rosenberg M (2001) Exploiting genomics to discover new antibiotics. *Trends in microbiology* 9(12):611-617.
27. Becker D*, et al.* (2006) Robust Salmonella metabolism limits possibilities for new antimicrobials. *Nature* 440(7082):303-307.
28. Wenzel RP (2004) The antibiotic pipeline--challenges, costs, and values. *N Engl J Med* 351(6):523-526.
29. Suttie JW (1985) Vitamin K-dependent carboxylase. *Annual review of biochemistry* 54:459-477.
30. Truglio JJ*, et al.* (2003) Crystal structure of Mycobacterium tuberculosis MenB, a key enzyme in vitamin K2 biosynthesis. *The Journal of biological chemistry* 278(43):42352-42360.
31. Bentinger M, Tekle M, & Dallner G (2010) Coenzyme Q--biosynthesis and functions. *Biochemical and biophysical research communications* 396(1):74-79.

32. Bishop DH, Pandya KP, & King HK (1962) Ubiquinone and vitamin K in bacteria. *The Biochemical journal* 83:606-614.
33. Haddock BA & Jones CW (1977) Bacterial respiration. *Bacteriological reviews* 41(1):47-99.
34. Bentley R & Meganathan R (1982) Biosynthesis of vitamin K (menaquinone) in bacteria. *Microbiological reviews* 46(3):241-280.
35. Meganathan R & Bentley R (1981) Biosynthesis of o-succinylbenzoic acid in a men- Escherichia coli mutant requires decarboxylation of L-glutamate at the C-1 position. *Biochemistry* 20(18):5336-5340.
36. Widhalm JR, van Oostende C, Furt F, & Basset GJ (2009) A dedicated thioesterase of the Hotdog-fold family is required for the biosynthesis of the naphthoquinone ring of vitamin K1. *Proceedings of the National Academy of Sciences of the United States of America* 106(14):5599-5603.
37. Shineberg B & Young IG (1976) Biosynthesis of bacterial menaquinones: the membrane-associated 1,4-dihydroxy-2-naphthoate octaprenyltransferase of Escherichia coli. *Biochemistry* 15(13):2754-2758.
38. Meganathan R (2001) Biosynthesis of menaquinone (vitamin K2) and ubiquinone (coenzyme Q): a perspective on enzymatic mechanisms. *Vitamins and hormones* 61:173-218.
39. Chen M*, et al.* (2013) Identification of a hotdog fold thioesterase involved in the biosynthesis of menaquinone in Escherichia coli. *J Bacteriol* 195(12):2768-2775.
40. Bentley SD*, et al.* (2002) Complete genome sequence of the model actinomycete Streptomyces coelicolor A3(2). *Nature* 417(6885):141-147.
41. Borodina I, Krabben P, & Nielsen J (2005) Genome-scale analysis of Streptomyces coelicolor A3(2) metabolism. *Genome research* 15(6):820-829.
42. Parkhill J*, et al.* (2000) The genome sequence of the food-borne pathogen Campylobacter jejuni reveals hypervariable sequences. *Nature* 403(6770):665-668.
43. Tomb JF*, et al.* (1997) The complete genome sequence of the gastric pathogen Helicobacter pylori. *Nature* 388(6642):539-547.
44. Marcelli SW*, et al.* (1996) The respiratory chain of Helicobacter pylori: identification of cytochromes and the effects of oxygen on cytochrome and menaquinone levels. *FEMS microbiology letters* 138(1):59-64.
45. Hiratsuka T*, et al.* (2008) An alternative menaquinone biosynthetic pathway operating in microorganisms. *Science* 321(5896):1670-1673.

46. Seto H, *et al.* (2008) Studies on a new biosynthetic pathway for menaquinone. *Journal of the American Chemical Society* 130(17):5614-5615.
47. Collins MD & Jones D (1981) Distribution of isoprenoid quinone structural types in bacteria and their taxonomic implication. *Microbiological reviews* 45(2):316-354.
48. Kobayashi K, *et al.* (2003) Essential Bacillus subtilis genes. *Proceedings of the National Academy of Sciences of the United States of America* 100(8):4678-4683.
49. Guest JR (1977) Menaquinone biosynthesis: mutants of Escherichia coli K-12 requiring 2-succinylbenzoate. *Journal of bacteriology* 130(3):1038-1046.
50. Dhiman RK, *et al.* (2009) Menaquinone synthesis is critical for maintaining mycobacterial viability during exponential growth and recovery from non-replicating persistence. *Molecular microbiology* 72(1):85-97.
51. Sassetti CM, Boyd DH, & Rubin EJ (2003) Genes required for mycobacterial growth defined by high density mutagenesis. *Molecular microbiology* 48(1):77-84.
52. Kurosu M & Begari E (2010) Vitamin K2 in electron transport system: are enzymes involved in vitamin K2 biosynthesis promising drug targets? *Molecules* 15(3):1531-1553.
53. Debnath J, *et al.* (2012) Discovery of selective menaquinone biosynthesis inhibitors against Mycobacterium tuberculosis. *Journal of medicinal chemistry* 55(8):3739-3755.
54. Kurosu M, Narayanasamy P, Biswas K, Dhiman R, & Crick DC (2007) Discovery of 1,4-dihydroxy-2-naphthoate [corrected] prenyltransferase inhibitors: new drug leads for multidrug-resistant gram-positive pathogens. *Journal of medicinal chemistry* 50(17):3973-3975.
55. Li X, *et al.* (2010) Synthesis and SAR studies of 1,4-benzoxazine MenB inhibitors: novel antibacterial agents against Mycobacterium tuberculosis. *Bioorganic & medicinal chemistry letters* 20(21):6306-6309.
56. Fang M, *et al.* (2010) Succinylphosphonate esters are competitive inhibitors of MenD that show active-site discrimination between homologous alpha-ketoglutarate-decarboxylating enzymes. *Biochemistry* 49(12):2672-2679.
57. Lu X, Zhang H, Tonge PJ, & Tan DS (2008) Mechanism-based inhibitors of MenE, an acyl-CoA synthetase involved in bacterial menaquinone biosynthesis. *Bioorganic & medicinal chemistry letters* 18(22):5963-5966.

58. Lu X, *et al.* (2012) Stable analogues of OSB-AMP: potent inhibitors of MenE, the o-succinylbenzoate-CoA synthetase from bacterial menaquinone biosynthesis. *Chembiochem : a European journal of chemical biology* 13(1):129-136.
59. Chirala SS, Huang WY, Jayakumar A, Sakai K, & Wakil SJ (1997) Animal fatty acid synthase: functional mapping and cloning and expression of the domain I constituent activities. *Proceedings of the National Academy of Sciences of the United States of America* 94(11):5588-5593.
60. Payne DJ, Warren PV, Holmes DJ, Ji Y, & Lonsdale JT (2001) Bacterial fatty-acid biosynthesis: a genomics-driven target for antibacterial drug discovery. *Drug discovery today* 6(10):537-544.
61. Campbell JW & Cronan JE, Jr. (2001) Bacterial fatty acid biosynthesis: targets for antibacterial drug discovery. *Annual review of microbiology* 55:305-332.
62. White SW, Zheng J, Zhang YM, & Rock (2005) The structural biology of type II fatty acid biosynthesis. *Annual review of biochemistry* 74:791-831.
63. Heath RJ, White SW, & Rock CO (2001) Lipid biosynthesis as a target for antibacterial agents. *Progress in lipid research* 40(6):467-497.
64. Baldock C, *et al.* (1996) A mechanism of drug action revealed by structural studies of enoyl reductase. *Science* 274(5295):2107-2110.
65. Baldock C, Rafferty JB, Stuitje AR, Slabas AR, & Rice DW (1998) The X-ray structure of Escherichia coli enoyl reductase with bound NAD+ at 2.1 A resolution. *Journal of molecular biology* 284(5):1529-1546.
66. Roujeinikova A, *et al.* (1999) Inhibitor binding studies on enoyl reductase reveal conformational changes related to substrate recognition. *The Journal of biological chemistry* 274(43):30811-30817.
67. Rozwarski DA, Vilcheze C, Sugantino M, Bittman R, & Sacchettini JC (1999) Crystal structure of the Mycobacterium tuberculosis enoyl-ACP reductase, InhA, in complex with NAD+ and a C16 fatty acyl substrate. *The Journal of biological chemistry* 274(22):15582-15589.
68. Xu H, *et al.* (2008) Mechanism and inhibition of saFabI, the enoyl reductase from Staphylococcus aureus. *Biochemistry* 47(14):4228-4236.
69. Rozwarski DA, Grant GA, Barton DH, Jacobs WR, Jr., & Sacchettini JC (1998) Modification of the NADH of the isoniazid target (InhA) from Mycobacterium tuberculosis. *Science* 279(5347):98-102.
70. Zhang YM, White SW, & Rock CO (2006) Inhibiting bacterial fatty acid synthesis. *The Journal of biological chemistry* 281(26):17541-17544.

71. Heath RJ & Rock CO (1995) Enoyl-acyl carrier protein reductase (fabI) plays a determinant role in completing cycles of fatty acid elongation in Escherichia coli. *The Journal of biological chemistry* 270(44):26538-26542.
72. Bergler H, Fuchsbichler S, Hogenauer G, & Turnowsky F (1996) The enoyl-[acyl-carrier-protein] reductase (FabI) of Escherichia coli, which catalyzes a key regulatory step in fatty acid biosynthesis, accepts NADH and NADPH as cofactors and is inhibited by palmitoyl-CoA. *European journal of biochemistry / FEBS* 242(3):689-694.
73. Slayden RA, Lee RE, & Barry CE, 3rd (2000) Isoniazid affects multiple components of the type II fatty acid synthase system of Mycobacterium tuberculosis. *Molecular microbiology* 38(3):514-525.
74. Cohn DL (2000) Treatment of latent tuberculosis infection: renewed opportunity for tuberculosis control. *Clinical infectious diseases : an official publication of the Infectious Diseases Society of America* 31(1):120-124.
75. Suarez J*, et al.* (2009) An oxyferrous heme/protein-based radical intermediate is catalytically competent in the catalase reaction of Mycobacterium tuberculosis catalase-peroxidase (KatG). *The Journal of biological chemistry* 284(11):7017-7029.
76. Zhang Y, Heym B, Allen B, Young D, & Cole S (1992) The catalase-peroxidase gene and isoniazid resistance of Mycobacterium tuberculosis. *Nature* 358(6387):591-593.
77. Rawat R, Whitty A, & Tonge PJ (2003) The isoniazid-NAD adduct is a slow, tight-binding inhibitor of InhA, the Mycobacterium tuberculosis enoyl reductase: adduct affinity and drug resistance. *Proceedings of the National Academy of Sciences of the United States of America* 100(24):13881-13886.
78. Ramaswamy SV*, et al.* (2003) Single nucleotide polymorphisms in genes associated with isoniazid resistance in Mycobacterium tuberculosis. *Antimicrobial agents and chemotherapy* 47(4):1241-1250.
79. Payne DJ*, et al.* (2002) Discovery of a novel and potent class of FabI-directed antibacterial agents. *Antimicrobial agents and chemotherapy* 46(10):3118-3124.
80. Heerding DA*, et al.* (2001) 1,4-Disubstituted imidazoles are potential antibacterial agents functioning as inhibitors of enoyl acyl carrier protein reductase (FabI). *Bioorganic & medicinal chemistry letters* 11(16):2061-2065.

81. Seefeld MA, *et al.* (2001) Inhibitors of bacterial enoyl acyl carrier protein reductase (FabI): 2,9-disubstituted 1,2,3,4-tetrahydropyrido[3,4-b]indoles as potential antibacterial agents. *Bioorganic & medicinal chemistry letters* 11(17):2241-2244.
82. Miller WH, *et al.* (2002) Discovery of aminopyridine-based inhibitors of bacterial enoyl-ACP reductase (FabI). *Journal of medicinal chemistry* 45(15):3246-3256.
83. Kuo MR, *et al.* (2003) Targeting tuberculosis and malaria through inhibition of Enoyl reductase: compound activity and structural data. *The Journal of biological chemistry* 278(23):20851-20859.
84. Yum JH, *et al.* (2007) In vitro activities of CG400549, a novel FabI inhibitor, against recently isolated clinical staphylococcal strains in Korea. *Antimicrobial agents and chemotherapy* 51(7):2591-2593.
85. Wehrli W (1977) Kinetic Studies of Interaction between Rifampicin and DNA-Dependent Rna-Polymerase of Escherichia-Coli. *European Journal of Biochemistry* 80(2):325-330.
86. Wehrli W, Knusel F, & Staeheli.M (1968) Action of Rifamycin on Rna-Polymerase from Sensitive and Resistant Bacteria. *Biochemical and biophysical research communications* 32(2):284-&.
87. Stubbings W, Bostock J, Ingham E, & Chopra I (2006) Mechanisms of the post-antibiotic effects induced by rifampicin and gentamicin in Escherichia coli. *The Journal of antimicrobial chemotherapy* 58(2):444-448.
88. Yao J, Zhang Q, Min J, He J, & Yu Z (2010) Novel enoyl-ACP reductase (FabI) potential inhibitors of Escherichia coli from Chinese medicine monomers. *Bioorganic & medicinal chemistry letters* 20(1):56-59.
89. McMurry LM, Oethinger M, & Levy SB (1998) Triclosan targets lipid synthesis. *Nature* 394(6693):531-532.
90. Levy CW, *et al.* (1999) Molecular basis of triclosan activity. *Nature* 398(6726):383-384.
91. Sivaraman S, *et al.* (2004) Inhibition of the bacterial enoyl reductase FabI by triclosan: a structure-reactivity analysis of FabI inhibition by triclosan analogues. *Journal of medicinal chemistry* 47(3):509-518.
92. Ward WH, *et al.* (1999) Kinetic and structural characteristics of the inhibition of enoyl (acyl carrier protein) reductase by triclosan. *Biochemistry* 38(38):12514-12525.

93. Li HJ, *et al.* (2014) A Structural and Energetic Model for the Slow-Onset Inhibition of the Mycobacterium tuberculosis Enoyl-ACP Reductase InhA. *ACS chemical biology*.
94. Qiu X, *et al.* (1999) Molecular basis for triclosan activity involves a flipping loop in the active site. *Protein science : a publication of the Protein Society* 8(11):2529-2532.
95. Lu H, *et al.* (2009) Slow-onset inhibition of the FabI enoyl reductase from francisella tularensis: residence time and in vivo activity. *ACS chemical biology* 4(3):221-231.
96. am Ende CW, *et al.* (2008) Synthesis and in vitro antimycobacterial activity of B-ring modified diaryl ether InhA inhibitors. *Bioorganic & medicinal chemistry letters* 18(10):3029-3033.
97. Luckner SR, Liu N, am Ende CW, Tonge PJ, & Kisker C (2010) A slow, tight binding inhibitor of InhA, the enoyl-acyl carrier protein reductase from Mycobacterium tuberculosis. *The Journal of biological chemistry* 285(19):14330-14337.

**Chapter II**

1. Massey RC, Horsburgh MJ, Lina G, Hook M, & Recker M (2006) The evolution and maintenance of virulence in Staphylococcus aureus: a role for host-to-host transmission? *Nature reviews. Microbiology* 4(12):953-958.
2. Kluytmans J, van Belkum A, & Verbrugh H (1997) Nasal carriage of Staphylococcus aureus: epidemiology, underlying mechanisms, and associated risks. *Clinical microbiology reviews* 10(3):505-520.
3. Lowy FD (1998) Staphylococcus aureus infections. *The New England journal of medicine* 339(8):520-532.
4. Chambers HF & Deleo FR (2009) Waves of resistance: Staphylococcus aureus in the antibiotic era. *Nature reviews. Microbiology* 7(9):629-641.
5. Gorwitz RJ, *et al.* (2008) Changes in the prevalence of nasal colonization with Staphylococcus aureus in the United States, 2001-2004. *The Journal of infectious diseases* 197(9):1226-1234.
6. CDC (2004) Staphylococcus aureus in Healthcare Settings.
7. Mylotte JM, McDermott C, & Spooner JA (1987) Prospective study of 114 consecutive episodes of Staphylococcus aureus bacteremia. *Reviews of infectious diseases* 9(5):891-907.

8. NIH (2012) Staph infections - hospital.
9. Gill SR, *et al.* (2005) Insights on evolution of virulence and resistance from the complete genome analysis of an early methicillin-resistant Staphylococcus aureus strain and a biofilm-producing methicillin-resistant Staphylococcus epidermidis strain. *J Bacteriol* 187(7):2426-2438.
10. Fleming A (1955) The story of penicillin. *Bulletin. Georgetown University. Medical Center* 8(4):128-132.
11. Chambers HF (2001) The changing epidemiology of Staphylococcus aureus? *Emerging infectious diseases* 7(2):178-182.
12. Kirby WM (1944) Extraction of a Highly Potent Penicillin Inactivator from Penicillin Resistant Staphylococci. *Science* 99(2579):452-453.
13. Cosgrove SE, *et al.* (2003) Comparison of mortality associated with methicillin-resistant and methicillin-susceptible Staphylococcus aureus bacteremia: a meta-analysis. *Clinical infectious diseases : an official publication of the Infectious Diseases Society of America* 36(1):53-59.
14. Parker MT & Hewitt JH (1970) Methicillin resistance in Staphylococcus aureus. *Lancet* 1(7651):800-804.
15. Lowy FD (2003) Antimicrobial resistance: the example of Staphylococcus aureus. *The Journal of clinical investigation* 111(9):1265-1273.
16. Small PM & Chambers HF (1990) Vancomycin for Staphylococcus aureus endocarditis in intravenous drug users. *Antimicrob Agents Chemother* 34(6):1227-1231.
17. Pantosti A & Venditti M (2009) What is MRSA? *The European respiratory journal* 34(5):1190-1196.
18. Edlund C, Barkholt L, Olsson-Liljequist B, & Nord CE (1997) Effect of vancomycin on intestinal flora of patients who previously received antimicrobial therapy. *Clinical infectious diseases : an official publication of the Infectious Diseases Society of America* 25(3):729-732.
19. Cantu TG, Yamanaka-Yuen NA, & Lietman PS (1994) Serum vancomycin concentrations: reappraisal of their clinical value. *Clinical infectious diseases : an official publication of the Infectious Diseases Society of America* 18(4):533-543.
20. Smith TL, *et al.* (1999) Emergence of vancomycin resistance in Staphylococcus aureus. Glycopeptide-Intermediate Staphylococcus aureus Working Group. *The New England journal of medicine* 340(7):493-501.
21. Walsh TR & Howe RA (2002) The prevalence and mechanisms of vancomycin resistance in Staphylococcus aureus. *Annual review of microbiology* 56:657-675.

22. Sievert DM, *et al.* (2008) Vancomycin-resistant Staphylococcus aureus in the United States, 2002-2006. *Clinical infectious diseases : an official publication of the Infectious Diseases Society of America* 46(5):668-674.
23. Pelaez F (2006) The historical delivery of antibiotics from microbial natural products--can history repeat? *Biochemical pharmacology* 71(7):981-990.
24. Brickner SJ, *et al.* (1996) Synthesis and antibacterial activity of U-100592 and U-100766, two oxazolidinone antibacterial agents for the potential treatment of multidrug-resistant gram-positive bacterial infections. *J Med Chem* 39(3):673-679.
25. Ford CW, *et al.* (1996) In vivo activities of U-100592 and U-100766, novel oxazolidinone antimicrobial agents, against experimental bacterial infections. *Antimicrob Agents Chemother* 40(6):1508-1513.
26. Swaney SM, Aoki H, Ganoza MC, & Shinabarger DL (1998) The oxazolidinone linezolid inhibits initiation of protein synthesis in bacteria. *Antimicrob Agents Chemother* 42(12):3251-3255.
27. Kaplan SL, *et al.* (2005) Three-year surveillance of community-acquired Staphylococcus aureus infections in children. *Clinical infectious diseases : an official publication of the Infectious Diseases Society of America* 40(12):1785-1791.
28. Klevens RM, *et al.* (2007) Invasive methicillin-resistant Staphylococcus aureus infections in the United States. *JAMA : the journal of the American Medical Association* 298(15):1763-1771.
29. Diep BA, *et al.* (2006) Complete genome sequence of USA300, an epidemic clone of community-acquired meticillin-resistant Staphylococcus aureus. *Lancet* 367(9512):731-739.
30. Hidron AI, *et al.* (2008) NHSN annual update: antimicrobial-resistant pathogens associated with healthcare-associated infections: annual summary of data reported to the National Healthcare Safety Network at the Centers for Disease Control and Prevention, 2006-2007. *Infection control and hospital epidemiology : the official journal of the Society of Hospital Epidemiologists of America* 29(11):996-1011.
31. Truglio JJ, *et al.* (2003) Crystal structure of Mycobacterium tuberculosis MenB, a key enzyme in vitamin K2 biosynthesis. *The Journal of biological chemistry* 278(43):42352-42360.
32. Li HJ, *et al.* (2011) Mechanism of the intramolecular Claisen condensation reaction catalyzed by MenB, a crotonase superfamily member. *Biochemistry* 50(44):9532-9544.
33. Li X, *et al.* (2010) Synthesis and SAR studies of 1,4-benzoxazine MenB inhibitors: novel antibacterial agents against Mycobacterium tuberculosis. *Bioorganic & medicinal chemistry letters* 20(21):6306-6309.

34. Li X, *et al.* (2011) CoA Adducts of 4-Oxo-4-Phenylbut-2-enoates: Inhibitors of MenB from the M. tuberculosis Menaquinone Biosynthesis Pathway. *ACS Med Chem Lett* 2(11):818-823.
35. Institute CaLS (2012) Methods for Dilution Antimicrobial Susceptibility Tests for Bacteria That Grow Aerobically; Approved Standard M7-A9.
36. Hiramatsu K, *et al.* (2013) Genomic Basis for Methicillin Resistance in Staphylococcus aureus. *Infect Chemother* 45(2):117-136.
37. Kurosu M, Siricilla S, & Mitachi K (2013) Advances in MRSA drug discovery: where are we and where do we need to be? *Expert Opin Drug Discov* 8(9):1095-1116.
38. Whistance GR, Brown BS, & Threlfall DR (1970) Biosynthesis of ubiquinone in non-photosynthetic gram-negative bacteria. *Biochem J* 117(1):119-128.
39. Pandya KP & King HK (1966) Ubiquinone and menaquinone in bacteria: a comparative study of some bacterial respiratory systems. *Arch Biochem Biophys* 114(1):154-157.
40. Fisher K & Phillips C (2009) The ecology, epidemiology and virulence of Enterococcus. *Microbiology* 155(Pt 6):1749-1757.
41. Orsi GB & Ciorba V (2013) Vancomycin resistant enterococci healthcare associated infections. *Ann Ig* 25(6):485-492.
42. Molton JS, Tambyah PA, Ang BS, Ling ML, & Fisher DA (2013) The global spread of healthcare-associated multidrug-resistant bacteria: a perspective from Asia. *Clin Infect Dis* 56(9):1310-1318.
43. Paternotte I, *et al.* (2001) Syntheses and hydrolysis of basic and dibasic ampicillin esters tailored for intracellular accumulation. *Bioorganic & medicinal chemistry* 9(2):493-502.
44. Moreira R, *et al.* (1996) Acyloxymethyl as a drug protecting group. Part 3. Tertiary O-amidomethyl esters of penicillin G: chemical hydrolysis and anti-bacterial activity. *Pharmaceutical research* 13(1):70-75.
45. Meganathan R, Bentley R, & Taber H (1981) Identification of Bacillus subtilis men mutants which lack O-succinylbenzoyl-coenzyme A synthetase and dihydroxynaphthoate synthase. *Journal of bacteriology* 145(1):328-332.
46. Taber HW, Dellers EA, & Lombardo LR (1981) Menaquinone biosynthesis in Bacillus subtilis: isolation of men mutants and evidence for clustering of men genes. *Journal of bacteriology* 145(1):321-327.
47. Chen C, Gonzalez FJ, & Idle JR (2007) LC-MS-based metabolomics in drug metabolism. *Drug Metab Rev* 39(2-3):581-597.

48. Reaves ML & Rabinowitz JD (2011) Metabolomics in systems microbiology. *Curr Opin Biotechnol* 22(1):17-25.
49. Honoré AH, Thorsen M, & Skov T (2013) Liquid chromatography-mass spectrometry for metabolic footprinting of co-cultures of lactic and propionic acid bacteria. *Anal Bioanal Chem* 405(25):8151-8170.
50. Nakagawa K*, et al.* (2010) Identification of UBIAD1 as a novel human menaquinone-4 biosynthetic enzyme. *Nature* 468(7320):117-121.
51. Okano T*, et al.* (2008) Conversion of phylloquinone (Vitamin K1) into menaquinone-4 (Vitamin K2) in mice: two possible routes for menaquinone-4 accumulation in cerebra of mice. *J Biol Chem* 283(17):11270-11279.
52. Geyer R, Peacock AD, White DC, Lytle C, & Van Berkel GJ (2004) Atmospheric pressure chemical ionization and atmospheric pressure photoionization for simultaneous mass spectrometric analysis of microbial respiratory ubiquinones and menaquinones. *J Mass Spectrom* 39(8):922-929.
53. White DC & Frerman FE (1967) Extraction, characterization, and cellular localization of the lipids of Staphylococcus aureus. *J Bacteriol* 94(6):1854-1867.
54. Bentley R & Meganathan R (1982) Biosynthesis of vitamin K (menaquinone) in bacteria. *Microbiol Rev* 46(3):241-280.
55. Osborne CS*, et al.* (2009) In vivo characterization of the peptide deformylase inhibitor LBM415 in murine infection models. *Antimicrob Agents Chemother* 53(9):3777-3781.
56. Reyes N, Aggen JB, & Kostrub CF (2011) In vivo efficacy of the novel aminoglycoside ACHN-490 in murine infection models. *Antimicrob Agents Chemother* 55(4):1728-1733.
57. Keel RA, Tessier PR, Crandon JL, & Nicolau DP (2012) Comparative efficacies of human simulated exposures of tedizolid and linezolid against Staphylococcus aureus in the murine thigh infection model. *Antimicrob Agents Chemother* 56(8):4403-4407.
58. Banevicius MA, Kaplan N, Hafkin B, & Nicolau DP (2013) Pharmacokinetics, pharmacodynamics and efficacy of novel FabI inhibitor AFN-1252 against MSSA and MRSA in the murine thigh infection model. *J Chemother* 25(1):26-31.
59. Louie A, Liu W, Kulawy R, & Drusano GL (2011) In vivo pharmacodynamics of torezolid phosphate (TR-701), a new oxazolidinone antibiotic, against methicillin-susceptible and methicillin-resistant Staphylococcus aureus strains in a mouse thigh infection model. *Antimicrob Agents Chemother* 55(7):3453-3460.
60. Andes D & Craig WA (2006) Pharmacodynamics of a new cephalosporin, PPI-0903 (TAK-599), active against methicillin-resistant Staphylococcus aureus in

murine thigh and lung infection models: identification of an in vivo pharmacokinetic-pharmacodynamic target. *Antimicrob Agents Chemother* 50(4):1376-1383.

61. Craig WA & Andes DR (2008) In vivo pharmacodynamics of ceftobiprole against multiple bacterial pathogens in murine thigh and lung infection models. *Antimicrob Agents Chemother* 52(10):3492-3496.
62. Schiebel J*, et al.* (2014) Rational Design of Broad-Spectrum Antibacterial Activity based on a Clinically Relevant Enoyl-ACP Reductase Inhibitor. *J Biol Chem*.

**Chapter III**

1. Proctor RA*, et al.* (2006) Small colony variants: a pathogenic form of bacteria that facilitates persistent and recurrent infections. *Nat Rev Microbiol* 4(4):295-305.
2. von Eiff C (2008) Staphylococcus aureus small colony variants: a challenge to microbiologists and clinicians. *Int J Antimicrob Agents* 31(6):507-510.
3. Colwell CA (1946) Small Colony Variants of Escherichia coli. *J Bacteriol* 52(4):417-422.
4. Bryan LE & Kwan S (1981) Aminoglycoside-resistant mutants of Pseudomonas aeruginosa deficient in cytochrome d, nitrite reductase, and aerobic transport. *Antimicrob Agents Chemother* 19(6):958-964.
5. HALL WH & SPINK WW (1947) In vitro sensitivity of Brucella to streptomycin; development of resistance during streptomycin treatment. *Proc Soc Exp Biol Med* 64(4):403-406.
6. Proctor RA & Peters G (1998) Small colony variants in staphylococcal infections: diagnostic and therapeutic implications. *Clin Infect Dis* 27(3):419-422.
7. Lannergård J*, et al.* (2008) Identification of the genetic basis for clinical menadione-auxotrophic small-colony variant isolates of Staphylococcus aureus. *Antimicrob Agents Chemother* 52(11):4017-4022.
8. Garcia LG*, et al.* (2012) Pharmacodynamic evaluation of the activity of antibiotics against hemin- and menadione-dependent small-colony variants of Staphylococcus aureus in models of extracellular (broth) and intracellular (THP-1 monocytes) infections. *Antimicrob Agents Chemother* 56(7):3700-3711.
9. Vaudaux P, Kelley WL, & Lew DP (2006) Staphylococcus aureus small colony variants: difficult to diagnose and difficult to treat. *Clin Infect Dis* 43(8):968-970.

10. Maduka-Ezeh A*, et al.* (2012) Thymidine auxotrophic Staphylococcus aureus small-colony variant endocarditis and left ventricular assist device infection. *J Clin Microbiol* 50(3):1102-1105.
11. von Eiff C, Proctor RA, & Peters G (2000) Staphylococcus aureus small colony variants: formation and clinical impact. *Int J Clin Pract Suppl* (115):44-49.
12. Tuchscherr L*, et al.* (2010) Staphylococcus aureus small-colony variants are adapted phenotypes for intracellular persistence. *J Infect Dis* 202(7):1031-1040.
13. Kahl BC*, et al.* (2003) Population dynamics of persistent Staphylococcus aureus isolated from the airways of cystic fibrosis patients during a 6-year prospective study. *J Clin Microbiol* 41(9):4424-4427.
14. von Eiff C, Proctor RA, & Peters G (2000) Small colony variants of Staphylococci: a link to persistent infections. *Berl Munch Tierarztl Wochenschr* 113(9):321-325.
15. Seaman PF, Ochs D, & Day MJ (2007) Small-colony variants: a novel mechanism for triclosan resistance in methicillin-resistant Staphylococcus aureus. *J Antimicrob Chemother* 59(1):43-50.
16. Proctor RA, van Langevelde P, Kristjansson M, Maslow JN, & Arbeit RD (1995) Persistent and relapsing infections associated with small-colony variants of Staphylococcus aureus. *Clin Infect Dis* 20(1):95-102.
17. Gómez-González C*, et al.* (2010) Clinical and molecular characteristics of infections with CO2-dependent small-colony variants of Staphylococcus aureus. *J Clin Microbiol* 48(8):2878-2884.
18. Slifkin M, Merkow LP, Kreuzberger SA, Engwall C, & Pardo M (1971) Characterization of CO 2 dependent microcolony variants of Staphylococcus aureus. *Am J Clin Pathol* 56(5):584-592.
19. McNamara PJ & Proctor RA (2000) Staphylococcus aureus small colony variants, electron transport and persistent infections. *Int J Antimicrob Agents* 14(2):117-122.
20. Koo SP, Bayer AS, Sahl HG, Proctor RA, & Yeaman MR (1996) Staphylocidal action of thrombin-induced platelet microbicidal protein is not solely dependent on transmembrane potential. *Infect Immun* 64(3):1070-1074.
21. Balwit JM, van Langevelde P, Vann JM, & Proctor RA (1994) Gentamicin-resistant menadione and hemin auxotrophic Staphylococcus aureus persist within cultured endothelial cells. *J Infect Dis* 170(4):1033-1037.
22. von Eiff C*, et al.* (2006) Phenotype microarray profiling of Staphylococcus aureus menD and hemB mutants with the small-colony-variant phenotype. *J Bacteriol* 188(2):687-693.

23. Bates DM, *et al.* (2003) Staphylococcus aureus menD and hemB mutants are as infective as the parent strains, but the menadione biosynthetic mutant persists within the kidney. *J Infect Dis* 187(10):1654-1661.
24. von Eiff C, *et al.* (1997) A site-directed Staphylococcus aureus hemB mutant is a small-colony variant which persists intracellularly. *J Bacteriol* 179(15):4706-4712.
25. Baumert N, *et al.* (2002) Physiology and antibiotic susceptibility of Staphylococcus aureus small colony variants. *Microb Drug Resist* 8(4):253-260.
26. Jamison JM, Gilloteaux J, Taper HS, & Summers JL (2001) Evaluation of the in vitro and in vivo antitumor activities of vitamin C and K-3 combinations against human prostate cancer. *J Nutr* 131(1):158S-160S.
27. Bolton-Smith C, Price RJ, Fenton ST, Harrington DJ, & Shearer MJ (2000) Compilation of a provisional UK database for the phylloquinone (vitamin K1) content of foods. *Br J Nutr* 83(4):389-399.
28. Beulens JW, *et al.* (2010) Dietary phylloquinone and menaquinones intakes and risk of type 2 diabetes. *Diabetes Care* 33(8):1699-1705.
29. Cox GB, Newton NA, Gibson F, Snoswell AM, & Hamilton JA (1970) The function of ubiquinone in Escherichia coli. *Biochem J* 117(3):551-562.
30. Søballe B & Poole RK (1999) Microbial ubiquinones: multiple roles in respiration, gene regulation and oxidative stress management. *Microbiology* 145 ( Pt 8):1817-1830.
31. Papa S, *et al.* (2002) The NADH: ubiquinone oxidoreductase (complex I) of the mammalian respiratory chain and the cAMP cascade. *J Bioenerg Biomembr* 34(1):1-10.
32. Hirota Y, *et al.* (2013) Menadione (vitamin K3) is a catabolic product of oral phylloquinone (vitamin K1) in the intestine and a circulating precursor of tissue menaquinone-4 (vitamin K2) in rats. *J Biol Chem* 288(46):33071-33080.
33. Okano T, *et al.* (2008) Conversion of phylloquinone (Vitamin K1) into menaquinone-4 (Vitamin K2) in mice: two possible routes for menaquinone-4 accumulation in cerebra of mice. *J Biol Chem* 283(17):11270-11279.
34. Nakagawa K, *et al.* (2010) Identification of UBIAD1 as a novel human menaquinone-4 biosynthetic enzyme. *Nature* 468(7320):117-121.
35. Kurosu M & Crick DC (2009) MenA is a promising drug target for developing novel lead molecules to combat Mycobacterium tuberculosis. *Med Chem* 5(2):197-207.

36. Dhiman RK*, et al.* (2009) Menaquinone synthesis is critical for maintaining mycobacterial viability during exponential growth and recovery from non-replicating persistence. *Mol Microbiol* 72(1):85-97.
37. Suhara Y, Wada A, & Okano T (2009) Elucidation of the mechanism producing menaquinone-4 in osteoblastic cells. *Bioorg Med Chem Lett* 19(4):1054-1057.
38. Davidson RT, Foley AL, Engelke JA, & Suttie JW (1998) Conversion of dietary phylloquinone to tissue menaquinone-4 in rats is not dependent on gut bacteria. *J Nutr* 128(2):220-223.
39. Kurosu M, Narayanasamy P, Biswas K, Dhiman R, & Crick DC (2007) Discovery of 1,4-dihydroxy-2-naphthoate [corrected] prenyltransferase inhibitors: new drug leads for multidrug-resistant gram-positive pathogens. *J Med Chem* 50(17):3973-3975.
40. Crick DC*, et al.* (2000) Polyprenyl phosphate biosynthesis in Mycobacterium tuberculosis and Mycobacterium smegmatis. *J Bacteriol* 182(20):5771-5778.
41. Institutes CaLS (2012) methods for antimicrobial susceptibility testes for aerobically growing bacteria.
42. Shineberg B & Young IG (1976) Biosynthesis of bacterial menaquinones: the membrane-associated 1,4-dihydroxy-2-naphthoate octaprenyltransferase of Escherichia coli. *Biochemistry* 15(13):2754-2758.

**Chpater IV**

1. Swinney DC (2004) Biochemical mechanisms of drug action: what does it take for success? *Nat Rev Drug Discov* 3(9):801-808.
2. Swinney DC (2009) The role of binding kinetics in therapeutically useful drug action. *Curr Opin Drug Discov Devel* 12(1):31-39.
3. Copeland RA, Pompliano DL, & Meek TD (2006) Drug-target residence time and its implications for lead optimization. *Nat Rev Drug Discov* 5(9):730-739.
4. Tummino PJ & Copeland RA (2008) Residence time of receptor-ligand complexes and its effect on biological function. *Biochemistry* 47(20):5481-5492.
5. Lu H & Tonge PJ (2010) Drug-target residence time: critical information for lead optimization. *Curr Opin Chem Biol* 14(4):467-474.
6. Zhang R & Monsma F (2009) The importance of drug-target residence time. *Curr Opin Drug Discov Devel* 12(4):488-496.
7. Kumar P*, et al.* (2009) Update of KDBI: Kinetic Data of Bio-molecular Interaction database. *Nucleic Acids Res* 37(Database issue):D636-641.

8. Leysen J, and Gommeren, W. (1986) Drug-receptor dissociation time, new tool for drug research: receptor binding affinity and drug-receptor dissociation profiles of Serontonin-S2, dopamine-D2, Histamine-H1 antagonists, and opiates. (Drug Develop. Res.), pp 119-131.
9. Tillotson B*, et al.* (2010) Hsp90 (heat shock protein 90) inhibitor occupancy is a direct determinant of client protein degradation and tumor growth arrest in vivo. *J Biol Chem* 285(51):39835-39843.
10. Gossas T*, et al.* (2012) Aliskiren displays long-lasting interactions with human renin. *Naunyn Schmiedebergs Arch Pharmacol* 385(2):219-224.
11. Lewandowicz A, Tyler PC, Evans GB, Furneaux RH, & Schramm VL (2003) Achieving the ultimate physiological goal in transition state analogue inhibitors for purine nucleoside phosphorylase. *J Biol Chem* 278(34):31465-31468.
12. Fuchs B*, et al.* (2000) Comparative pharmacodynamics and pharmacokinetics of candesartan and losartan in man. *J Pharm Pharmacol* 52(9):1075-1083.
13. Disse B, Speck GA, Rominger KL, Witek TJ, & Hammer R (1999) Tiotropium (Spiriva): mechanistical considerations and clinical profile in obstructive lung disease. *Life Sci* 64(6-7):457-464.
14. Lu H*, et al.* (2009) Slow-onset inhibition of the FabI enoyl reductase from francisella tularensis: residence time and in vivo activity. *ACS Chem Biol* 4(3):221-231.
15. MacKenzie FM & Gould IM (1993) The post-antibiotic effect. *J Antimicrob Chemother* 32(4):519-537.
16. Stubbings W, Bostock J, Ingham E, & Chopra I (2006) Mechanisms of the post-antibiotic effects induced by rifampicin and gentamicin in Escherichia coli. *J Antimicrob Chemother* 58(2):444-448.
17. Yan S, Bohach GA, & Stevens DL (1994) Persistent acylation of high-molecular-weight penicillin-binding proteins by penicillin induces the postantibiotic effect in Streptococcus pyogenes. *J Infect Dis* 170(3):609-614.
18. Nikravesh A*, et al.* (2007) Antisense PNA accumulates in Escherichia coli and mediates a long post-antibiotic effect. *Mol Ther* 15(8):1537-1542.
19. Seefeld MA*, et al.* (2003) Indole naphthyridinones as inhibitors of bacterial enoyl-ACP reductases FabI and FabK. *J Med Chem* 46(9):1627-1635.
20. Payne DJ, Gwynn MN, Holmes DJ, & Pompliano DL (2007) Drugs for bad bugs: confronting the challenges of antibacterial discovery. *Nat Rev Drug Discov* 6(1):29-40.

21. Kaplan N, *et al.* (2012) Mode of action, in vitro activity, and in vivo efficacy of AFN-1252, a selective antistaphylococcal FabI inhibitor. *Antimicrob Agents Chemother* 56(11):5865-5874.
22. Gerusz V, *et al.* (2012) From triclosan toward the clinic: discovery of nonbiocidal, potent FabI inhibitors for the treatment of resistant bacteria. *J Med Chem* 55(22):9914-9928.
23. Escaich S, *et al.* (2011) The MUT056399 inhibitor of FabI is a new antistaphylococcal compound. *Antimicrob Agents Chemother* 55(10):4692-4697.
24. Park HS, *et al.* (2007) Antistaphylococcal activities of CG400549, a new bacterial enoyl-acyl carrier protein reductase (FabI) inhibitor. *J Antimicrob Chemother* 60(3):568-574.
25. Yum JH, *et al.* (2007) In vitro activities of CG400549, a novel FabI inhibitor, against recently isolated clinical staphylococcal strains in Korea. *Antimicrob Agents Chemother* 51(7):2591-2593.
26. Xu H, *et al.* (2008) Mechanism and inhibition of saFabI, the enoyl reductase from Staphylococcus aureus. *Biochemistry* 47(14):4228-4236.
27. Schiebel J, *et al.* (2014) Rational Design of Broad Spectrum Antibacterial Activity Based on a Clinically Relevant Enoyl-Acyl Carrier Protein (ACP) Reductase Inhibitor. *J Biol Chem* 289(23):15987-16005.
28. Campbell JW & Cronan JE (2001) Bacterial fatty acid biosynthesis: targets for antibacterial drug discovery. *Annu Rev Microbiol* 55:305-332.
29. Borgaro JG, Chang A, Machutta CA, Zhang X, & Tonge PJ (2011) Substrate recognition by β-ketoacyl-ACP synthases. *Biochemistry* 50(49):10678-10686.
30. Machutta CA, *et al.* (2010) Slow onset inhibition of bacterial beta-ketoacyl-acyl carrier protein synthases by thiolactomycin. *J Biol Chem* 285(9):6161-6169.
31. Schiebel J, *et al.* (2013) Structural basis for the recognition of mycolic acid precursors by KasA, a condensing enzyme and drug target from Mycobacterium tuberculosis. *J Biol Chem* 288(47):34190-34204.
32. Kapilashrami K, *et al.* (2013) Thiolactomycin-based β-ketoacyl-AcpM synthase A (KasA) inhibitors: fragment-based inhibitor discovery using transient one-dimensional nuclear overhauser effect NMR spectroscopy. *J Biol Chem* 288(9):6045-6052.
33. Oishi H, *et al.* (1982) Thiolactomycin, a new antibiotic. I. Taxonomy of the producing organism, fermentation and biological properties. *J Antibiot (Tokyo)* 35(4):391-395.
34. Sasaki H, *et al.* (1982) Thiolactomycin, a new antibiotic. II. Structure elucidation. *J Antibiot (Tokyo)* 35(4):396-400.

35. Noto T, Miyakawa S, Oishi H, Endo H, & Okazaki H (1982) Thiolactomycin, a new antibiotic. III. In vitro antibacterial activity. *J Antibiot (Tokyo)* 35(4):401-410.
36. Hamada S*, et al.* (1990) Antimicrobial activities of thiolactomycin against gram-negative anaerobes associated with periodontal disease. f1. *Oral Microbiol Immunol* 5(6):340-345.
37. Axten JM*, et al.* (2012) Discovery of 7-methyl-5-(1-{[3-(trifluoromethyl)phenyl]acetyl}-2,3-dihydro-1H-indol-5-yl)-7H-pyrrolo[2,3-d]pyrimidin-4-amine (GSK2606414), a potent and selective first-in-class inhibitor of protein kinase R (PKR)-like endoplasmic reticulum kinase (PERK). *J Med Chem* 55(16):7193-7207.
38. Foley TL*, et al.* (2014) 4-(3-Chloro-5-(trifluoromethyl)pyridin-2-yl)-N-(4-methoxypyridin-2-yl)piperazine-1-carbothioamide (ML267), a potent inhibitor of bacterial phosphopantetheinyl transferase that attenuates secondary metabolism and thwarts bacterial growth. *J Med Chem* 57(3):1063-1078.

**Chpater V**

1. Miller PW, Long NJ, Vilar R, & Gee AD (2008) Synthesis of 11C, 18F, 15O, and 13N radiolabels for positron emission tomography. *Angew Chem Int Ed Engl* 47(47):8998-9033.
2. Turkington TG (2001) Introduction to PET instrumentation. *J Nucl Med Technol* 29(1):4-11.
3. Gambhir SS (2002) Molecular imaging of cancer with positron emission tomography. *Nat Rev Cancer* 2(9):683-693.
4. Karp JS*, et al.* (1990) Continuous-slice PENN-PET: a positron tomograph with volume imaging capability. *J Nucl Med* 31(5):617-627.
5. Phelps ME, Hoffman EJ, Mullani NA, & Ter-Pogossian MM (1975) Application of annihilation coincidence detection to transaxial reconstruction tomography. *J Nucl Med* 16(3):210-224.
6. Anonymous (2010) A Vital legacy: Biological and Environmental Research in the Atomic Age. (U.S. Department of Energy, The Office of Biological and Environmental Research), pp 25-26.
7. Signore A, Mather SJ, Piaggio G, Malviya G, & Dierckx RA (2010) Molecular imaging of inflammation/infection: nuclear medicine and optical imaging agents and methods. *Chem Rev* 110(5):3112-3145.

8. Rajagopalan KN & DeBerardinis RJ (2011) Role of glutamine in cancer: therapeutic and imaging implications. *J Nucl Med* 52(7):1005-1008.
9. Qu W, *et al.* (2012) Preparation and characterization of L-[5-11C]-glutamine for metabolic imaging of tumors. *J Nucl Med* 53(1):98-105.
10. Herrmann K, *et al.* (2011) (18)F-FDG-PET/CT in evaluating response to therapy in solid tumors: where we are and where we can go. *Q J Nucl Med Mol Imaging* 55(6):620-632.
11. Fowler JS, *et al.* (2003) Low monoamine oxidase B in peripheral organs in smokers. *Proc Natl Acad Sci U S A* 100(20):11600-11605.
12. Fowler JS, *et al.* (2003) Monoamine oxidase A imaging in peripheral organs in healthy human subjects. *Synapse* 49(3):178-187.
13. Lister-James J, *et al.* (2011) Florbetapir f-18: a histopathologically validated Beta-amyloid positron emission tomography imaging agent. *Semin Nucl Med* 41(4):300-304.
14. Clark CM, *et al.* (2011) Use of florbetapir-PET for imaging beta-amyloid pathology. *JAMA* 305(3):275-283.
15. Botnar RM & Makowski MR (2012) Cardiovascular magnetic resonance imaging in small animals. *Prog Mol Biol Transl Sci* 105:227-261.
16. Schuster A, *et al.* (2012) Platelets in cardiovascular imaging. *Curr Vasc Pharmacol* 10(5):619-625.
17. Welling MM & Alberto R (2010) Performance of a 99mTc-labelled 1-thio-beta-D-glucose 2,3,4,6-tetra-acetate analogue in the detection of infections and tumours in mice: a comparison with [18F]FDG. *Nucl Med Commun* 31(3):239-248.
18. Kosterink JG (2011) Positron emission tomography in the diagnosis and treatment management of tuberculosis. *Curr Pharm Des* 17(27):2875-2880.
19. Kubota R, *et al.* (1992) Intratumoral distribution of fluorine-18-fluorodeoxyglucose in vivo: high accumulation in macrophages and granulation tissues studied by microautoradiography. *J Nucl Med* 33(11):1972-1980.
20. Solanki KK, Mather SJ, Janabi MA, & Britton KE (1988) A rapid method for the preparation of 99Tcm hexametazime-labelled leucocytes. *Nucl Med Commun* 9(10):753-761.
21. Fischman AJ, *et al.* (1997) Pharmacokinetics of 18F-labeled trovafloxacin in normal and Escherichia coli-infected rats and rabbits studied with positron emission tomography. *Clin Microbiol Infect* 3(3):379.
22. Fischman AJ, *et al.* (1992) Pharmacokinetics of 18F-labeled fleroxacin in rabbits with Escherichia coli infections, studied with positron emission tomography. *Antimicrob Agents Chemother* 36(10):2286-2292.

23. Langer O*, et al.* (2005) In vitro and in vivo evaluation of [18F]ciprofloxacin for the imaging of bacterial infections with PET. *Eur J Nucl Med Mol Imaging* 32(2):143-150.
24. Siaens RH, Rennen HJ, Boerman OC, Dierckx R, & Slegers G (2004) Synthesis and comparison of 99mTc-enrofloxacin and 99mTc-ciprofloxacin. *J Nucl Med* 45(12):2088-2094.
25. Singh N & Bhatnagar A (2010) Clinical Evaluation of Efficacy of (99m)TC - Ethambutol in Tubercular Lesion Imaging. *Tuberc Res Treat* 2010:618051.
26. Babich JW*, et al.* (1996) 18F-labeling and biodistribution of the novel fluoro-quinolone antimicrobial agent, trovafloxacin (CP 99,219). *Nucl Med Biol* 23(8):995-998.
27. Rohwer JM, Meadow ND, Roseman S, Westerhoff HV, & Postma PW (2000) Understanding glucose transport by the bacterial phosphoenolpyruvate:glycose phosphotransferase system on the basis of kinetic measurements in vitro. *J Biol Chem* 275(45):34909-34921.
28. Natarajan A & Srienc F (2000) Glucose uptake rates of single E. coli cells grown in glucose-limited chemostat cultures. *J Microbiol Methods* 42(1):87-96.
29. Bates DM*, et al.* (2003) Staphylococcus aureus menD and hemB mutants are as infective as the parent strains, but the menadione biosynthetic mutant persists within the kidney. *J Infect Dis* 187(10):1654-1661.